Drought and Defoliation-induced Alterations to the Structure and Function of the Vascular Tissue in Trees

by

Rachel M. Hillabrand

A thesis submitted in partial fulfillment of the requirements for the degree of

Doctor of Philosophy

in

Forest Biology and Management

Department of Renewable Resources
University of Alberta

Abstract

Observations of tree dieback and mortality from climate change-induced drought has been documented across the world, however the mechanisms of tree mortality are not fully understood. Infestations of insect pests may also contribute to the process of drought-induced dieback. Tree physiological processes are linked to the vascular tissue which provides the transport of water and sugars through the xylem and phloem. These processes are critical for tree functioning; recent research has emphasized the importance of xylem functional traits as predictors of mortality. The determination of structural and functional changes to the vascular tissue induced by drought and defoliation can provide evidence for how these stress events increase the vulnerability of trees to dieback and mortality. This thesis advances this objective through different research approaches using the species trembling aspen (*Populus tremuloides* Michx.) and balsam poplar (*Populus balsamifera* L.): firstly, by examining drought-stressed trees to provide evidence for previously hypothesized xylem pit membrane damage, secondly, by examining tree rings to discover unknown xylem structural changes due to drought and defoliation, and thirdly, by examining defoliated trees for a comprehensive look at alterations in xylem and phloem structure and function.

Results of these analyses indicated a variety of structural and functional changes due to drought and defoliation. Drought-induced, irreversible damage to xylem pit membranes was observed and interpreted as a cause for the phenomenon of cavitation fatigue. The examination of tree rings revealed that the mean xylem vessel diameters correlated more strongly to precipitation when the trees were young, than when they were mature. Additionally, tree rings showed more pronounced alterations to xylem structure in response to insect defoliation than to drought. Xylem

structural changes due to defoliation increased the vulnerability of trees to cavitation, and defoliation reduced sieve tube diameters and fiber area in the phloem.

Altogether, these data show that vascular tissue alterations due both drought and defoliation increase the vulnerability of trees to drought-induced dieback. Mature trees may be less sensitive to drought than young trees, but when drought is severe, drought promotes mortality through irreversible damage to the xylem pit membranes. The resource limitation resulting from insect defoliation contributes to increased risk for tree physiological dysfunction by reductions in tree hydraulic safety and efficiency through xylem structural changes, and reduced phloem transport efficiency and reduced mechanical strength in stems through phloem structural changes.

Preface

This research has been conducted in collaboration with multiple partners. Contributions by the thesis author (**RH**) and others are detailed below.

Intellectual Contributions to Publications and Chapters:

A version of Chapter 2 has been published as: **Hillabrand R.M.**, Hacke U.G. & Lieffers V.J. (2016) Drought-induced xylem pit membrane damage in aspen and balsam poplar. *Plant, Cell & Environment* 39: 2210-2220. This study was conceived by **RH** and UH, with input from VL. **RH** set up the study, collected data, and performed the analyses. **RH** wrote the manuscript with input and edits from UH and VL.

A version of Chapter 3 has been published as: **Hillabrand R.M.**, Lieffers V.J., Hogg E.H., Martinez-Sancho E., Menzel A. & Hacke U.G. (2018) Functional xylem anatomy of aspen exhibits greater change due to insect defoliation than to drought. *Tree Physiology*, https://doi.org/10.1093/treephys/tpy075. The general idea of the study was conceived by **RH**, with input by UH and VL. Tree core collection was assisted by VL and EH, and EMS assisted **RH** with tree core methods and statistical analysis. **RH** made all tree core micro-sections and measurements. **RH** wrote the manuscript with input and edits from VL, EH, EMS, AM, and UH.

A version of Chapter 4 has been submitted to a peer-reviewed journal as: **Hillabrand R.M.**, Hacke U.G. & Lieffers V.J. (2018) Defoliation constrains xylem and phloem functionality. This study was conceived by **RH**, with input from UH and VL. **RH** set up the study, collected data, and performed the analyses. **RH** wrote the manuscript with input and edits from UH and VL.

Acknowledgements

The completion of this thesis would not have been possible without many sources of support.

Thank you to my supervisors Dr. Uwe Hacke and Dr. Vic Lieffers for their support in the research undertaken to write this thesis. Thank you also to my committee members, Dr. Ted Hogg and Dr. Andreas Hamann, for their helpful feedback.

Thank you to current and former graduate students, summer students, and post-docs who have provided their help and advice: Cayla Brocious, Stefan Schreiber, Joan Laur, Na-Yeong Park, Ryan Stanfield, Jaime Sebastian-Azcona, Lauren Sinclair, Killian Fleurial, Miriam Isaac-Renton, Morgane Merlin, Erin Wiley, Nathan Lauer, David Love, David Montwé, and many others.

Thank you to our collaborators at the Technical University Munich who hosted me for a month long stay and taught me about dendrochronology, especially: Elisabet Martínez-Sancho, Isabel Dorado Liñán, Hannes Seidel, and Annette Menzel.

Thank you to the University staff who provided their assistance and expertise in scanning electron microscopy: Nathan Gerein and George Braybrook. Thank you also to Arlene Oatway in the Microscopy Unit for teaching me tissue preparation methods for light microscopy.

And, thank you to my family and friends who have always supported and believed in me.

Table of Contents

List of Tables

Chapter 2: Drought-induced xylem pit membrane damage in aspen and balsam poplar

Chapter 3: Functional xylem anatomy of aspen exhibits greater change due to insect defoliation than to drought

Chapter 4: Defoliation constrains xylem and phloem functionality

List of Figures

Chapter 2: Drought-induced xylem pit membrane damage in aspen and balsam poplar

Chapter 3: Functional xylem anatomy of aspen exhibits greater change due to insect defoliation than to drought

Chapter 4: Defoliation constrains xylem and phloem functionality

1 Introduction

1.1 Drought-induced tree mortality

An emerging issue over the last decade has been the observation of tree mortality due to climate-change induced drought (Allen et al. 2010). This is also true here in Canada, where drought has contributed to increasing rates of tree mortality in the boreal forest (Peng et al. 2011; Chen & Luo 2015) and has led to severe dieback in the aspen parkland of western Canada (Michaelian et al. 2011).

Forests provide many critical resources to the world that, in turn, may be at risk. Forestry and the production of wood products are large industries that strongly contribute to individual economies; the forest industry contributes over 20 billion dollars towards Canada's GDP (Natural Resources Canada 2017). Forests also provide key ecosystem services such as carbon sequestration. It is estimated that globally, forests sequester ~2.4 Pg carbon per year (Pan et al. 2011). The mortality of adult trees due to drought may significantly change ecosystems, leading to changes in species composition or the introduction of non-native species (Suarez & Kitzberger 2008) altering the way in which forest resources can be used. Therefore, the ability to predict the severity of die-back due to drought has emerged as an essential topic for future forest management. However, our understanding of the complex physiological process of tree death is limited (McDowell et al. 2008). This includes understanding how the underlying physiological mechanisms of tree functioning are impacted by drought.

The mechanism of tree death due to drought is generally discussed through two main hypotheses: hydraulic failure and carbon starvation. These are somewhat analogous to thinking that the tree dies either from thirst, or hunger, and hinge on the ability of the vascular tissue to transport both water and sugar. There has been much discussion of these hypotheses concerning if

trees die from one or the other or a combination of both, and the possible role of biotic agents such as insects (McDowell et al. 2008; Sala et al. 2010; Sevanto et al. 2014; Adams et al. 2017). It is possible that some trees are more predisposed to dying from one or the other based on their stomatal behavior (McDowell et. al. 2008). And, experimentally it has been shown that within the same species both types of mechanisms can be induced (Sevanto et al. 2014). However, recently, it has been shown in individual species and through meta-analyses of many species that vulnerability to hydraulic failure and hydraulic dysfunction are best predictors of mortality for drought stressed trees (Skelton et al. 2015; Anderegg et al. 2016; Adams et al. 2017). This result emphasizes that measurements of functional traits, especially hydraulic traits can play a role in furthering our ability to understand tree death.

Furthermore, in order to advance our understanding of tree death it is necessary to understand the ways in which individual species respond to drought and environmental stress. Models can inform us about the future trends of tree species distribution, but they are improved by studies at the species level because the response of trees to stress can be species-specific. As mentioned, a key area of study is the vascular function of trees. This includes studying alterations in both the xylem and the phloem, the tissues through which the essential functions of water and sugar transport occur. Knowledge of the ways in which vascular transport is impacted by environmental stress in different species is a stepping stone to making broader predictions. By integrating these properties of vascular structure and function into model frameworks, uncertainties surrounding the impact of climate change on woody plants may be resolved (Anderegg 2014; Sperry & Love 2015; Anderegg et al. 2015a).

1.2 The influence of insects

Global change may not only lead into increases in tree mortality due to drought, but also tree mortality facilitated by insect attack (McDowell et al. 2009; Anderegg et al. 2015b). The types of insect attack that influence tree function are various. Some insects carry fungal pathogens with them while other insects attack more directly through herbivory and defoliation. High temperatures may increase the risk for insect outbreaks directly through increasing the developmental rates of insects, and drought may also reduce trees' resources for defense (Weed et al. 2013). Therefore, understanding the contribution of insects to tree mortality is an important part of modeling tree mortality to climate change (Anderegg et al. 2015b; Foster 2017). Generalizing the response of insects to climate change can be difficult because the response can also be species-specific (Pureswaran et al. 2018); however, evidence suggests that insect outbreaks of defoliators here in the northern and boreal regions may be triggered by warmer spring temperatures (Chen et al. 2017).

The physical effects of insect defoliation on trees can be quite visible through observable reductions in tree ring growth (Jones et al. 2004; Foster 2017). However, although growth suppression indicates a substantial impact on tree productivity, insect defoliation may also have direct impacts on the vascular tissue. These species-specific responses may influence the mechanisms through which defoliation promotes tree dysfunction. Defoliation has been shown to lead to increases in xylem conduit size in *Aesculus* and *Tsuga*, increasing efficiency but potentially decreasing the mechanical integrity of the wood (Salleo et al. 2003; Huggett et al. 2018). But not all trees may exhibit similar responses, and not all tree species have been studied for their responses to defoliaton. Trembling aspen, a diffuse-porous species and widespread boreal tree, is affected by a defoliator (*Malacosoma disstria* Hbn.), the forest tent caterpillar (Hildahl & Reeks 1960;

Peterson & Peterson 1992). Multiple years of defoliation by the caterpillar may lead to substantial mortality (Man & Rice 2010). There exists potential to better understand the effect of defoliation on this tree through further study of its vascular structure and function.

1.3 The vascular tissue – xylem

The vascular tissue of each tree is the network through which water, nutrients, and sugar are transported (Evert 2006). Its importance to tree physiological health cannot be overstated. Underlying the transport of water in trees is the xylem tissue. The xylem is made up of hollow cells, dead at maturity, that act as conduits for the water movement from the roots all the way to the leaves. In angiosperms, these are the xylem vessels, which are surrounded by a matrix of xylem fibers for structural support. An approximation of water flow through xylem vessels is modelled by the Hagen-Poiseuille equation of fluid flow through a capillary:

$$K_{capillary} = \frac{r^4 \pi}{8\eta} \tag{1.1}$$

where the hydraulic conductivity (K) is proportional to the radius of the capillary (r) raised to the 4th power, over the viscosity (η) of water (Tyree & Zimmerman 2002). This equation has large implications for alterations in vessel size: small changes in radius can lead to exponential changes in flow. Differences in vessel size may be observed among different species with varying life strategies. And, within species, various environmental conditions during xylem development, such as drought, can alter vessel traits which may lead to greater vulnerability to hydraulic failure. This plasticity of xylem vessel properties in response to the environment has been shown not only for drought (Arend & Fromm 2007; Beikircher & Mayr 2009; Corcuera et al. 2011), but also for

altered nutrient (Placova et al. 2013) and shade conditions (Schoonmaker et al. 2010; Plavcova & Hacke 2012).

Dysfunction of xylem vessels due to drought occurs when vessels become embolised, or filled with air. The liquid state of water is meta-stable in the xylem because of the high tensions in the water column, and cavitation and subsequent embolism formation inside a xylem conduit can happen via air-seeding from adjacent conduits (Lens et al. 2013). Air-seeding may especially occur between conduits through pores in xylem pit membranes (Sperry & Tyree 1988; Tyree & Zimmerman 2002). Pit membranes are porous structures within the xylem cell walls that connect adjacent conduits to allow water movement between them. During the progression of a drought, pressure differences between water-filled and air-filled vessels become increasingly large, leading to air-seeding events and increasing embolism.

A particular concern of tree hydraulic function is that the resistance of xylem to embolism formation is weakened in some species after drought, a phenomenon labelled "cavitation fatigue" (Hacke et al. 2001; Stiller & Sperry 2002; Anderegg et al. 2013). It has been hypothesized that drought may cause damage to xylem pit membranes (Hacke et al. 2001; Stiller & Sperry 2002). Specifically, that repeated flexing of the membrane may cause loosening or rupturing of the membrane leading to larger pores, and thus, increased air-seeding at smaller pressures differences (Hacke et al. 2001). However, this hypothesis requires experimental evidence that has been so far lacking.

1.4 Tree rings as a record of xylem structure and function

Another component of studying alterations in xylem structure and function is its change over time. Tree rings provide a record of xylem structure over many years, offering insight into

adjustments of the water transport system to different environmental factors (Fonti et al. 2010). Besides tree ring width, wood anatomical data, such as vessel and fiber properties, are preserved which were produced during years of environment stress. Studying the xylem at different points over a tree's lifetime offers opportunity to examine the response of trees not only to recent environmental change, but also to the environmental conditions of years past. Changes in xylem properties over time have been observed in trees as a long-term response to drought and altered environmental conditions (Eilmann et al. 2009; Bryukhanova & Fonti 2013) as well as in the specific year of stress (Corcuera et al. 2004).

Additionally, physiological information can be gathered from isotopic analyses of tree rings. Not only is the structure of the xylem preserved in tree rings, but so too are the isotopic ratios of carbon, oxygen, and hydrogen isotopes that were taken in by the tree as CO_2 and H_2O every year. These molecules are processed into the wood that makes up the rings, and can provide consistent data about tree response to environmental conditions through the measured ratio of the elemental isotopes. For example, carbon has two stable isotopes: ^{12}C and ^{13}C. The ratio of these two isotopes within wood is expressed in parts per thousand (‰) as:

$$\delta^{13}C = (R_{sample}/R_{standard} - 1)1000 \quad (1.2)$$

where R_{sample} and $R_{standard}$ are ratios of $^{13}C/^{12}C$ within the sample and the global standard, VPDB (McCarroll & Loader 2004). $\delta^{13}C$ values in wood are reflective of the rate of stomatal conductance, or more specifically, the rate of CO_2 diffusion through the stomatal opening and the rate of CO_2 carboxylation during photosynthesis. Stomatal conductance can be very sensitive to changes in temperature and humidity. Trees will close their stomata during high temperatures and dry

conditions to reduce water loss, but this prevents CO_2 diffusion into the leaf. With open stomata, ^{12}C would be preferentially taken in due to its mass. However, because there is a low internal concentration of CO_2 , the tree discriminates less between ^{12}C and ^{13}C during times of stomatal closure (McCaroll & Loader 2004). This means there will be a higher $\delta^{13}C$ signal in wood analyzed from drought years. In this way, drought years from decades ago can be identified and validated in tree ring chronologies, and their xylem anatomy examined.

1.5 The vascular tissue – phloem

Phloem is the tissue through which sugars produced through photosynthesis are transported from the sources to sinks throughout the tree (Van Bel 2003). Like the xylem, the phloem includes tube-like cells for transport. Unlike the xylem, the phloem cells which are used for transport (sieve tubes) are alive at maturity. This presents challenges to the study and observation of phloem transport, because the cells respond immediately to any damage which may occur as a consequence of manipulation. This has led to a lack of ability to validate hypotheses of phloem transport function (Knoblauch & Peters 2010). Though under-studied, understanding phloem physiology and its contribution to plant ecology can be critical to understand how plants respond to their environment (Savage et al. 2016). Luckily, the study of phloem is growing and new techniques are emerging to examine the phloem function in greater detail (Mullendore et al. 2015; Knoblauch et al. 2016).

Even though physiological measurements of the phloem are challenging, anatomical measurements can give useful insight into the function. Just like for the xylem, the Hagen-Poiseuille model can be used to infer potential changes in phloem flow. How drought stress impacts the phloem is a topic of recent interest. The exchange of water between the xylem and the

phloem suggests that drought stress would have impact on transport in both (Sevanto 2014, 2018). This is supported by observations of phloem structure that include changes in the size of sieve elements due to water stress, likely caused by a reduction in turgor pressure within the cells (Woodruff 2013; Dannoura et al. 2018). However, studies examining the impact of insect defoliation on the phloem have been lacking.

1.6 *Populus* as study species

The genus *Populus* contains around 30 species, comprising fast-growing trees with economic uses as sources for fuel, fiber, and lumber (Stettler et al. 1996). *Populus* species are considered early successional and can establish in ecologically disturbed areas; even the less drought tolerant cottonwood species can establish readily on disturbed sites given sufficient precipitation (Braatne et al. 1996). Trembling aspen (*P. tremuloides*) is also the most widespread tree species in North America (Peterson & Peterson 1992), and may provide understory forage for both livestock and wild ungulates (Rodgers 2017). However, massive declines of aspen due to drought have been documented in recent years (Worrall et al. 2008, 2013; Michaelian et al. 2011) which have likely been influenced in some areas by multi-year defoliation (Worrall et al. 2013). The species balsam poplar (*P. balsamifera*) has a similar range and attributes (Peterson & Peterson 1992). Like aspen, is also known to be defoliated by the forest tent caterpillar (Hogg & Schwarz 1999). These two species have clear risk for die-back or mortality due to both drought and insect defoliation. Being widespread species that are part of an economically and ecologically useful genus presents a strong motive to learn more about the impact of both drought and defoliation on their vascular structure and function. Understanding how both of these factors influence tree mortality is important for the future management of these species.

1.7 Research objectives

With the above information in mind, there exists an opportunity to determine unknown mechanisms of tree dieback and mortality that result from alterations in vascular tissue structure and function. The overall objectives of this research are to both discover structural changes resulting from drought and defoliation stress and to determine how the resulting functional changes may increase the vulnerability of trees to drought stress. These research aims will be achieved throughout the 3 data chapters, by experimentally inducing both drought and defoliation stress in trees, and by examining tree rings. Both aspen and balsam poplar will be used as research species when available.

1.8 Thesis organization

This thesis is organized into five chapters, three of which are research chapters. Chapter 1 provides a general introduction to the research described within this thesis. Chapters 2 through 4 describe each research project undertaken:

Beginning by experimentally inducing drought, the first data chapter of this thesis will investigate previously hypothesized drought-induced changes to xylem pit membrane structure to provide evidence for a mechanism of cavitation fatigue. The second data chapter of this thesis will broaden the scope of the research to discover unknown influences of drought and defoliation by examining changes to xylem vessels and fibers through the use of tree cores. Thirdly, based on conclusions of the second data chapter, the effects of defoliation on tree vascular function will be brought to the forefront by measuring hydraulic conductivity in defoliated trees and examining

both xylem and phloem structure. Along with these measurements of vascular tissue structure and function, potential mechanisms of tree mortality and dieback will be discussed.

Chapter 5 concludes this thesis and synthesizes the findings of this research. It highlights the novel findings and discusses how structural and functional alterations lead to trees with increased risk for drought-induced mortality.

1.9 References

Adams H.D., Zeppel M.J.B., Anderegg W.R.L., Hartmann H., Landhäusser S.M., Tissue D.T., …, McDowell N.G. (2017) A multi-species synthesis of physiological mechanisms in drought-induced tree mortality. *Nature Ecology & Evolution* 1: 1285-1291.

Allan C.D., Macalady A.K., Chenchouni H., Bachelet D., Mcdowell N., Vennetier M., ..., Cobb N. (2010) A global overview of drought and heat-induced tree mortality reveals emerging climate change risks for forests. *Forest Ecology and Management* 259: 660-684.

Anderegg W.R.L., Plavcová L., Anderegg L.D.L., Hacke U.G., Berry J.A. & Field C.B. (2013) Drought's legacy: Multiyear hydraulic deterioration underlies widespread aspen forest die-off and portends increased future risk. Global *Change Biology* 19:1188-1196.

Anderegg W.R.L. (2014) Spatial and temporal variation in plant hydraulic traits and their relevance for climate change impacts on vegetation. *New Phytologist* 205: 1008-1014.

Anderegg W.R.L., Flint A., Huang C., Flint L., Berry J.A., Davis F.W., Sperry J.S. & Field C.B. (2015a) Tree mortality predicted from drought-induced vascular damage. *Nature Geoscience* 8: 367-371.

Anderegg W.R.L., Hicke J.A., Fisher R.A., Allen C.D., Aukema J., Bentz B., …, Zeppel M. (2015b) Tree mortality from drought, insects, and their interactions in a changing climate. *New Phytologist* 208:674-683.

Anderegg W.R.L., Klein T., Bartlett M., Sack L., Pellegrini A.F.A., Choat B. & Jansen S. (2016) Meta-analysis reveals that hydraulic traits explain cross-species patterns of drought-induced tree mortality across the globe. *PNAS* 113: 5024-5029.

Arend M. & Fromm J. (2007) Seasonal change in the drought response of wood cell development in poplar. *Tree Physiology* 27: 985-992.

Beikircher B. & Mayr S. (2009) Intraspecific differences in drought tolerance and acclimation in hydraulics of *Ligustrum vulgare* and *Viburnum lantana*. *Tree Physiology* 29: 765-775.

Braatne J.H., Rood S.B. & Heilman P.E. (1996) Life history, ecology, and conservation of riparian cottonwoods in North America. In Biology of *Populus* (eds R.F Stettler, H.D. Bradshaw Jr., P.E. Heilman, & T.M. Hinckley), pp. 57-85. Ottawa: NRC Research Press.

Chen L., Huang J., Dawson A., Zhai L., Stadt K.J., Comeau P.G. & Whitehouse C. (2018) Contributions of insects and droughts to growth decline of trembling aspen mixed boreal forest of western Canada. *Global Change Biology* 24: 655-667.

Chen H.Y.H. & Luo Y. (2015) Net aboveground biomass declines of four major forest types with forest ageing and climate change in western Canada's boreal forests. *Global Change Biology* 21: 3675-3684.

Corcuera L., Camarero J.J. & Gil-Pelegrin E. (2004) Effects of a severe drought on *Quercus ilex* radial growth and xylem anatomy. *Trees* 16: 83-92.

Corcuera L., Cochard H., Gil-Pelegrin E., Notivol E. (2011) Phenotypic plasticity in mesic populations of *Pinus pinaster* improves resistance to xylem embolism (P_{50}) under severe drought. *Trees* 25: 1033-1042.

Dannoura M., Epron D., Desalme D., Massonnet C., Tsuji S., Plain C., Priault P., Gérant D. (2018) The impact of prolonged drought on phloem anatomy and phloem transport in young beech trees. *Tree Physiology,* https://doi.org/10.1093/treephys/tpy070

Eilmann B., Zweifel R., Buchmann N., Fonti P. & Rigling A. (2009) Drought-induced adaptation of xylem in Scots pine and pubescent oak. *Tree Physiology* 29: 1011-1020.

Evert R.F. (2006) Esau's Plant Anatomy: meristems, cells, and tissues of the plant body: their structure, function, and development (3rd ed.). Hoboken, NJ: Wiley-Interscience.

Fonti P., von Arx G., García-González I., Eilmann B., Sass-Klaassen U., Gärtner H., Eckstein D. (2010) Studying global change through investigation of the plastic responses of xylem anatomy in tree rings. *New Phytologist* 185:42-53.

Foster J.R. (2017) Xylem traits, leaf longevity and growth phenology predict growth and mortality response to defoliation in northern temperate forests. *Tree Physiology* 37: 1151-1165.

Hacke U.G., Stiller V., Sperry J.S., Pittermann J. & McCulloh K.A. (2001) Cavitation Fatigue. Embolism and refilling cycles can weaken the cavitation resistance of xylem. *Plant Physiology* 125: 779-786.

Hildahl V. & Reeks W.A. (1960) Outbreaks of the forest tent caterpillar, *Malacosoma disstria* Hbn., and their effects on stands of trembling aspen in Manitoba and Saskatchewan. *The Canadian Entomologist* 92: 199-209.

Hogg E.H. & Schwarz A.G. (1999) Tree-ring analysis of declining aspen stands in west-central Saskatchewan. Information Report Nor-X-359. Forestry Canada, Northern Forestry Centre, Edmonton, Alberta.

Huggett B.A., Savage J.A., Hao G., Preisser E.L., Holbrook N.M. (2018) Impact of hemlock woolly adelgid (*Adelges tsugae*) infestation on xylem structure and function and leaf physiology in eastern hemlock (*Tsuga canadensis*). *Functional Plant Biology* 45: 501-508.

Jones B., Tardif J. & Westwood R. (2004) Weekly xylem production in trembling aspen (*Populus tremuloides*) in response to artificial defoliation. *Canadian Journal of Botany* 82:590-597.

Knoblauch M. & Peters W.S (2010) Münch, morphology, microfluidics – our structural problem with the phloem. *Plant, Cell and Environment* 33: 1439- 1452.

Knoblauch M., Knoblauch J., Mullendore D.L., Savage J.A., Babst B.A., Beecher S.D., …, Holbrook N.M. (2016) Testing the Münch hypothesis of long distance phloem transport in plants. *eLife* 5.

Lens F., Tixier A., Cochard H., Sperry J.S., Jansen S. & Herbette S. (2013) Embolism resistance as a key mechanism to understand adaptive plant strategies. *Current Opinion in Plant Biology* 16: 287-292.

McCarroll D. & Loader N.J. (2004) Stable isotopes in tree rings. *Quaternary Science Reviews* 23: 771-801.

McDowell N., Pockman W.T., Allen C.D., Breshears D.D., Cobb N., Kolb T., ..., Yepez E.A. (2008) Mechanisms of plant survival and mortality during drought: why do some plants survive while others succumb to drought? *New Phytologist* 178: 719-739.

Man R. & Rice J.A. (2010) Response of aspen stands to forest tent caterpillar defoliation and subsequent overstory mortality in northeastern Ontario, Canada. *Forest Ecology and Management* 260: 1853-1860.

Michaelian M., Hogg E.H., Hall R.J. & Arsenault E. (2011) Massive mortality of aspen following severe drought along the southern edge of the Canadian boreal forest. *Global Change Biology* 17: 2084-2094.

Mullendore D.L., Froelich D.R., Beecher S., Ross-Elliott T.J., Knoblauch J. & Knoblauch M. (2015) Investigation of Structure-Function relationship of Long-Distance transport in plants: new imaging tools to answer old questions. *Microscopy and Microanalysis* 21:1491-1492.

Natural Resources Canada (2017) Statistical Data, Forests: https://cfs.nrcan.gc.ca/statsprofile.

Pan Y., Birdsey R.A., Fang J., Houghton R., Kauppi P.E., Kurz W.A., …, Hayes D. (2011) A large and persistent carbon sink in the world's forests. *Science* 333: 988-993.

Peng C., Ma Z., Lei X., Zhu Q., Chen H., Wang W., …, Zhou X. (2011) A drought-induced pervasive increase in tree mortality across Canada's boreal forests. *Nature Climate Change* 1: 467-471.

Peterson E.B. & Peterson N.M. (1992) Ecology, management, and use of aspen and balsam poplar in the Prairie Provinces. Special Report 1. Forestry Canada, Northern Forestry Centre, Edmonton, Alberta.

Plavcová L. & Hacke U.G. (2012) Phenotypic and developmental plasticity of xylem in hybrid poplar saplings subjected to experimental drought, nitrogen fertilization, and shading. *Journal of Experimental Botany* 63: 6481-6491.

Plavcová L., Hacke U.G., Almeida-Rodriguez A.M., Li E. & Douglas C.J. (2013) Gene expression patterns underlying changes in xylem structure and function in response to increased nitrogen availability in hybrid poplar. *Plant, Cell and Environment* 36: 186-199.

Pureswaran D., Roques A., Battisti A. (2018) Forest Insects and Climate Change. *Current Forestry Reports* 4: 35-50.

Rodgers P.C. (2017) Guide to Quaking Aspen Ecology and Management. BLM-UT-G1017-001-8000. Western Aspen Alliance, Utah State University, Logan, Utah.

Sala A., Piper F. & Hoch G. (2010) Physiological mechanisms of drought-induced tree mortality are far from being resolved. *New Phytologist* 186: 274-281.

Salleo S., Nardini A., Raimondo F., Assunta Lo Gullo M., Pace F., Giacomich P. (2003) Effects of defoliation caused by the leaf miner *Cameraria ohridella* on wood production and efficiency in *Aesculus hippocastanum* growing in north-eastern Italy. *Trees* 17: 367-375.

Savage J.A., Clearwater M.J., Haines D.F., Klein T., Mencuccini M., Sevanto S., Turgeon R. & Zhang C. (2016) Allocation, stress tolerance and carbon transport in plants: how does phloem physiology affect plant ecology. *Plant, Cell and Environment* 39: 709-725.

Schoonmaker A.L., Hacke U.G., Landhausser S.M., Lieffers V.J., Tyree M.T. (2010) Hydraulic acclimation to shading in boreal conifers of varying shade tolerance. *Plant, Cell and Environment* 33: 382-393.

Sevanto S., McDowell N.G., Dickman L.T., Pangle R. & Pockman W.T. (2014) How do trees die? A test of the hydraulic failure and carbon starvation hypotheses. *Plant, Cell and Environment*, 37, 153-161.

Sevanto S. (2014) Phloem transport and drought. *Journal of Experimental Botany* 65: 1751-1759.

Sevanto S. (2018) Drought impacts on phloem transport. *Current Opinion in Plant Biology* 43: 76-81.

Skelton R.P., West A.G. & Dawson T.E. (2015) Predicting plant vulnerability to drought in biodiverse regions using functional traits. *PNAS* 112: 5744-5749.

Sperry J.S. & Tyree M.T. (1988) Mechanism of water stress-induced xylem embolism. *Plant Physiology* 88: 581-587.

Sperry J.S. & Love D.M. (2015) What plant hydraulics can tell us about responses to climate-change droughts. *New Phytologist* 207: 14-17.

Settler R.F., Bradshaw Jr. H.D., Heilman P.E. & Hinckley T.M. (1996) Biology of *Populus* and its Implications for Management and Conservation. Ottawa: NRC Research Press.

Stiller V. & Sperry J.S. (2002) Cavitation fatigue and its reversal in sunflower (*Helianthus annuus* L.) *Journal of Experimental Botany* 53: 1155-1161.

Suarez M.L. & Kitzberger T. (2008) Recruitment patterns following a severe drought: long-term compositional shifts in Patagonian forests. *Canadian Journal of Forest Research*, 38, 3002-3010.

Tyree M.T. & Zimmerman M. (2002) Xylem Structure and the Ascent of Sap. Berlin: Springer Verlag.

Van Bel A.J.E. (2003) The phloem, a miracle of ingenuity. *Plant, Cell and Environment* 26: 125-149.

Weed A.S., Ayres M.P. & Hicke J. (2013) Consequences of climate change for biotic disturbances in North American forests. *Ecological Monographs* 83: 441-470.

Woodruff D.R. (2014) The impacts of water stress on phloem transport in Douglas-fir trees. *Tree Physiology* 34: 5-14.

Worrall J.J., Egeland L., Eager T., Mask R.A., Johnson E.W., Kemp P.A. & Shepperd W.D. (2008) Rapid mortality of *Populus tremuloides* in southwestern Colorado, USA. *Forest Ecology and Management* 255:686-696.

Worrall J.J., Rehfeldt G.E., Hamann A., Hogg E.H., Marchetti S.B., Michaelian M. & Gray L.K. (2013) Recent declines of *Populus tremuloides* in North America linked to climate. *Forest Ecology and Management* 299: 35-51.

2 Drought-induced xylem pit membrane damage in aspen and balsam poplar

2.1 Summary

Drought induces an increase in a tree's vulnerability to a loss of its hydraulic conductivity in many tree species, including two common in western Canada, trembling aspen (*Populus tremuloides*) and balsam poplar (*Populus balsamifera*). Termed "cavitation fatigue" or "air-seeding fatigue", the mechanism of this phenomenon is not well understood, but hypothesized to be a result of damage to xylem pit membranes. To examine the validity of this hypothesis, the effect of drought on the porosity of pit membranes in aspen and balsam poplar was investigated. Controlled drought and bench dehydration treatments were used to induce fatigue in aspen and balsam poplar and scanning electron microscopy (SEM) was used to image pit membranes for relative porosity evaluations from air-dried samples after ethanol dehydration. A significant increase in the diameter of the largest pore was found in the drought and dehydration treatments of aspen, while an increase in the percentage of porous pit membranes was found in the dehydration treatments of both species. Additionally, the location of the largest pore per pit membrane was observed to tend toward the periphery of the membrane.

2.2 Introduction

Around the world, major forest die-back events have been linked with episodes of drought and high temperatures (Allan et al. 2010). This has been evident in western Canada, where a severe drought during 2001-2002 caused massive mortality in the aspen parkland and adjacent boreal forest eco-regions (Michaelian et al. 2011), regions where tree growth and productivity is limited

by moisture (Hogg et. al. 2008). The degree of die-back in western Canada is particularly concerning because climate models predict that there will be an expansion of the drier prairie climate (Mbogga et al. 2009) and a northward shift in the ecosystem suitability for aspen (Worrall et al. 2013), the most widespread tree species in North America. Thus, the ability to predict the impact of climate change and severity of die-back due to drought has emerged as an essential topic for future forest management. However, our understanding of the complex physiological process of tree death is limited. During drought, trees may experience impaired hydraulics, reduced carbon uptake, and diminished defenses against insect attacks (McDowell et al. 2008), all which may contribute to the ultimate death of a tree. In order to advance our understanding of tree death, it is necessary to first understand the influence of each of these processes.

We focus here on the impact of drought on a tree's hydraulic structure and function. Water moves through the xylem down a gradient in negative pressure driven by transpiration at the leaf surface. At these pressures, the liquid state of water is meta-stable in the xylem and transport can be disrupted by the process of air-seeding, which involves cavitation and subsequent embolism formation inside a xylem conduit (Lens et al. 2013). During the progression of a drought, pressures in the xylem become increasingly negative and air-seeding events leading to embolism become more frequent. Moreover, after a cycle of drought and subsequent refilling of embolised xylem vessels, the resistance of xylem to embolism formation is weakened in some species (Hacke et al. 2001; Stiller & Sperry 2002; Anderegg et al. 2013). Known in the literature as "cavitation fatigue", this phenomenon will be referred to as "air-seeding fatigue" in this manuscript.

Air-seeding fatigue is characterized by an increase in percent loss of hydraulic conductivity (PLC) at the least negative xylem pressures. Although trees produce new xylem each year, this hydraulic impairment may have lasting effects. A severe drought in Colorado led to massive aspen

mortality which continued multiple years after the initial drought. This die-back was termed Sudden Aspen Decline (SAD) due to its rapid progression (Worrall et al. 2010). Physiological measurements found that trees affected by SAD exhibited fatigue eight years after the drought event, suggesting that these trees have some reliance on older xylem and may be at increased risk for mortality in future drought events (Anderegg et al. 2013).

The mechanism of air-seeding fatigue is not well understood, but it has been hypothesized that drought may cause damage to xylem structural features known as inter-vessel pit membranes (Hacke et al. 2001; Stiller & Sperry 2002). Pit membranes are a feature of bordered pits which line the xylem cell walls and connect adjacent conduits to allow lateral water movement between them. Layers of cellulose microfibrils and possibly, components of unknown chemistry (Lee et al. 2012), act as a filter that is porous for water movement, but also function to block air entry from embolised conduits into functional, water-filled conduits. However, the "air-seeding hypothesis" predicts that air enters xylem conduits through pores in the cell wall (Zimmerman 1983) and since the largest pores in the cell walls appear to exist in the inter-vessel pit membranes, this should be the primary place for air-seeding (Sperry & Tyree 1988). Surface tension holds the air-water meniscus at pores in the pit membrane until the pressure difference between adjacent embolised and water-filled xylem conduits exceeds a critical pressure difference ΔP, leading to air-entry into the functional conduit. This mechanism can be predicted with the equation:

$$\Delta P = \frac{4T\cos\propto}{D} \tag{2.1}$$

where D is the diameter of the largest pore in the pit membrane at which the air-water interface exists, T is the surface tension of the xylem sap , and α is the contact angle between xylem sap and

the pit membrane, assumed to be 0 with total contact. Based on the thickness of the pit membrane, a correction factor (κ) may also be added to the equation to account for pore shape (Schenk et al. 2015). As a mechanism for fatigue, it is hypothesized that repeated flexing of the membrane may cause loosening or rupturing of membrane microfibrils leading to larger pores, and thus, increased air-seeding at smaller pressures differences (Hacke et al. 2001). However, experimental evidence observing changes in pit membrane porosity due to drought has been lacking.

If damage to pit membranes occurs because of residual strain or rupture due to pit membrane flexing during drought, it may be related to the primary location of air-seeding in the membrane. Experimental evidence has suggested that a larger deflection ability of the membrane is associated with increased porosity (Choat et al. 2004) and pit membrane behavior modelling suggests that before air-seeding occurs, the pit membrane may aspirate against the pit border (Fig. 2.1a) leaving only the center of the membrane to experience strain or deformation at increasingly negative pressures (Sperry & Hacke 2004; Tixier et al. 2014). Following this prediction, we might expect to observe a higher percentage of pores arising in the center of the pit membrane if pit membrane damage is influencing air-seeding fatigue. Alternatively, the membrane may be moderately deflected (Fig. 2.1b). However, assuming that the membrane has uniform thickness, as in most angiosperms, maximum strain causing air-seeding would still be expected to be in the middle of the membrane (Tixier et al. 2014). Still, in angiosperm species, it has been observed that large pores of several hundred nanometers in diameter tend to occur toward the periphery of the membrane (Sano 2005). As the mechanism of air-seeding fatigue is still not fully understood, quantifying the location of large pores in the pit membranes would advance the knowledge on this topic.

In this study, we employed scanning electron microscopy (SEM) to view pit membranes. SEM allows a detailed observation of the pit membrane surface and has been a useful tool in past research linking pit membrane porosity with air-seeding pressures across species (Jansen et al. 2009; Lens et al. 2011) as well as in experimental shading treatments (Plavcova et al. 2011). However, there are valid concerns about experimental artefacts arising from SEM sample preparation (Jansen et al. 2008; Plavcova et al. 2011) and these were addressed as much as possible in the methodology (See Discussion).

The main objective of this study was to test the hypothesis that pit membrane damage may be caused by drought in trees experiencing air-seeding fatigue. Here we studied the phenomenon in trembling aspen (*Populus tremuloides*) and the co-occurring species balsam poplar (*P. balsamifera*). We hypothesized that pit membranes of trees exhibiting air-seeding fatigue will be more porous, providing evidence supporting pit membrane damage as a mechanism for the phenomenon. To address and describe changes in porosity, we ask (1) does the percentage of visibly porous pit membranes increase in trees exhibiting fatigue? And (2) does the diameter of the largest pore (D_{max}) in visibly porous membranes increase in trees exhibiting fatigue? Finally we observe and quantify the location of the largest pores in the pit membranes.

2.3 Materials and Methods

Plant material and experimental design

Drought experiments to induce air-seeding fatigue were carried out on seedlings of aspen and balsam poplar in the greenhouse. Aspen plants were grown in March 2014 from seed collected in Edmonton, AB in 2010 and balsam poplars were grown from branch cuttings from at least 8 separate trees, collected in the North Saskatchewan River valley (53º31′40″N, 113º30′45″W) in

May 2014. Both species were established and maintained in a peat-based soil (Sunshine Mix #4, Sun Gro Horticulture, Agawam, MA, USA). For the first month, seedlings were kept in Styrofoam planting trays and fertilized once a week with a 1 g/L solution of a high phosphorus fertilizer, 10:52:10 N:P:K, to promote growth. After establishment, seedlings were transplanted to 3 L round pots and the fertilizer was adjusted to a 20:20:20 N:P:K solution. Climate conditions in the greenhouse were semi-controlled with daily ambient temperatures ranging from 17 – 29ºC and a relative humidly ranging from 21– 32%.

In July 2014, after 4 months of growth, aspen trees were randomly assigned to two treatments: to be drought stressed or well-watered controls. Drought stress was induced by completely withholding water for the duration of the drought. Balsam poplar trees were randomly assigned to the same treatments after 4 months of growth in September 2014. The droughts took place over the course of a month and control trees of both species were harvested throughout the duration of the experimental droughts. Aspen and balsam poplar experiencing drought were harvested for measurements after they reached a target stem water potential of at least -1.9 MPa and -1.7 MPa, respectively. These pressures were determined pre-treatment to correspond to 50% loss of hydraulic conductivity (P50) in each species and chosen because preliminary experimentation indicated that soon after reaching the P50, the leaves on the seedlings withered, preventing water potential measurements. Stem water potential was monitored daily by excising a leaf that had been covered by aluminum tape overnight to prevent transpiration and immediately placing it in a pressure chamber (Model 1000, PMS Instrument Company, Albany, OR, USA). The water potential was recorded as the internal chamber pressure required for xylem sap to extrude from the leaf petiole.

During a second set of experiments, branches from trees of the same species were harvested from the North Saskatchewan River valley, downslope of the University of Alberta (53º31′40″N, 113º30′45″W). This was done to determine if the greenhouse drought treatments were representative of the effect of drought on xylem pit membranes in the field. Six 'field aspen' and six 'field balsam poplar' trees were selected with individuals of the same species at least 10 m apart. Midday leaf water potentials were recorded for each tree. In early August 2015, sun-exposed branches 3-7 years old and between 1 and 4 meters high were harvested from both species over the period of a week for hydraulic conductivity measurements. Though conditions in the summer were very dry, it was assessed via conductivity measurements that the field trees did not exhibit the increased vulnerability to a loss of hydraulic conductivity associated with air-seeding fatigue. Therefore, branches from several trees were harvested again for bench dehydration to simulate a drought and induce fatigue for another experimental replication of drought within the species studied. These branches of both species were collected throughout the duration of another week. Branches were allowed to dehydrate overnight for at least 12 hours. Leaves were covered again with aluminum tape and stem water potentials for all branches were < -3.5 MPa after dehydration, corresponding to complete embolism in these species. The exact values could not be determined because the required balancing pressure exceeded the specifications of the pressure chamber used (Model 600D, PMS Instrument Company, Albany, OR, USA). Finally, hydraulic conductivity measurements for these branches were made.

Hydraulic conductivity

All treatments were harvested for hydraulic conductivity (K_h) measurements. Sample segments consisted of stems (greenhouse trees) and branches (field trees). Multiple cuts were made

under water at each end of the segment until a segment 14.2 cm long was produced. A section distal from the final segment was saved and refrigerated for scanning electron microscopy (SEM). K_h was measured with a flow-balance system and recorded by computer software as bulk flow divided by the pressure gradient (Sperry et al. 1988). The system was filled with a measuring solution of 20mM KCl and 1mM $CaCl_2$ in distilled, filtered (0.2 μm) water. Following measurements of native K_h, segments were submerged in the measuring solution for vacuum infiltration to remove embolism for at least 1 hour. Subsequently, the maximum conductivity of the segments was measured. Each segment was spun to increasingly negative pressures using the standard centrifuge method (Alder et al. 1997; Hacke et al. 2015). At each pressure K_h was measured and recorded. The K_h values were converted into percent loss of conductivity (PLC) from their maximum, and then averaged for each treatment per experiment to create vulnerability curves. Additionally, K_h values were normalized by xylem area to compare specific conductivity (K_s), which indicated the effectiveness of the vacuum infiltration at removing embolism. Drought-stressed and dehydrated segments were discarded if their maximum K_s values did not reach the range of control segment values to ensure vulnerability curve measurements began with embolism fully removed from the segments.

Scanning electron microscopy

Refrigerated samples were cut to 1.5 cm segments and rehydrated in water for 1 day. Samples were prepared following the procedure from Plavcova et al. (2011) in which samples were sequentially dehydrated through an ethanol series, air-dried, and split longitudinally with a razor blade acting as a wedge. The imaging of samples was completed with field-emission scanning electron microscopes: a JEOL 6301F (greenhouse trees) and a Zeiss Sigma 300 VP (field

trees) with accelerating voltages of 2kV and 1kV, respectively. Approximately 3.25 hours were spent imaging pit membranes from 2-4 trees per each treatment within each experiment. The total number of imaged pits (n) per treatment reflects the ease of locating pit membranes during the time allotted, but was standardized such that the same total number of images was collected for each treatment within each experiment. Within field trees, the imaging was restricted to the longitudinal edges of the section in order to capture xylem from the current year.

Not all imaged pit membranes contained resolvable pores. Within visibly porous pit membranes, the diameter of the largest pore (D_{max}) was estimated from its area using image analysis software (ImagePro Premier, Media Cybernetics, Rockville, MD, USA). Additionally, the radius of each pit membrane and the distances from the center of the largest pore to the edge of each pit membrane were recorded. This distance calculation allowed a categorization of the pore as located within the periphery of the membrane (less than half the radius) or within the center of the membrane (more than half the radius). From the total number of pit membranes imaged, 22 were omitted from the distance calculation because a partial covering of the membrane by the pit border prevented an accurate measurement of the membrane radius. For further understanding of the relation between D_{max} and its location, pores were divided into categories based on size. Pores with a diameter greater than 0.3 μm were considered exceptionally large, as they were relatively rare in occurrence and resembled the large, peripheral pit membrane pores observed by Sano (2005). Smaller pores were divided into two more categories with pore diameters between 0.1 – 0.3 μm and < 0.1 μm.

Statistical Analysis

Calculations were performed using the statistical software package R 3.2.1 (R Core Team 2015, Vienna, Austria). Hydraulic conductivity was compared between control and drought-stressed or dehydrated trees along the length of the vulnerability curves. 95% confidence intervals were calculated to establish differences between the mean conductivities along the curves at each xylem pressure where conductivity was measured. Pit membrane porosity was statistically evaluated in two ways. The pit membrane data for each experiment was evaluated for significant changes in the number of visibly porous pit membranes between treatments. For this analysis, pit membranes in each treatment were divided into two categories: porous or non-porous. This categorical data was analyzed with a z test of proportions (Agresti, 1990). Additionally, the mean D_{max} in visibly porous membranes was analyzed for significant differences between treatments in all experiments via a two-sample Student's t test. The data for each treatment was transformed to meet the assumptions of normality by an inverse transformation of the datasets prior to the test.

2.4 Results

Air-seeding fatigue

Drought and bench dehydration treatments exhibited increases in the loss of hydraulic conductivity associated with air-seeding fatigue and revealed a connection between the degree of fatigue and the degree of water stress experienced by the tree. The vulnerability curves of drought-stressed, greenhouse-grown aspen and balsam poplar (open symbols, Fig. 2.2a-b) showed evidence of air-seeding fatigue with an immediate increase in PLC at the least negative pressures. In contrast to the sigmoidal shape of the control treatment curves, the drought treatment curves lost conductivity more steadily as xylem pressures became more negative; 95% confidence intervals were lower in the control treatments than in drought-stressed treatments at -0.5 or -1.0 MPa for

both greenhouse experiments. However, the drought treatment curves converged back with the control curves, reaching the same loss in conductivity near the stem water potentials to which the drought-stressed seedlings were subjected (arrows, Fig. 2.2a-b).

The initial hydraulic conductivity measurements of the field trees were designated the control treatment because despite dry conditions in the summer of 2015, air-seeding fatigue was not observed (solid symbols, Fig. 2.2c-d). Measured midday leaf water potentials of field trees averaged -1.7 MPa and -1.3 MPa in aspen and balsam poplar, respectively, which did not meet or exceed the P50 value of their control vulnerability curves (Table 2.S1). The dehydration treatments stressed the branches of the field trees to water potentials < -3.5 MPa, and, in turn, the vulnerability curves of the dehydration treatments displayed an increase in PLC throughout the curve. 95% confidence intervals only overlapped at distant points of the vulnerability curves in field trees: -3 and -3.5 MPa in field aspen and -0.5 in field balsam poplar (Fig. 2.2c-d).

Aspen vulnerability curves exhibited greater plasticity than balsam poplar. This is apparent when comparing the curves of controls from the greenhouse and the field within species. Field-grown aspen branches exhibited more resistant xylem; the curve was less steep than the curve of greenhouse-grown aspen stems and P50 values between them differed by 0.6 MPa (closed symbols in Fig. 2.2a, c; Table 2.S1). By contrast, the curves of balsam poplar controls were relatively indistinguishable and their P50 values differed only by 0.1 MPa (compare closed symbols in Fig. 2.2b, d; Table 2.S1). Greater plasticity of aspen is also apparent when comparing the P50 values between the control and dehydration curves from the field-grown branches within each experiment (Table 2.S1); the P50 of field aspen differed by 1.2 MPa between treatments, while field balsam poplar differed only by 0.6 MPa between the control and dehydration treatment.

Maximum specific conductivity values (K_s) between treatments were unchanged. 95% confidence intervals overlapped at 0 PLC in all experiments (Fig. 2.3), suggesting that the vacuum infiltration was effective in removing embolism in these treatments.

Pit membrane porosity

Scanning electron microscopy revealed a wide variation in pit membrane porosity within and between treatments (Figs. 2.4-2.5, 2.S1-2.S2). Non-porous membranes were most common (Figs. 2.4a-b, 2.5a) while porous pit membranes varied both in pore size and in the distribution of pores within the membrane. Variations in membrane texture were also present within samples from the same treatments (Fig. 2.5a, e). While most membrane pores were less than 0.1 μm in diameter, occasionally exceptionally large pores were observed (Figs. 2.4c-d, 2.S1d, 2.S2d). Both non-porous and porous membranes were found in all treatments. However, the proportions of porous pit membranes were not significantly different between treatments for aspen or balsam poplar in the greenhouse experiments; the z test of proportions was not calculated for the aspen as both the control and drought treatments contained the same proportion of porous pit membranes (Table 2.1). In contrast, for both species in the field experiments, the proportion of porous pit membranes was significantly larger in the dehydration treatments than in the control (Table 2.1). It is notable that non-stressed field-grown trees had a low fraction of porous membranes (16.7% and 11.9% for aspen and balsam poplar, respectively). By contrast, well-watered greenhouse controls already had 33.3% and 53.3% porous membranes.

The diameter of the largest membrane pore (D_{max}) showed substantial variation across treatments in all experiments (Fig. 2.6a-d, Table 2.1). In the greenhouse aspen experiment, the mean D_{max} was significantly larger in the drought treatment (Table 2.1). This was not the case for

the greenhouse balsam poplar experiment; however, like aspen, the variance of D_{max} was increased in balsam poplar experimental drought treatment (Fig. 2.6a-b). In the field aspen experiment, the mean D_{max} was significantly larger in the dehydration treatment, but again there was no significant difference in D_{max} between the balsam poplar control and dehydration treatments (Table 2.1). Although the mean D_{max} in the drought and dehydration treatments of balsam poplar did not differ significantly from the control treatments, the general trends of the treatment distributions were similar across all experiments. As illustrated by Fig. 2.6, the interquartile range, a measure of variability, was 2-22 times larger in the drought and dehydration treatments. And, in all but one case, the median of D_{max} was also increased in the drought and dehydration treatments (Fig. 2.6a-d).

While many pit membranes contained a multitude of pores and were partially or uniformly porous, the largest pore within each porous pit membrane was examined for its location. Fig. 2.7 shows the number of pores per size class in either the periphery or center of the membrane for each experiment regardless of treatment applied. Larger pores tended to occur in the periphery of the membrane. This was especially apparent in greenhouse experiments (Fig. 2.7a-b). In the greenhouse-grown aspen, none of the largest pores were located in center of the membrane, while pores of all size classes were found in the periphery (Fig. 2.7a). Pores in the largest size category (> 0.3 μm) were exclusively found in the periphery of the membrane. Pores in the second-largest category, with diameters between 0.3 and 0.1 μm, were also restricted to the periphery, with the exception of field balsam poplar (Fig. 2.7d). Most pores were less than 0.1 μm in diameter and their location was more evenly distributed (Fig. 2.7).

2.5 Discussion

Our imaging of pit membranes with SEM for aspen and balsam poplar documents increases in pit membrane porosity due to both controlled drought and bench dehydration. Though some pores were very large, the numerous visible pores we observed in both species are in agreement with previous SEM imaging of *Populus* species (Plavcova et al. 2011; Sperry et al. 1991). Within the experiments performed, significant increases in porosity for drought-stressed and dehydrated trees were found both by evaluating (1) the number of porous pit membranes and (2) the diameter of the largest pore in visibly porous pit membranes. Aspen and balsam poplar were chosen for these experiments due to their widespread distribution in North America, and because the pit membranes of *Populus* species have relatively large pores (Jansen et al. 2009; Plavcova et al. 2011). In our evaluation of pit membrane porosity, we focused on the largest pore per pit membrane because according to the air-seeding hypothesis, the largest pore would be the first to permit air-seeding when exposed to an air-water interface (Zimmerman 1983; Sperry & Tyree 1988).

Pit membrane porosity

The significant increases in the diameter of the largest pore in the drought and dehydration treatments of aspen, and an observed similar trend in greenhouse-grown balsam poplar (Fig. 2.6, Table 2.1) support an increase in pore size as a mechanism for air-seeding fatigue. These results agree with previous work where pit membrane pore diameter has been linked with air-seeding pressure (Jarbeau et al. 1995; Jansen et al. 2009; Lens et al. 2011).

Aside from the trend for increased pore size in drought and dehydration treatments relative to controls, there were two other trends that deserve discussion. First, consistent with the observed greater xylem vulnerability of balsam poplar, the D_{max} of control plants was larger in balsam poplar

than in aspen. This was the case in greenhouse plants and in branches collected from the field (Table 2.1). Second, we observed differences in membrane structure depending on the growing conditions (i.e., greenhouse *versus* field). In the present study, the D_{max} of drought-stressed greenhouse samples was ~2-fold larger than the D_{max} of dehydrated branches from field-grown trees (Table 2.1) within each species, despite the fact that dehydrated branches experienced more negative xylem pressures and greater embolism levels than greenhouse samples.

Controls in the greenhouse experiment were kept well-watered and received adequate levels of fertilizer while trees growing in the river valley likely experienced variable growing conditions and more negative water potentials. It is conceivable that these differences in growing conditions (particularly in water potential) and may have influenced pit membrane structure, especially pit membrane thickness. Although pit membrane thickness was not measured, the greenhouse-grown seedlings of both species appeared to have thinner membranes which would correlate with increased porosity (Jansen et al. 2009) and decreased embolism resistance (Lens et al. 2011; Scholz et al. 2013; Li et al. 2016). Our results would also be consistent with balsam poplar having thinner membranes than aspen. Likewise, environmental conditions appear to have also influenced the number of pit membranes which were visibly porous. The fact that we found significant differences in the fraction of porous membranes in field-grown trees, but not in greenhouse-grown plants, appears to be due to the low fraction of porous membranes in field controls. Even well-watered greenhouse samples, by contrast, had a relatively high fraction of porous membranes, and these fractions did not increase further in response to the drought treatment, though the average D_{max} was increased (Table 2.1).

Scanning electron microscopy

SEM is a useful tool for observing pit membrane pores; however, we caution that the viewing of pit membranes with SEM may overestimate their porosity. While some studies have been unable to locate expected pore sizes with SEM (Shane et al. 2000; Choat et. al. 2003), there is still concern that exceptionally large pores could be artifacts of SEM preparation; some protocols have been known to increase porosity, and air-drying of samples has been recommended (Jansen et al. 2008). However, in poplar, an ethanol dehydration series before air-drying samples yielded pit membranes with pores that were significantly smaller than in samples which were air-dried directly from water immersion (Plavcova et al. 2011). The effect of sample preparation may vary by species, and with this evidence ethanol dehydration was used to minimize the occurrence of artificially enlarged pores in this study. Viewing of pit membranes with atomic force microscopy (AFM) has also cautioned that air-dried pit membranes may be reduced in thickness and have a more compact microfibrillar structure (Pesacreta et al. 2005), complicating the study of pit membrane surface features. Though artifacts from SEM preparation may be difficult to prevent whatever the method, at the very least, measurements of pit membrane pore size provide an estimation of the relative porosity between and among species. It is also possible that large pores in pit membranes represent developmental irregularities or actual physical damage which contribute to air-seeding, and therefore should be included in analysis of pit membrane porosity (Plavcova et al. 2013).

Location of the largest pores

All of the pores in the largest size category (>3 μm) were located in the periphery of the membrane (Fig. 2.7). This result is consistent with previous observations of large pores (Sano 2005; Sano & Jansen 2006). The locations of the largest pores per pit membrane for both

treatments in each experiment were combined, as there appeared to be no impact of the treatments on the location of the largest pore (Fig. 2.S3). Moreover, the presence of these exceptionally large pores in both the control and drought treatments (Figs. 2.4c-d, 2.S1d, 2.S2d) indicates that some instances of large pores may be developmental. Though the exact size of the pore may be altered in SEM imaging, these observations are consistent with the idea that there are rare large pores that contribute to air-seeding in non-stressed plants (Wheeler et al. 2005; Choat et al. 2008). If they are actually the result of damage to the membrane periphery, the mechanism remains unclear. Although, the recently discussed idea of "nano-bubbles" existing within the xylem vessels suggests that the breakup of expanding bubbles within the pit chamber would create a large pressure wave (Schenk et al. 2015). It seems possible that bubble expansion and break-up could cause damage to the periphery of the membrane.

Whether or not these pores are developmental or drought-induced, pores in the periphery would be unlikely to cause an increase in air-seeding if the pit membrane is already sealed against the pit border when pressures permitting air-seeding occur (Sperry & Hacke 2004; Tixier et al. 2014). The situation may be similar to aspirated torus-margo pits in gymnosperms where the large pores of the margo are sealed by the pit border (Hacke et al. 2004). Though examining the location of the largest pores did not provide support for an increase in their abundance in the center of the membrane, this does not preclude the possibility that pores in the center of the pit membrane influence air-seeding fatigue. Visible pores frequently occurred in the center of the membrane (Figs. 2.4, Fig. 2.5). In some cases (e.g., Fig. 2.4f, Fig. 2.5f) there was a line of pores in the center of the membrane, suggesting that pores were created by mechanical stress. These 'line pores' were noticed in branches from field-grown trees, and in all but one case out of 16, they were observed in the dehydration treatments. Though these were observed only a few times, the fact that they

were almost always observed in the dehydration treatment is consistent with the air-seeding mechanism outlined in Fig. 2.1a.

Vulnerability curve shape changes

The vulnerability curves of fatigued samples differed from the curves of controls in a manner that reflects the degree of water stress samples experienced. Similar findings were reported by Hacke et al. (2001) and Stiller and Sperry (2002). In this study, the drought-stressed greenhouse-grown trees experienced more moderate stress (less negative water potentials) than what was experienced by the dehydrated branches collected from the field. Moreover, the greenhouse-grown trees exhibited drought-stressed vulnerability curves which converged with the control curves. The convergence of the vulnerability curves in these trees could be explained by the proportion of pit membranes damaged by the drought treatment. Because the trees in the greenhouse drought treatments were harvested just after reaching 50% PLC, potentially there were a proportion of xylem vessels and their associated pit membranes which did not experience embolism. These pit membranes would not have been damaged and, in turn, the pressure difference required for air-seeding would be unchanged in those pit membranes, leading to the absence of air-seeding fatigue at the water potentials more negative than the harvest value.

Our results are consistent with the idea that this pit membrane damage is irreversible. Previous studies have suggested irreversible damage by observing multi-year air-seeding fatigue in aspen (Anderegg et al. 2013) and by modeling behavior of pit membrane flexing in angiosperm species, where it is suggested that pit membranes experience residual plastic strains that lead to structural damage during air-seeding (Tixier et al. 2014). The observed porosity in this study is

also consistent with observations of pit membrane degradation in older xylem of aspen (Sperry et al. 1991).

2.6 Conclusions

This study indicates that controlled drought and bench dehydration treatments result in increased porosity in the xylem pit membranes of aspen and balsam poplar as viewed by SEM. Resulting drought-induced increases in the diameter of the largest pores in the pit membranes and drought-induced increases in the percentage of visibly porous pit membranes suggest a reduction in the pressures required for air-seeding across these membranes and a possible mechanism for air-seeding fatigue. Moreover, the degree of fatigue exhibited by stressed trees was observed to change based on the most negative water potential experienced by the samples, implying a relationship between the proportion of pit membranes damaged and air-seeding fatigue. Pit membrane pores observed with SEM suggest that this damage may be irreversible and detrimental to the future health and productivity of drought-stressed trees. It remains unclear how this damage to the membrane occurs, however as we learn more about pit membrane ultrastructure and pit membrane changes in response to drought, this research will be advanced. At a forest stand level, future species-specific investigations into xylem changes due to drought will improve our knowledge of the process of tree death and further the ability to predict tree-dieback

2.7 References

Agresti A. (1990) Categorical Data Analyses. New York: John Wiley & Sons.

Alder N.N., Pockman W.T., Sperry J.S. & Nuismer S. (1997) Use of centrifugal force in the study of xylem cavitation. *Journal of Experimental Botany* 48: 665-674.

Allan C.D., Macalady A.K., Chenchouni H., Bachelet D., Mcdowell N., Vennetier M., ..., Cobb N. (2010) A global overview of drought and heat-induced tree mortality reveals emerging climate change risks for forests. *Forest Ecology and Management* 259: 660-684.

Anderegg W.R.L., Plavcova L., Anderegg L.D.L., Hacke U.G., Berry J.A. & Field C.B. (2013) Drought's legacy: multiyear hydraulic deterioration underlies widespread aspen forest die-off and portends increased future risk. *Global Change Biology* 19: 1188-1196.

Choat B., Ball M., Luly J. & Holtum J. (2003) Pit membrane porosity and water stress-induced cavitation in four co-existing dry rainforest tree species. *Plant Physiology* 131: 41-48.

Choat B., Cobb A.R. & Jansen S. (2008) Structure and function of bordered pits: new discoveries and impacts on whole-plant hydraulic function. *New Phytologist* 177: 608-626.

Choat B., Jansen S., Zwieniecki M.A., Smets E. & Holbrook N.M. (2004) Changes in pit membrane porosity due to deflection and stretching: the role of vestured pits. *Journal of Experimental Botany* 55: 1569-1575.

Hacke U.G., Sperry J.S. & Pittermann J. (2004) Analysis of circular bordered pit function II. Gymnosperm tracheids with torus-margo pit membranes. *American Journal of Botany* 91: 386-400.

Hacke U.G., Stiller V., Sperry J.S., Pittermann J. & McCulloh K.A. (2001) Cavitation Fatigue. Embolism and refilling cycles can weaken the cavitation resistance of xylem. *Plant Physiology* 125: 779-786.

Hacke U.G., Venturas M.D., MacKinnon E.D., Jacobsen A.L., Sperry J.S & Pratt R.B. (2015) The standard centrifuge method accurately measures vulnerability curves of long-vesselled olive stems. *New Phytologist* 205: 116-127.

Hogg E.H., Brandt J.P. & Michaelian M. (2008) Impacts of a regional drought on the productivity, dieback, and biomass of western Canadian aspen forests. *Canadian Journal of Forest Research* 38: 1373-1384.

Jansen S., Choat B. & Pletsers A. (2009) Morphological variation of intervessel pit membranes and implications to xylem function in angiosperms. *American Journal of Botany* 96: 409-419.

Jansen S., Pletsers A. & Sano Y. (2008) The effect of preparation techniques on SEM-imaging of pit membranes. *IAWA Journal* 29: 161-178.

Jarbeau J.A., Ewers F.W. & Davis S.D. (1995) The mechanism of water-stress-induced embolism in two species of chaparral shrubs. *Plant, Cell and Environment* 18: 189-196.

Lee J., Holbrook N.M. & Zwieniecki M. A. (2012) Ion induced changes in the structure of bordered pit membranes. *Frontiers in Plant Science* 3: 55.

Lens F., Sperry J.S., Christman M.A., Choat B., Rabaey D. & Jansen S. (2011) Testing hypotheses that link wood anatomy to cavitation resistance and hydraulic conductivity in the genus *Acer*. *New Phytologist* 190: 709-723.

Lens F., Tixier A., Cochard H., Sperry J.S., Jansen S. & Herbette S. (2013) Embolism resistance as a key mechanism to understand adaptive plant strategies. *Current Opinion in Plant Biology* 16: 287-292.

Li S., Lens F., Espino S., Karimi Z., Klepsch M., Schenk H.J., …, Jansen S. (2016) Intervessel pit membrane thickness as a key determinant of embolism resistance in angiosperm xylem. *IAWA Journal* 37: 152-171.

Mbogga M.S., Hamann A. & Wang T. (2009) Historical and projected climate data for natural resource management in western Canada. *Agricultural and Forest Meteorology* 149: 881-890.

McDowell N., Pockman W.T., Allen C.D., Breshears D.D., Cobb N., Kolb T., ..., Yepez E.A. (2008) Mechanisms of plant survival and mortality during drought: why do some plants survive while others succumb to drought? *New Phytologist* 178: 719-739.

Michaelian M., Hogg E.H., Hall R.J. & Arsenault E. (2011) Massive mortality of aspen following severe drought along the southern edge of the Canadian boreal forest. *Global Change Biology* 17: 2084-2094.

Pesacreta T.C., Groom L.H. & Rials T.G. (2005) Atomic force microscopy of the intervessel pit membrane in the stem of *Sapium sebiferum* (Euphorbiaceae). *IAWA Journal* 26: 397-426.

Plavcova L., Hacke U.G. & Sperry J.S. (2011) Linking irradiance-induced changes in pit membrane ultrastructure with xylem vulnerability to cavitation. *Plant, Cell and Environment* 34: 501-513.

Plavcova L., Jansen S., Klepsch M. & Hacke U.G. (2013) Nobody's perfect: can irregularities in pit structure influence vulnerability to cavitation? *Frontiers in Plant Science* 4: 453.

Sano Y. (2005) Inter- and intraspecific structural variations among intervascular pit membranes, as revealed by field-emission scanning electron microscopy. *American Journal of Botany* 92: 1077-1084.

Sano Y. & Jansen S. (2006) Perforated pit membranes in imperforate tracheary elements of some angiosperms. *Annals of Botany* 97: 1045-1053.

Schenk H.J., Steppe K. & Jansen S. (2015) Nanobubbles: a new paradigm for air-seeding in xylem. *Trends in Plant Science* 20: 199-205.

Scholz A., Rabaey D., Stein A., Cochard H., Smets E. & Jansen S. (2013) The evolution and function of vessel and pit characters with respect to cavitation resistance across 10 *Prunus* species. *Tree Physiology* 33: 684-694.

Shane M.W., McCully M.E. & Canny M.J. (2000) Architecture of branch-root junctions in maize: structure of the connecting xylem and the porosity of the pit membranes. *Annals of Botany* 85: 613-624.

Sperry J.S., Donnelly J.R. & Tyree M.T. (1988) A method for measuring hydraulic conductivity and embolism in xylem. *Plant, Cell and Environment* 11: 35-40.

Sperry J.S. & Hacke U.G. (2004) Analysis of circular bordered pit function I. Angiosperm vessels with homogenous pit membranes. *American Journal of Botany* 91: 369-385.

Sperry J.S., Perry A.H. & Sullivan J.E.M. (1991) Pit membrane degradation and air-embolism formation in ageing xylem vessels of *Populus tremuloides* Michx. *Journal of Experimental Botany* 42: 1399-1406.

Sperry J.S. & Tyree M.T. (1988) Mechanism of water stress-induced xylem embolism. *Plant Physiology* 88: 581-587.

Stiller V. & Sperry J.S. (2002) Cavitation fatigue and its reversal in sunflower (*Helianthus annuus* L.) *Journal of Experimental Botany* 53: 1155-1161.

Tixier A., Herbette S., Jansen S., Capron M., Tordjeman P., Cochard H. & Badel E. (2014) Modelling the mechanical behavior of pit membranes in bordered pits with respect to cavitation resistance in angiosperms. *Annals of Botany* 114: 325-334.

Wheeler J.K., Sperry J.S., Hacke U.G. & Hoang N. (2005) Inter-vessel pitting and cavitation in woody Rosaceae and other vesselled plants: a basis for a safety versus efficiency trade-off in xylem transport. *Plant, Cell and Environment* 28: 800-812.

Worrall J.J., Marchetti S.B., Egeland L., Mask R.A., Eager T. & Howell B. (2010). Effects and etiology of sudden aspen decline in southwestern Colorado, USA. *Forest Ecology and Management* 260: 638-648.

Worrall J.J., Rehfeldt G.E., Hamann A., Hogg E.H., Marchetti S.B., Michaelian M. & Gray L.K. (2013) Recent declines of *Populus tremuloides* in North America linked to climate. *Forest Ecology and Management* 299: 35-51.

Zimmerman M. (1983) Xylem Structure and the Ascent of Sap. Berlin: Springer Verlag.

2.8 Figures and Tables

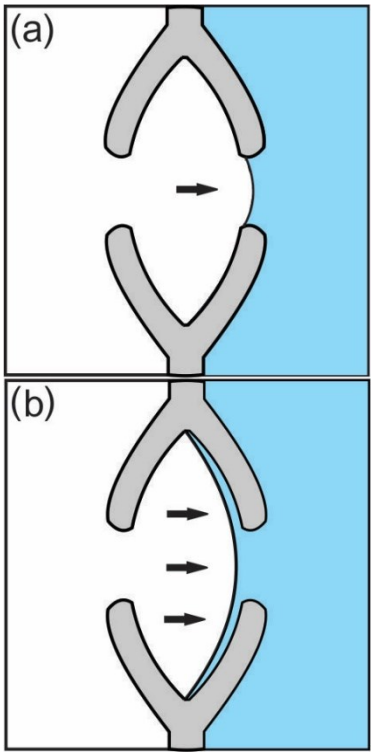

Figure 2.1
An illustration of pit membrane strain during drought. (a) A pit membrane linking air-filled and water-filled xylem vessels aspirates against the pit borders with the increasing pressure differential during drought, allowing only the center of the membrane to flex further toward the water-filled vessel. (b) A pit membrane flexes but is not yet appressed to the pit borders.

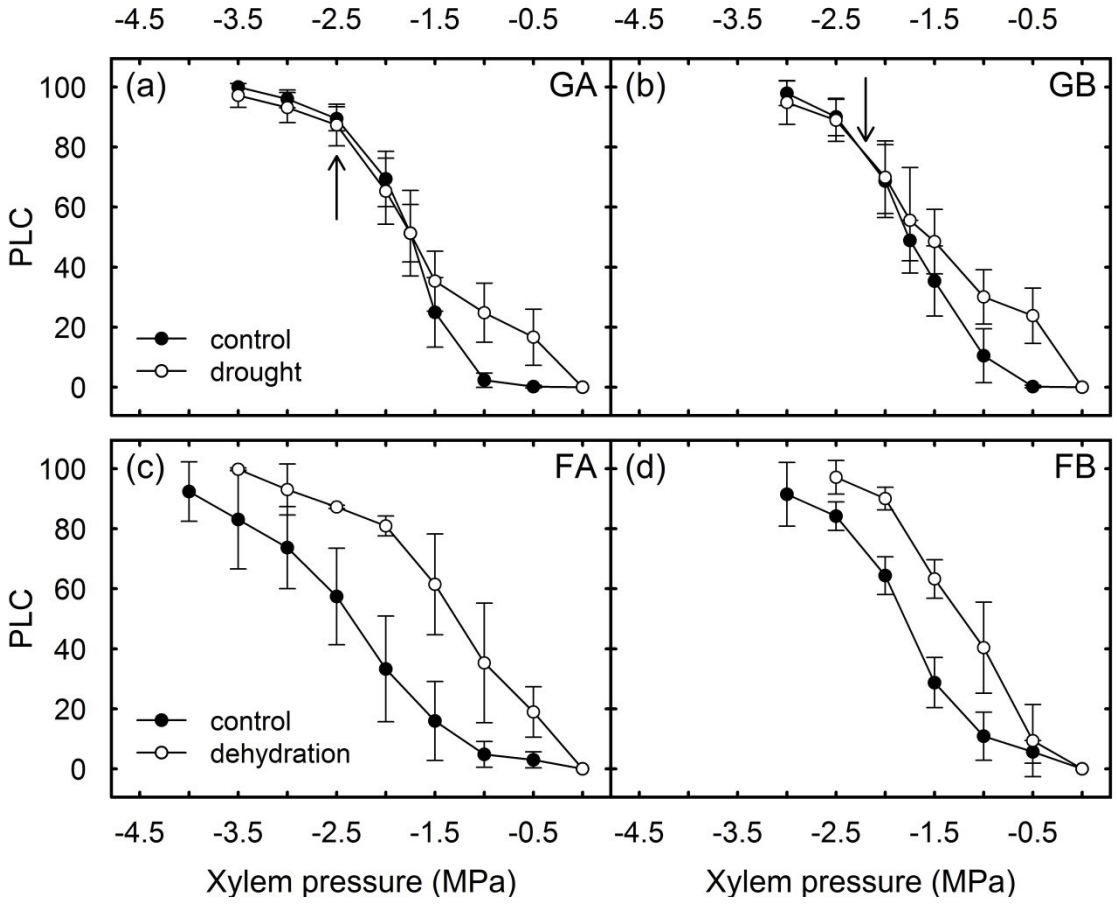

Figure 2.2

Vulnerability curves of aspen (a, c) and balsam poplar (b, d) showing percentage loss of conductivity (PLC) as a function of xylem pressure. Graphs are separated as (a) greenhouse aspen (GA; control: n=12, drought: n=10), (b) greenhouse balsam poplar (GB; control: n=8, drought: n=6), (c) field aspen (FA; control: n=6, dehydration: n=3), and (d) field balsam poplar (FB; control: n=6, dehydration: n=4). Arrows (a, b) indicate the average xylem pressure the seedlings in the greenhouse drought treatments reached before they were harvested. Error bars represent 95% confidence intervals.

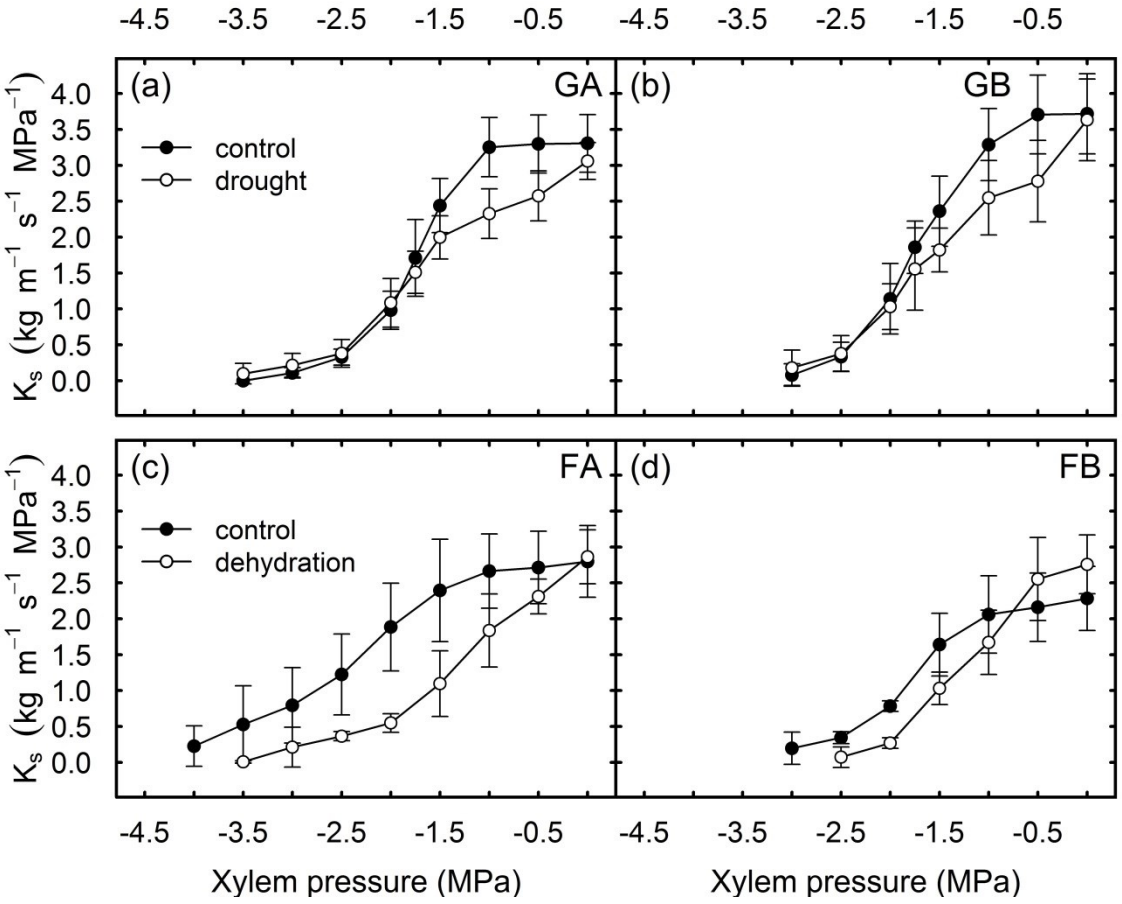

Figure 2.3

Vulnerability curves of aspen (a, c) and balsam poplar (b, d) showing specific conductivity (K_S) as a function of xylem pressure. Graphs are separated as (a) greenhouse aspen (GA; control: n=12, drought: n=10), (b) greenhouse balsam poplar (GB; control: n=8, drought: n=6), (c) field aspen (FA; control: n=6, dehydration: n=3), and (d) field balsam poplar (FB; control: n=6, dehydration: n=4). Error bars represent 95% confidence intervals.

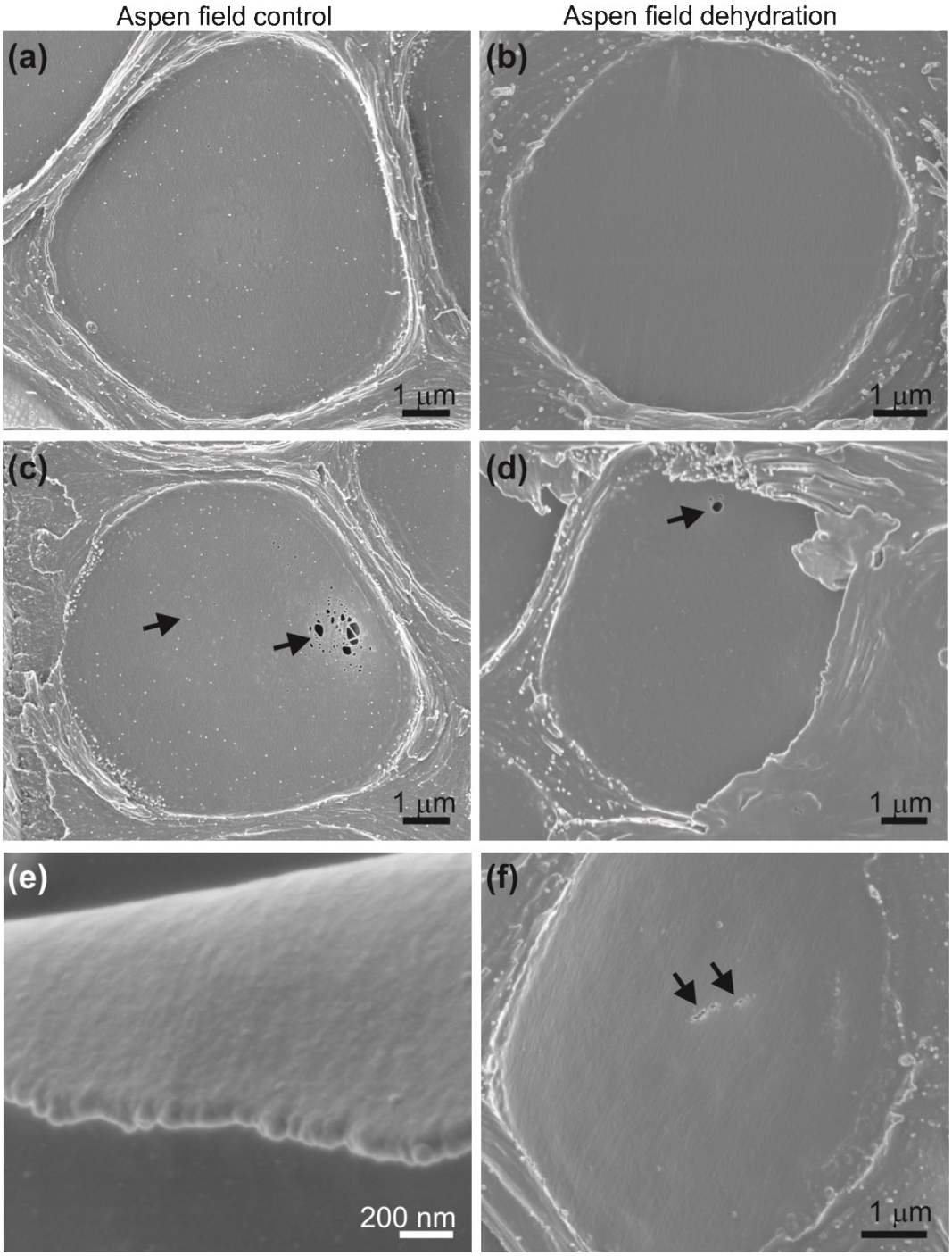

Figure 2.4

SEM images of field aspen. The left column indicates pit membranes from the control treatment; the right indicates pit membranes from the dehydration treatment. (a) A non-porous membrane from the control treatment. (b) A non-porous membrane from the dehydration treatment (c) A pit membrane from the control treatment with both small (left arrow) and large pores (right arrow). (d) A large pore is visible in a pit membrane from the dehydration treatment; the presence of these large pores in both the control and dehydration treatments suggests that they are developmental in nature and are not necessarily caused by drought stress. (e) A close up of the edge of a torn pit membrane with a smooth surface; microfibrils are not clearly visible. (f) A line of pores through the center of a pit membrane is visible, possibly due to mechanical stress

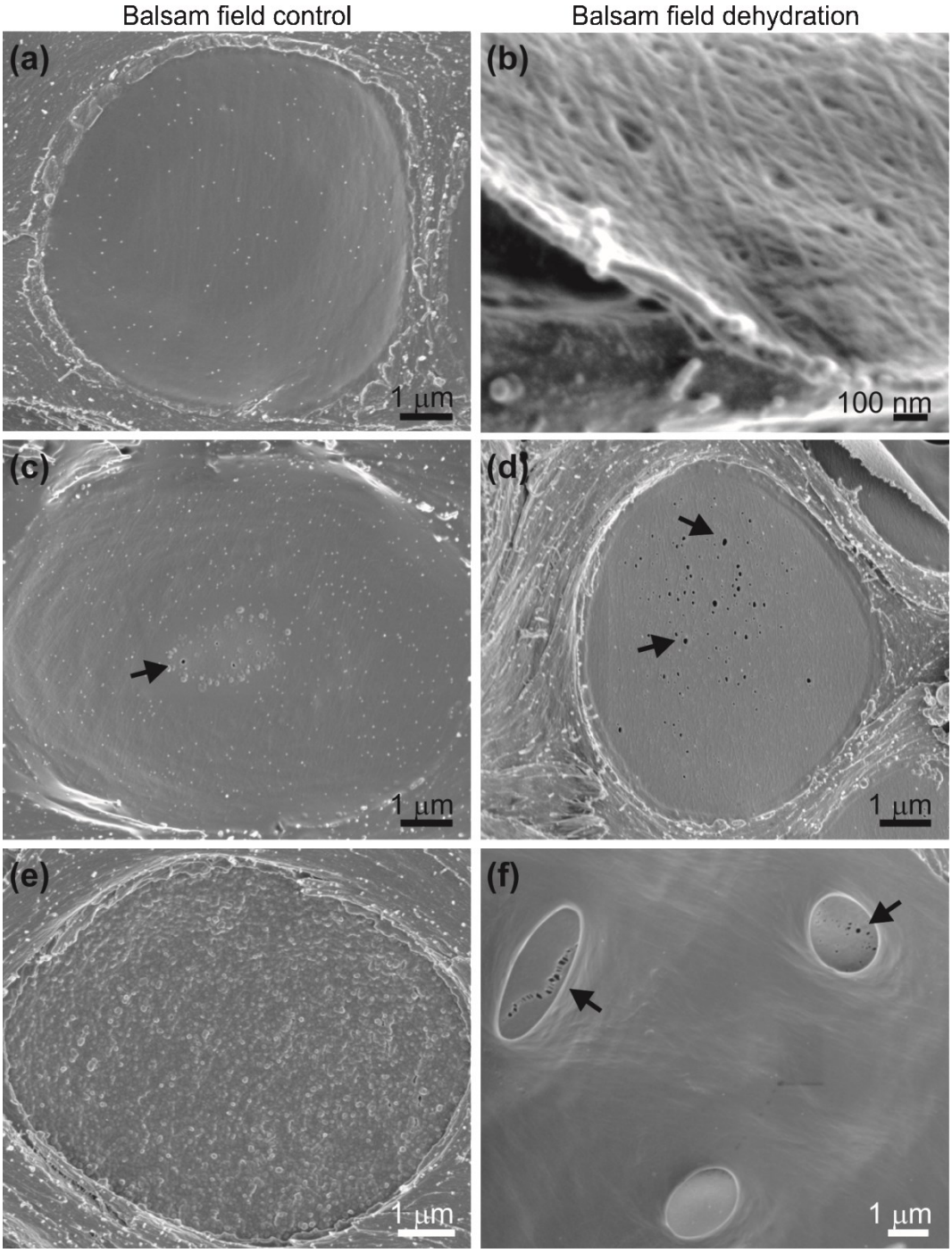

Figure 2.5

SEM images of field balsam poplar. The left column indicates pit membranes from the control treatment; the right indicates pit membranes from the dehydration treatment. (a) A non-porous membrane from the control treatment. (b) A close up of the edge of a torn pit membrane, with a visible network of microfibrils. (c) Small pores (arrow) in the center of a pit membrane from the control treatment. (d) Multiple pores (arrows) in a pit membrane from the dehydration treatment. (e) A pit membrane from the control treatment with a rough texture or layer on the surface; layers of unknown composition were observed occasionally in all treatments. (f) Pores (arrows) in pit membranes are visible through the aperture of the pit border, including a line of pores through the center of the membrane (left arrow).

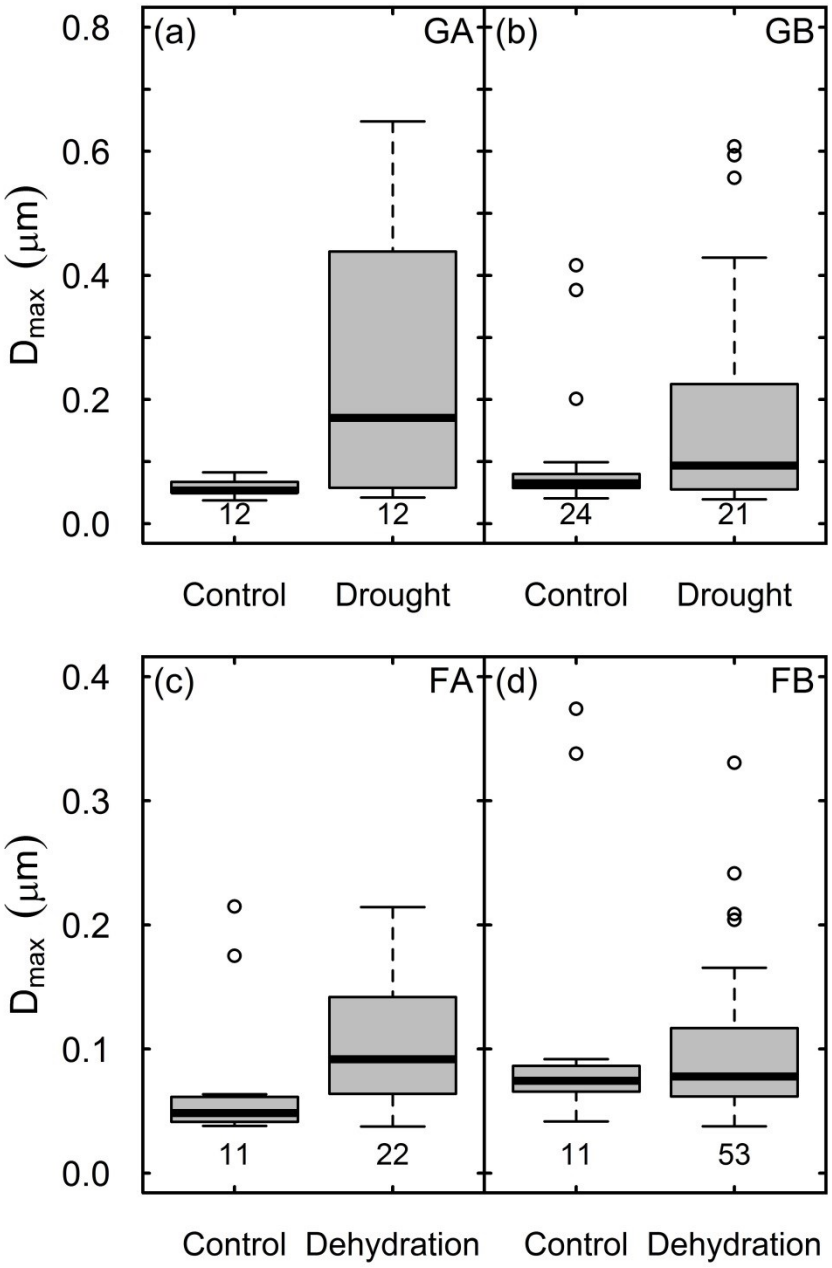

Figure 2.6

The distributions of the diameter of the largest pore per pit membrane (D_{max}) in all treatments. Points are considered outliers at1.5 times the interquartile range and the black line within each box indicates the median. Numbers below the boxplots indicate the number of visibly porous membranes per treatment. Graphs are separated as (a) GA; greenhouse aspen, (b) GB; greenhouse balsam poplar, (c) FA; field aspen, and (d) FB; field balsam poplar.

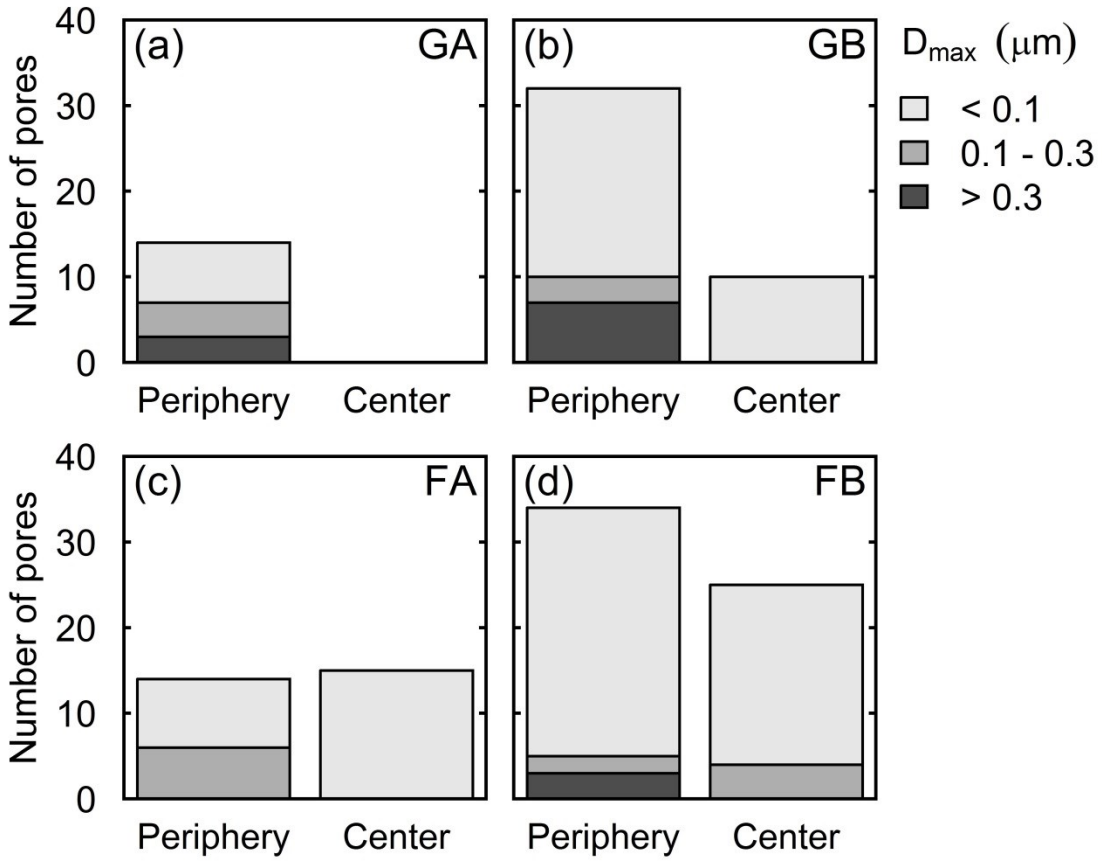

Figure 2.7

The location of the largest pores in the pit membranes. The distance of the largest pore to the edge of the membrane was characterized as being less than half the radius of the membrane (in the periphery) and more than half the radius (in the center). Pore sizes were categorized by D_{max}. Graphs are separated as (a) GA; greenhouse aspen, (b) GB; greenhouse balsam poplar, (c) FA; field aspen, and (d) FB; field balsam poplar.

Table 2.1 Pit membrane characteristics for greenhouse and field experiments.

Characters shown are total number of pit membranes (n) imaged per treatment, the percent of porous pit membranes from the total; the results of a z test of proportions are indicated (*$P \leq 0.05$, **$P \leq 0.01$), and the mean diameter of the largest pore (D_{max}) ± standard deviation; the results of two sample Student's t tests are indicated (*$P \leq 0.05$, **$P \leq 0.01$).

	Pit membrane total	% porous pit membranes	D_{max} (μm)
Greenhouse			
Aspen			
control	36	33.3	0.06 ± 0.01
drought	36	33.3	0.25 ± 0.24**
Balsam poplar			
control	45	53.3	0.10 ± 0.10
drought	45	46.7	0.19 ± 0.20
Field			
Aspen			
control	66	16.7	0.07 ± 0.06
dehydration	66	33.3**	0.11 ± 0.05*
Balsam poplar			
control	92	11.9	0.12 ± 0.12
dehydration	92	57.6**	0.10 ± 0.06

2.9 Supporting Information

Table 2.S1. Hydraulic characteristics for greenhouse and field experiments.

Hydraulic characters shown are treatment means of stem water potential (ψStem) ± standard deviation immediately prior to hydraulic conductivity measurements, mean midday leaf water potential (ψLeaf) ± standard deviation of field trees measured August 19, 2015 (nd, not determined), mean maximum specific conductivity (Kg m^{-1} s^{-1} MPa^{-1}) at 0 MPa (K_s max) measured after the removal of embolism with vacuum infiltration ± standard deviation, the xylem pressure corresponding to 50% loss of conductivity (P50) of each treatment vulnerability curve which was estimated from a Weibull curve fit.

	ψStem (MPa)	ψLeaf (MPa)	K_s max	P50 (MPa)
Greenhouse				
Aspen				
control	-0.41 ± 0.05	nd	3.30 ± 0.71	-1.78
drought	-2.54 ± 0.61	nd	3.06 ± 0.41	-1.66
Balsam				
control	-0.32 ± 0.07	nd	3.72 ± 0.81	-1.73
drought	-2.17 ± 0.29	nd	3.63 ± 0.71	-1.55
Field				
Aspen				
control	nd	-1.68 ± 0.24	2.80 ± 0.62	-2.39
dehydration	< -3.50	nd	2.86 ± 0.33	-1.23
Balsam				
control	nd	-1.33 ± 0.11	2.28 ± 0.56	-1.81
dehydration	< -3.50	nd	2.76 ± 0.42	-1.20

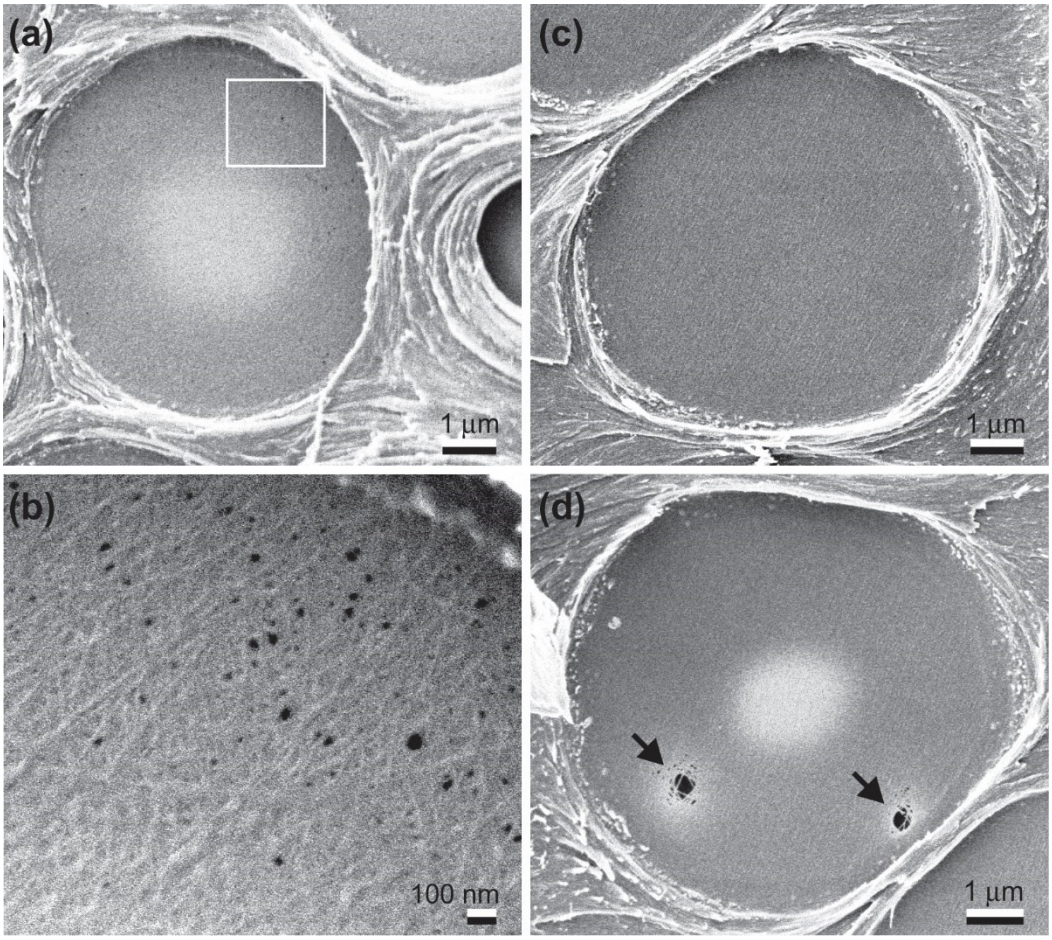

Figure 2.S1
SEM images of greenhouse aspen. Variations in porosity are visible. (a) Small pores are scattered around the periphery of the membrane from the control treatment; the white box indicates the area shown magnified in the image below. (b) A close up view of the pit membrane section denoted by the white box with pores and membrane microfibrils visible. (c) No pores are visible in a membrane from the drought treatment. (d) Two exceptionally large pores are observed in the periphery of the membrane (arrows) from the drought treatment.

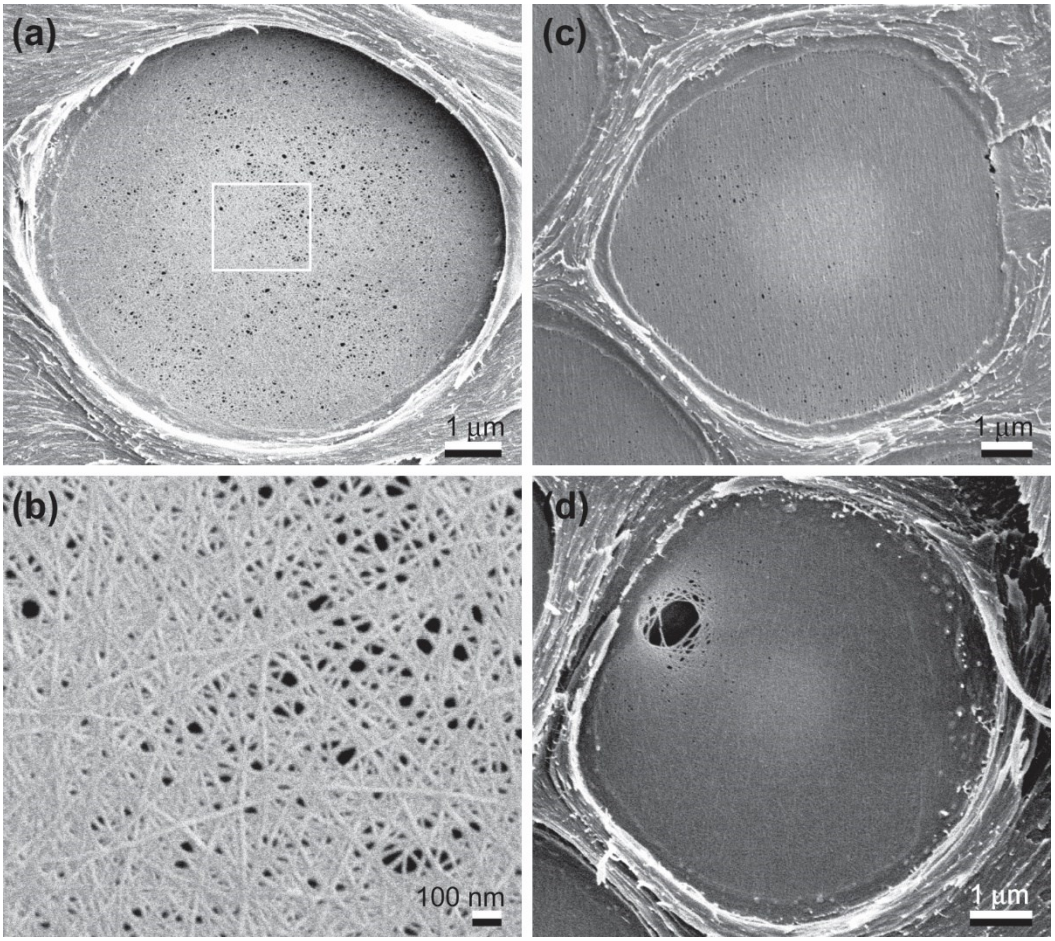

Figure 2.S2
SEM images of greenhouse balsam poplar. Variations in porosity are visible. (a) Small pores are uniformly distributed across the membrane from the control treatment; the white box indicates the area shown magnified in the image below. (b) A close up view of the pit membrane section denoted by the white box with membrane microfibrils clearly visible. (c) Small pores are visible in both the periphery and center of the membrane from the drought treatment, though they are more concentrated to one side. (d) An exceptionally large pore is observed in the periphery of the membrane from the drought treatment.

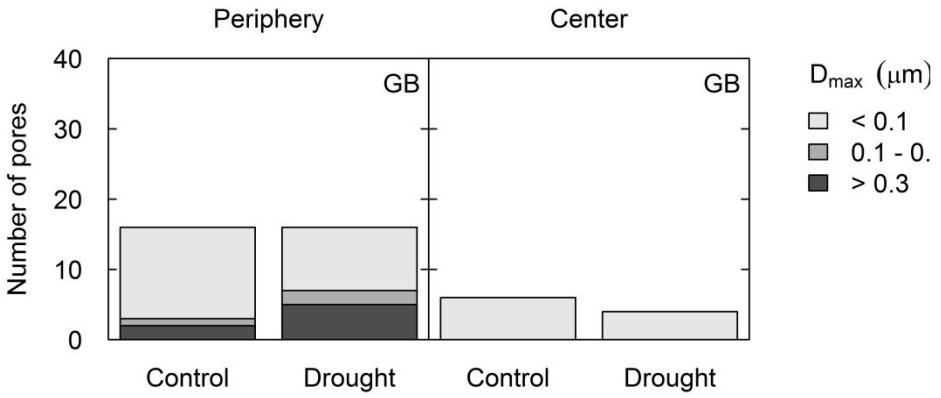

Figure 2.S3
An example of the location of the largest pores in the pit membranes separated by treatment. The data illustrated here is from the greenhouse balsam poplar (GB) experiment. The distance of the largest pore to the edge of the membrane was characterized as being less than half the radius of the membrane (in the periphery) and more than half the radius (in the center). Pores were categorized by D_{max}. The proportion of pit membranes in the periphery or center did not appear to change depending on the treatment applied.

3 Functional xylem anatomy of aspen exhibits greater change due to insect defoliation than to drought

3.1 Summary

The study of tree rings can reveal long-term records of a tree's response to the environment. This dendroecological approach, when supplemented with finer-scale observations of the xylem anatomy, can provide novel information about a tree's year-to-year anatomical and hydraulic adjustments. Here we use this method in aspen (*Populus tremuloides* Michx.) to identify xylem response to drought and insect defoliation. Surprisingly, we found that precipitation influenced vessel diameter mostly in the trees' youth, while this correlation was less pronounced at maturity. This is likely due to a reduction in stress the stand experiences as it ages, and reflects an ability to mediate drought stress as trees mature. Defoliation events caused consistent and profound changes in fiber anatomy likely leading to reduced structural support to vessels. We therefore expect that in years of defoliation trees may be vulnerable to drought-induced cavitation when leaf area recovers. This study highlights how the inclusion of cellular level measurements in tree ring studies provides additional information on how stress events may alter tree functioning through alterations in structure.

3.2 Introduction

The variation in tree ring width is widely used to study tree growth response to changing environmental conditions; sensitivity to the environment can be observed especially in areas where tree growth is limited by precipitation or temperature (Fritts 1976; Speer 2010). However, there is also variation within the cellular structure of tree rings. Tree rings are composed of cells belonging to the water-transporting xylem tissue: cells with a direct link to tree physiology. Analyses of

xylem structure along a time series have been less widely studied than tree ring width, but remain an important source of information about year to year physiological adjustments to the environment (Fonti et al. 2010).

With the global rise of tree dieback due to climate change-induced drought (e.g., Allen et al. 2010, Venturas et al. 2016, Adams et al. 2017), understanding the anatomical structure of the xylem could provide additional insight into this high-interest topic of tree death (McDowell et al. 2008). Drought may lead to narrower vessels, and this will correspond with lower transport efficiency (Plavcová & Hacke, 2012; Hacke et al. 2017), and xylem pit membranes can become more porous (and leaky to air), resulting in increased vulnerability to drought-induced cavitation (Hillabrand et al. 2016). Additional aspects of cellular xylem anatomy may also be altered by drought and should be explored further. Although most studies of functional xylem anatomy have focused on vessel size, the structure of fibers can also influence water transport. Increased fiber wall area was positively correlated with cavitation resistance in at least one study (Jacobsen et al. 2005), suggesting a mechanical role for fibers in cavitation resistance. Similarly, inter-vessel wall thickness also remains an important contributor to the integrity of the vessel structure (Hacke et al. 2001).

Here we asked how the xylem anatomy of trembling aspen (*Populus tremuloides* Michx.) is altered by stress events like drought and insect defoliation. Aspen is a promising study system, because its ecophysiology and water relations have been extensively studied (e.g., Galvez et al. 2011; Schreiber et al. 2011; Anderegg et al. 2013; Schreiber et al. 2015), and because it is the most widespread tree species in North America (Peterson & Peterson 1992). Aspen stands have experienced massive dieback as a result of severe drought (Worrall et al. 2008; Michaelian et al.

2011), but xylem anatomy has not been studied in this context and over longer time scales, i.e., decades.

Increases in drought due to climate change and insect outbreaks may interact to promote tree mortality (Anderegg et al. 2015). In western Canada, a major defoliator of trembling aspen is the forest tent caterpillar (Hogg et al. 2005). Defoliation by the caterpillar often first occurs in early spring before the leaves are fully expanded; as a result, these defoliation events lead to the formation of distinctive "white rings" with reduced width and density (Hogg et al. 2002; Sutton & Tardif 2005). Forest tent caterpillar outbreaks in aspen stands may last successive years (Cooke & Roland 2000; 2007), leading to the formation of multiple adjacent white rings. Though the fiber wall thickness appears to be influenced by defoliation events (Sutton & Tardif 2005), the impact of defoliation on the xylem anatomy remains under-studied. It is also unknown whether defoliation events can alter xylem structure in the following year, i.e., whether there is a lag effect.

Besides stress-induced changes in xylem anatomy, the cellular dimensions of xylem are known to change radially, from pith to bark, i.e., there is a trend for an increase in conduit size with age (Lachenbruch et al. 2011). As a tree grows larger, it experiences different micro-environments and mechanical demands. Wood produced in the early years of a tree's life is generally characterized by large gradients of change in anatomy. In the growth rings of later years, this change becomes more gradual (Lachenbruch et al. 2011). Disturbance events such as drought and insect defoliation could therefore impact the structure of the wood to different degrees based on the age of the tree at the time of disturbance.

The radial extent of change varies by species, and though this pattern is found in both hardwoods and softwoods, anatomical changes due to age are understudied in diffuse-porous wood (Lachenbruch et al. 2011). In *Populus* species, research in this area has mainly focused on wood

density and fiber length, important commercial traits (Koubaa et al.1998; DeBell et al. 2002). Analyses of hydraulic traits such as vessel diameter would provide an additional insight into how trembling aspen respond to their environment and stress events over time.

For this study, aspen trees were chosen from Ministik forest, a site in central Alberta where aspen trees have experienced both periods of drought and defoliation over their lifetimes. This provided an opportunity to observe potential changes in tree ring anatomy with environmental stress and provide a comprehensive examination of aspen xylem anatomy over time. Our objectives were to 1) determine how drought and defoliation events influence the structure and inferred function of the xylem anatomy, and 2) to determine how xylem anatomy changes due to age and whether age alters the response to drought and defoliation.

3.3 Methods

Tree core sampling and cross-dating

Tree cores were collected from an even-aged stand of trembling aspen that originated around 1926 in Ministik, Alberta, Canada (53° 16' 40.8" N, 112° 54' 46.8" W). Two increment cores were taken at 1.3 m height from 20 aspen trees along with measurements of diameter at breast height (DBH). The cores were dried and sanded with progressively finer sand paper. Cores were visually cross-dated using a binocular microscope (Fritts 1976). Tree-ring width (*rw*) was measured to a precision of 0.01 mm using a LINTAB measuring device (Rinntech, Heidelberg, Germany). The program COFECHA was used to check the quality and correct dating of the series (Holmes 1983).

Identification of drought and defoliation events

Years of drought were identified using the Climate Moisture Index (CMI), a measure derived from the difference between annual precipitation and annual potential evapotranspiration (Hogg 1994; Hogg et al. 2013), calculated yearly over successive 12-month periods ending on the 31st of July (Hogg et al. 2005). With this index, four separate years were identified as having values below -15 cm and were classified as 'drought years' for this study: 1949, 1950, 2002, and 2009. Five years of severe defoliation, primarily by forest tent caterpillar, were identified by the repeated presence of 'white rings' (Hogg et al. 2002) in the chronology: 1960, 1987, 1988, 1994, and 1995.

Thin section preparation and wood anatomical variables

To measure wood anatomical characteristics spanning the years 1946-1963 (Age Group 1) and 1984-2012 (Age Group 2), thin sections were produced to represent each year by four to six individual trees. The lengths of these two Age Groups were determined by beginning 3 years prior to the first stress event and ending at 3 years post last year of stress. Transverse thin sections were prepared using a sliding microtome (Leica SM2400). The tissue was stabilized with a starch-based non-Newtonian solution to fill the cells and keep the structure rigid during the cut (Schneider & Gärtner 2013). Afterwards, the sections were stained with a combination dye of safranin and astrablue to indicate lignification (Gärtner & Schweingruber 2013).

Prepared slides were imaged using a light microscope (Leica DM3000) with a mounted camera. The resulting images were stitched together to create larger sections containing adjacent tree rings. Images were analyzed with ImagePro Premier (Media Cybernetics, Rockville, MD, USA) for wood anatomical variables.

The average diameter (*dv*) was taken from all vessels across an entire ring between 3-4 xylem rays. From this, the hydraulically weighted mean vessel diameter (*dh*) (Sperry et al. 1994) was calculated per ring as:

$$dh = \frac{\sum dv^5}{\sum dv^4} \quad (3.1)$$

Xylem vessel contact fraction (*cf*) was measured as the total length of contact between vessels per the total perimeter of all vessels (Wheeler et al. 2005) across an entire ring for the same vessels on which the diameter measurements were made. Using xylem rays as an outline surrounding measured vessels, vessel lumen fraction (*lf*) was measured as the total vessel lumen area per total xylem area. A greater vessel lumen fraction corresponds with a higher percentage of xylem cross-sectional area dedicated to water transport.

All sections containing rings representing defoliation years were also analyzed for the fiber lumen fraction. The fiber lumen fraction was calculated by selecting two sections of fibers from the middle of each ring and determining the ratio of total fiber lumen area to total fiber lumen and wall area. Higher values of fiber lumen fraction correspond with larger fibers and/or thinner fiber walls.

Additionally, sections in Age Group 2 were analyzed for vessel roundness and inter-vessel double wall thickness (*t*); the lower quality of the sections in Age Group 1 did not allow for accurate measurements of *t*. With *t*, the thickness to span ratio *tb* was calculated as $(t/b)^2$ to estimate vessel resistance to implosion (Hacke et al. 2001), with *b* represented by *dh*. Within each ring, only vessel pairs within +/- 5 μm of the calculated *dh* were chosen for these measurements.

Vessel roundness was calculated by ImagePro Premier with an area to perimeter ratio:

$$roundness = \frac{Perimeter^2}{4\pi Area} \quad (3.2)$$

where a value of 1 represents the ratio of a perfect circle. Values greater than 1 deviate from the ideal shape.

Stable carbon isotope analysis

Additional cores were chosen for analysis of carbon isotope discrimination. In total, each year in the analysis was represented by four individual trees in same Age Groups as used the anatomical analyses. Entire rings were separated using a scalpel for the same years of interest as chosen for the thin sections. As some rings were very small, we did not extract cellulose; whole wood was used to ensure there was enough material for the analysis. Samples were weighed, cut into slivers, and sent to be analyzed at the University of British Columbia Stable Isotope Laboratory (*http://isotopes.forestry.ubc.ca/)* for the isotope ratio $^{13}C/^{12}C$, expressed as $\delta^{13}C$ in parts per thousand (‰) relative to the standard V-PDB. These values ($\delta^{13}C_p$) were used to calculate the physiological discrimination of ^{13}C by the tree ($\Delta^{13}C$), accounting for changes in the atmospheric ratio ($\delta^{13}C_a$) over time (McCarroll & Loader 2004):

$$\Delta^{13}C = \frac{\delta^{13}C_a - \delta^{13}C_p}{1 - \delta^{13}C_p/1000} \quad (3.3)$$

Statistical analysis

Data analysis was completed using R statistical software (R Core Team 2016). Significant changes in mean values of $\delta^{13}C$, fiber lumen fraction, and vessel roundness were assessed with

analysis of variance (ANOVA) performed using linear mixed models with wood Age Group and tree core id as random effects to assess these changes independent of age.

Time series of tree ring width and wood anatomical data were detrended using a 10 –year cubic smoothing spline with a 50% frequency cut-off to remove age trends. First order autocorrelation was non-significant in the detrended series. This detrending procedure was applied to series in both Age Group 1 and Age Group 2, and carried out using the *dplR* package (Bunn 2008).

After detrending, correlation matrices of Pearson's r were calculated using the standardized data to assess the relationships between wood anatomical variables, as well as anatomical variables and climate. Years of defoliation were removed from the calculation of correlations between wood anatomical variables and climate since changes in wood anatomy due to defoliation events were not climate-driven.

Annual and seasonal climate data for Ministik, AB was generated through interpolation with the BioSIM software tool, available at *ftp://ftp.cfl.forestry.ca/regniere/software/BioSIM/* (Régnière et al. 2016). Annual variables such as mean annual temperature (T_aj) and total annual precipitation (P_aj), as well as the CMI and additional Soil Moisture Index (SMI) values (Hogg et al., 2013) were calculated from the previous August 1st to July 31st. Total growing season precipitation (P_gs) included the months of May through September. A mean of the last 4 years CMI (CMI_4y) was also included based on strong correlations with ring width (Hogg et al. 2008), as well as a mean of the last 2 years SMI (SMI_2y).

For further investigation of correlations between wood anatomical variables, standard major axis regression was used to model the relationship. This analysis was used because the wood

anatomical variables could not be considered to be independent of one another (Warton et al. 2006).

3.4 Results

The chronology of aspen ring width showed considerable variation year to year from 1933 to 2014. Years with CMI values lower than -15 cm, considered as severe drought, showed narrow ring width, but not as narrow as years of defoliation (Fig. 3.1).

Stable carbon isotope analysis of the tree rings showed inter-annual variation in $\Delta^{13}C$ values and generally supported the choice of years of severe drought as previously determined with the CMI (Fig 3.2a). Expectedly, mean drought year $\Delta^{13}C$ was significantly lower than those of defoliation or control, meaning that drought years were significantly more enriched in ^{13}C. Mean $\Delta^{13}C$ for the defoliation years was significantly higher than control (Fig. 3.2b).

Pearson's r correlations between wood anatomical variables in the separate wood age groups showed similar results (Fig. 3.3a-b). However, correlations between wood anatomical variables and climate generally showed a stronger relationship in the Age Group 1 than in the Age Group 2, including *rw*, *dv*, and *dh* (Fig. 3.3c-d; see Tables 3.S1-3.S4 for *P*-values). A strong positive relationship between vessel diameter (*dv* and *dh*) and precipitation variables was found in Age Group 1, but was less pronounced for Group 2. The relationship between vessel diameter and growing season precipitation (P_aj) was even stronger than the relationship between ring width and P_aj (Fig. 3.4a-b), though both these relationships were not found in Age Group 2. Age Group 1 ring width and vessel diameter was also found to correlate strongly with the current year CMI and SMI, while the Age Group 2 ring width was more strongly correlated with the mean of the last four years for the CMI (CMI_4y) and two years for the SMI (SMI_2y). The relationship between

$\Delta^{13}C$ data and climate was significantly positive for all climate variables in Age Group 2 except T_aj, while in Age Group 1, $\Delta^{13}C$ was only significantly correlated with CMI_4y.

Between wood anatomical variables, a significant negative correlation was found between ring width and vessel lumen fraction (Fig. 3.3). In both Age Groups, defoliation rings were characterized by small width and increased vessel lumen fraction (Fig. 3.5a-b). Drought years did not exhibit this characterization as strongly. Another significant negative correlation was found between vessel diameter and contact fraction, indicating that tree rings with smaller vessels also had vessels in greater contact with another. Drought and defoliation years did not appear to be characterized by either extreme (Fig. 3.6).

No anatomical variables strongly characterized drought rings by having significantly different means in drought years. By contrast, defoliation rings were characterized by having increased fiber lumen fraction and decreased vessel roundness (Fig. 3.7). Fiber lumen fraction was significantly greater in the years that experienced defoliation as compared to the year immediately prior to or post a 1-2 year defoliation event (Fig. 3.7a). Fiber lumen fraction measurements were taken as close to the middle of each ring as possible and high fiber lumen fraction seemed to reflect both thinner walls and larger fiber lumens (Fig. 3.7b). No lag effect was seen; following defoliation, mean fiber lumen fraction returned to a value equal to the year prior the defoliation. Additionally, the vessels within the defoliation years were significantly less round as compared to vessels in the years prior to and post a defoliation event (Fig. 3.7c). Vessels exhibited wavy margins in defoliation years (Fig. 3.7d), indicating a weakened structure. The combination dye of safranin and astrablue also suggested that white rings were less lignified by the darker staining (See Fig. 3.7b).

3.5 Discussion

Our first objective was to determine wood structural changes induced by drought and defoliation. We found that these two types of stress events have different impacts on xylem anatomy. This may be expected from the ^{13}C data, which showed contrasting influences of these events on tree water relations in the year of their occurrence. The enrichment of drought years in ^{13}C, and the reduced ^{13}C in defoliation years is a proxy indicator of stomatal behavior; stomatal closure in drought years results in increased fixation of ^{13}C (McCarroll & Loader 2004), while the ^{13}C values of defoliation years likely reflect more favorable tree water potentials due to reduced leaf area for transpiration. Additionally, direct measures have shown increased stomatal conductance in residual leaves following partial defoliation in aspen (Hart et al. 2000).

We begin our discussion with drought and will then consider the impact of insect defoliation. In Age Group 1, mean vessel diameter was strongly correlated with growing season precipitation. In fact, vessel diameters were more sensitive to precipitation than ring width was. Surprisingly, however, this sensitivity differed between tree rings formed in youth and at maturity. Therefore, when considering both Age Groups, vessel diameter could not serve as a defining characteristic of drought years.

Subsequently, our finding was that correlations between precipitation variables and wood anatomical variables (*rw, dv, dh*) were generally stronger in Age Group 1 than Age Group 2 (Fig. 3.3). We suggest that when the trees in the aspen stand are young, they are more growth-limited by water stress than they are at maturity. Competition for soil water may be a factor; young aspen stands can carry more leaf area than mature stands (Pinno et al. 2001), leading to more water lost through transpiration in young stands. Older trees may also mediate stress by using larger amounts of stored water (Phillips et al. 2003; Scholz et al. 2011) and by having larger or deeper roots.

Additionally, older trees may mediate stress through a greater stomatal sensitivity to the environment as indicated by the significant $\Delta^{13}C$ correlations with climate variables in Age Group 2. The ability to mediate water stress would then provide an explanation for why the relationship in Age Group 2 for ring width is stronger for an average of multiple past years CMI and SMI, than the concurrent year.

Compared with drought, insect defoliation caused more consistent and profound changes in xylem anatomy. The "white rings", that were formed during years of defoliation had significantly increased fiber lumen fraction (less cell walls per cross sectional area) and decreased vessel roundness in both Age Groups. Interestingly, defoliation primarily altered fiber properties, and observed changes in vessel anatomy may be partially explicable in the light of their support by the altered fiber matrix surrounding the vessels. Increased fiber lumen fraction in the xylem of defoliation years seemed to be due to both thinner fiber walls and larger fiber lumens. This finding contrasts slightly with the observations of Sutton & Tardif (2005), who found thinner fiber walls, but also smaller fiber lumens in white rings of aspen. It may be that the size of the lumen area is more variable depending on environmental conditions of the time i.e. precipitation, while the fiber wall thickening is more directly impacted by the loss of photosynthates in the early spring. Regardless, the fiber cellular dimensions recovered in the following year; there was no lag effect.

Though the inter-vessel wall thicknesses were not found to be significantly thinner in defoliation years, the vessel walls were found to be "wavy" and less circular. This is likely due to the thinner-walled fibers being unable to keep the xylem structure rigid, which allowed the vessel walls to be pulled inward due to the negative hydrostatic pressure within the vessels (Jacobsen et al. 2005). Consequently, we might expect that vessels in white rings are more susceptible to cavitation as the compromised structure may create nucleation points for air through micro-

fractures in the cell wall or stretching of pit membranes (Jacobsen et al. 2005). White rings may also weaken the wood structurally and functionally, if cell walls are reduced in lignin content (Kitin et al. 2010; Voelker et al. 2011) and may provide pathways for the spread of pathogens, similar to frost damage (Diamandis & Koukos 1992). And, despite the recovery of the xylem structure in the year following defoliation, loss of stored carbon from the tree may be a long-term risk factor for tree dysfunction. In mature aspen, loss of root tissue carbon reserves from defoliation can take up to 2 years to recover (Landhäusser & Lieffers 2012). In the year of defoliation, the reduced leaf area and reduced total transpiration are not likely to generate very low water potentials and may mitigate the risk of cavitation. However, there is potential for delayed effects. Trees may be at an increased risk for cavitation if drought occurs in the year following defoliation. An early season drought, before the current year's xylem is fully functional, may be especially detrimental to twigs containing only wood formed in a defoliation year. We conclude that the changes caused by insect defoliation may have a range of negative effects on tree performance in future years.

The anatomy and the extent of fiber production were also highly variable across years. This was observed in the correlation between ring width and vessel lumen fraction, which inversely describes the percentage of area occupied by fibers. Although vessels were produced throughout the growing season as is typical in diffuse porous growth, vessels comprised a larger cross-sectional area in earlywood than in latewood. In other words, earlywood had a higher vessel lumen area than latewood. It appears that the increased vessel lumen area of smaller rings is a result of early truncation of growth in years of unfavorable conditions, reducing the addition of fiber area to the latewood. This correlation characterized defoliation years as small rings with high vessel lumen fraction, likely because defoliation causes early cessation of radial growth (Jones et al. 2004).

The fact that fiber properties appeared to be more sensitive to defoliation events than vessel properties may indicate that trees prioritized the need for maintaining adequate water transport (at least in the short term) over structural support during these years. As already mentioned though, transport and structural support go hand in hand, hence alterations in fiber properties are likely to have a negative effect on transport, at least when water potentials become negative enough to trigger cavitation – presumably when full leaf area recovers.

The maintenance of adequate water transport may also be influenced by the arrangement of vessels. The grouping of vessels, expressed as contact fraction, exhibited the strongest correlation with mean vessel diameter: rings with smaller vessels had vessels that were in greater contact with each other. Similar patterns are found between mean vessel area and vessel frequency in growth rings of other species (Leal et al. 2004; Martínez-Sancho et al. 2017; Noyer et al. 2017). Greater contact between vessels is an anatomical character with conflicting attributes. It can offer redundancy in the hydraulic pathway (Carlquist 1984), but it also may increase the vulnerability of vessels to embolism by providing more surface area for air-seeding (Loepfe et al. 2007). It is possible that the benefits of increased contact are maximized when vessels are small, and the risk of embolism is low.

3.6 Conclusions

Although vessel diameters were sensitive to precipitation in Age Group 1, this was not the case in Age Group 2. We suggest that older trees were more buffered from the impacts of drought through a larger root system, increased stomatal sensitivity, and reduced stand leaf area as compared with their youth. White rings produced by defoliation had a weaker fiber matrix than control or drought rings in both Age Groups. Also, likely due to the weakened fiber structure,

white rings had vessels with reduced circularity, implying that these vessels would be more susceptible to cavitation. Fortunately, the year of defoliation is less likely to generate strongly negative water potentials that would promote cavitation. Surprisingly, the fiber properties in growth rings were more influenced by stress than were the vessels. Perhaps this is because vessel development, with its direct tie to water transport, is more conserved. These measurements increase our knowledge about annual adjustments in xylem cellular anatomy in aspen, and associated physiological implications which could not be seen from chronologies of ring width alone.

3.7 References

Adams H.D., Zeppel M.J.B., Anderegg W.R.L., Hartmann H., Landhäusser S.M., Tissue D.T., …, McDowell N.G. (2017) A multi-species synthesis of physiological mechanisms in drought-induced tree mortality. *Nature Ecology & Evolution* 1: 1285-1291.

Allan C.D., Macalady A.K., Chenchouni H., Bachelet D., Mcdowell N., Vennetier M., ..., Cobb N. (2010) A global overview of drought and heat-induced tree mortality reveals emerging climate change risks for forests. *Forest Ecology and Management* 259: 660-684.

Anderegg W.R.L., Hicke J.A., Fisher R.A., Allen C.D., Aukema J., Bentz B., …, Zeppel M. (2015) Tree mortality from drought, insects, and their interactions in a changing climate. *New Phytologist* 208:674-683.

Anderegg W.R.L., Plavcová L., Anderegg L.D.L., Hacke U.G., Berry J.A. & Field C.B. (2013) Drought's legacy: Multiyear hydraulic deterioration underlies widespread aspen forest die-off and portends increased future risk. *Global Change Biology* 19:1188-1196.

Bunn A.G. (2008) A dendrochronology program library in R (dplR). *Dendrochronologia* 26:115-124.

Carlquist S. (1984) Vessel grouping in dicotyledon wood. *Aliso* 10:505-525.

Cooke B.J. & Roland J. (2007) Trembling aspen responses to drought and defoliation by forest tent caterpillar and reconstruction of recent outbreaks in Ontario. *Canadian Journal of Forest Research* 37:1586-1598.

Cooke B.J. & Roland J. (2000) Spatial analysis of large-scale patterns of forest tent caterpillar outbreaks. *Écoscience* 7:410-422.

DeBell D.S., Singleton R., Harrington C.A. & Gartner B.L. (2002) Wood density and fiber length in young *Populus* stems: Relation to clone, age, growth rate, and pruning. *Wood and Fiber Science* 34:529-539.

Diamandis S. & Koukos P. (1992) Effect of bacteria on the mechanical and chemical properties of wood in poplars damaged by frost cracks. *Forest Pathology* 22:362-370.

Fonti P., von Arx G., García-González I., Eilmann B., Sass-Klaassen U., Gärtner H. & Eckstein D. (2010) Studying global change through investigation of the plastic responses of xylem anatomy in tree rings. *New Phytologist* 185:42-53.

Fritts H.C. (1976) Tree rings and climate. London: Academic Press Inc.

Galvez D.A., Landhäusser S.M. & Tyree M.T. (2011) Root carbon reserve dynamics in aspen seedlings: Does simulated drought induce reserve limitation? *Tree Physiology* 31:250-257.

Gärtner H. & Schweingruber F. (2013) Microscopic preparation techniques for plant stem analysis. Remagen: Verlag Dr. Kessel.

Hacke U.G., Sperry J.S., Pockman W.T., Davis S.D. & McCulloh K.A. (2001) Trends in wood density and structure are linked to prevention of xylem implosion by negative pressure. *Oecologia* 126:457-461.

Hacke U.G., Spicer R., Schreiber S.G. & Plavcová L. (2017) An ecophysiological and developmental perspective on variation in vessel diameter. *Plant, Cell and Environment* 40:831-845.

Hart M., Hogg E.H. & Lieffers V.J. (2000) Enhanced water relations of residual foliage following defoliation in *Populus tremuloides*. *Canadian Journal of Botany* 78:583-590.

Hillabrand R.M., Hacke U.G. & Lieffers V.J. (2016) Drought-induced xylem pit membrane damage in aspen and balsam poplar. *Plant, Cell and Environment* 39:2210-2220.

Hogg E.H., Barr A.G. & Black T.A. (2013) A simple soil moisture index for representing multi-year drought impacts on aspen productivity in the western Canadian interior. *Agricultural and Forest Meteorology* 178-179:173-182.

Hogg E.H., Brandt J.P. & Michaelian M. (2008) Impacts of a regional drought on the productivity, dieback, and biomass of western Canadian aspen forests. *Canadian Journal of Forest Research* 38:1373-1384.

Hogg E.H., Brandt J.P. & Kochtubajda B. (2005) Factors affecting interannual variation in growth of western Canadian aspen forests during 1951-2000. *Canadian Journal of Forest Research* 35:610-622.

Hogg E.H., Hart M. & Lieffers V.J. (2002) White tree rings formed in trembling aspen saplings following experimental defoliation. *Canadian Journal of Forest Research* 32:1929-1934.

Hogg E.H. (1994) Climate and the southern limit of the western Canadian boreal forest. *Canadian Journal of Forest Research* 24:1835-1845.

Holmes R.L. (1983) Computer-assisted quality control in tree-ring dating and measurement. *Tree-Ring Bulletin* 43:70-78.

Jacobsen A.L., Ewers F.W., Pratt R.B., Paddock III W.A. & Davis S.D. (2005) Do xylem fibers affect vessel cavitation resistance? *Plant Physiology* 139:546-556.

Jones B., Tardif J. & Westwood R. (2004) Weekly xylem production in trembling aspen (*Populus tremuloides*) in response to artificial defoliation. *Canadian Journal of Botany* 82:590-597.

Kitin P., Voelker S.L., Meinzer F.C., Beeckman H., Strauss S.H. & Lachenbruch B. (2010) Tyloses and phenolic deposits in xylem vessels impede water transport in low-lignin transgenic poplars: A study by cryo-fluorescence microscopy. *Plant Physiology* 154:887-898.

Koubaa A., Hernandez R.E., Beaudoin M. & Poliquin J. (1998) Interclonal, intraclonal, and within-tree variation in fiber length of poplar hybrid clones. *Wood and Fiber Science* 30:40-47.

Lachenbruch B., Moore J. & Evans R. (2011) Radial variation in wood structure and function in woody plants, and hypotheses for its occurrence. In: Meinzer F.C., Lachenbruch B. & Dawson T.E. (eds) Size- and Age-Related Changes in Tree Structure and Function. Springer, Dordrecht, pp. 121-164.

Landhäusser S.M. & Lieffers V.J. (2012) Defoliation increases risk of carbon starvation in root systems of mature aspen. *Trees* 26:653-661.

Leal S., Pereira H., Grabner M. & Wimmer R. (2004) Tree-ring structure and climatic effects in young *Eucalyptus globulus* Labill. grown at two Portuguese sites: preliminary results. *Dendrochronologia* 21:139-146.

Loepfe L., Martinez-Vilalta J., Piñol J., Mencuccini M. (2007) The relevance of xylem network structure for plant hydraulic efficiency and safety. *Journal of Theoretical* Biology 247:788-803.

Martínez-Sancho E., Dorado-Liñán I., Heinrich I., Helle G. & Menzel A. (2017) Xylem adjustment of sessile oak at its southern distribution limits. *Tree Physiology* 37:903-914.

McCarroll D. & Loader N.J. (2004) Stable isotopes in tree rings. *Quaternary Science Reviews* 23: 771-801.

McDowell N., Pockman W.T., Allen C.D., Breshears D.D., Cobb N., Kolb T., …, Yepez E.A. (2008) Mechanisms of plant survival and mortality during drought: Why do some plants survive while others succumb to drought? *New Phytologist* 178: 719-739.

Michaelian M., Hogg E.H., Hall R.J. & Arsenault E. (2011) Massive mortality of aspen following severe drought along the southern edge of the Canadian boreal forest. *Global Change Biology* 17:2084-2094.

Noyer E., Lachenbruch B., Dlouhá J., Collet C., Ruelle J., Ningre F. & Fournier M. (2017) Xylem traits in European beech (*Fagus sylvatica* L.) display a large plasticity in response to canopy release. *Annals of Forest Science* 74:1-11.

Peterson E.B. & Peterson N.M. (1992) Ecology, management, and use of aspen and balsam poplar in the Prairie Provinces. Special Report 1. Forestry Canada, Northern Forestry Centre, Edmonton, Alberta.

Phillips N.G., Ryan M.G., Bond B.J., McDowell N.G., Hinckley T.M. & Čermák J. (2003) Reliance on stored water increases with tree size in three species in the pacific northwest. *Tree Physiology* 23:237-245.

Pinno B.D., Lieffers V.J. & Stadt K.J. (2001) Measuring and modelling the crown and light transmission characteristics of juvenile aspen. *Canadian Journal of Forest Research* 31:1930-1939.

Plavcová L. & Hacke U.G. (2012) Phenotypic and developmental plasticity of xylem in hybrid poplar saplings subjected to experimental drought, nitrogen fertilization, and shading. *Journal of Experimental Botany* 63:6481-6491.

R Core Team (2016) R: A language and environment for statistical computing. R Foundation for Statistical Computing, Vienna, Austria. URL http://www.R-project.org/.

Régnière J., St.-Amant R. & Béchard A. (2016) BioSIM 10.0 User's Manual, Information Report LAU-X-137E. Natural Resources Canada, Canadian Forest Service, Ottawa, ON, Canada.

Schneider L. & Gärtner H. (2013) The advantage of using a starch based non-Newtonian fluid to prepare micro sections. *Dendrochronologia* 31:175-178.

Scholz F.G., Phillips N., Bucci S., Meinzer F.C. & Goldstein G. (2011) Hydraulic capacitance: Biophysics and functional significance of internal water sources in relation to tree size. In: Meinzer F.C., Lachenbruch B. & Dawson T.E. (eds) Size- and Age-Related Changes in Tree Structure and Function. Springer, Dordrecht, pp. 341-361.

Schreiber S.G., Hacke U.G., Hamann A. & Baltzer J. (2015) Variation of xylem vessel diameters across a climate gradient: Insight from a reciprocal transplant experiment with a widespread boreal tree. *Functional Ecology* 29:1392-1401.

Schreiber S.G., Hacke U.G., Hamann A. & Thomas B.R. (2011) Genetic variation of hydraulic and wood anatomical traits in hybrid poplar and trembling aspen. *New Phytologist* 190:150-160.

Speer J.H. (2010) Fundamentals of tree ring research. Tucson: The University of Arizona Press.

Sperry J.S., Nichols K.J., Sullivan J.E.M. & Eastlack S.E. (1994) Xylem embolism in ring-porous, diffuse-porous, and coniferous trees of northern Utah and interior Alaska. *Ecology* 75: 1736-1752.

Sutton A. & Tardiff J. (2005) Distribution and anatomical characteristics of white rings in *Populus tremuloides*. *IAWA Journal* 26:221-238.

Venturas M.D., MacKinnon E.D., Dario H.L., Jacobsen A.L., Pratt R.B. & Davis S.D. (2016) Chaparral shrub hydraulic traits, size, and life history types relate to species mortality during California's historic drought of 2014. *PLOS ONE* 11:e0159145.

Voelker S.L., Lachenbruch B., Meinzer F.C., Kitin P. & Strauss S.H. (2011) Transgenic poplars with reduced lignin show impaired xylem conductivity, growth efficiency and survival. *Plant, Cell and Environment* 34:655-668.

Warton D.I., Wright I.J., Falster D.S. & Westoby M. (2006) Bivariate line-fitting methods for allometry. *Biological Reviews* 81:259-291.

Wheeler J.K., Sperry J.S., Hacke U.G. & Hoang N. (2005) Inter-vessel pitting and cavitation in woody Rosaceae and other vesselled plants: A basis for a safety versus efficiency trade-off in xylem transport. *Plant, Cell and Environment* 28:800-812.

Worrall J.J., Egeland L., Eager T., Mask R.A., Johnson E.W., Kemp P.A., Shepperd W.D. (2008) Rapid mortality of *Populus tremuloides* in southwestern Colorado, USA. *Forest Ecology & Management* 255:686-696.

3.8 Figures

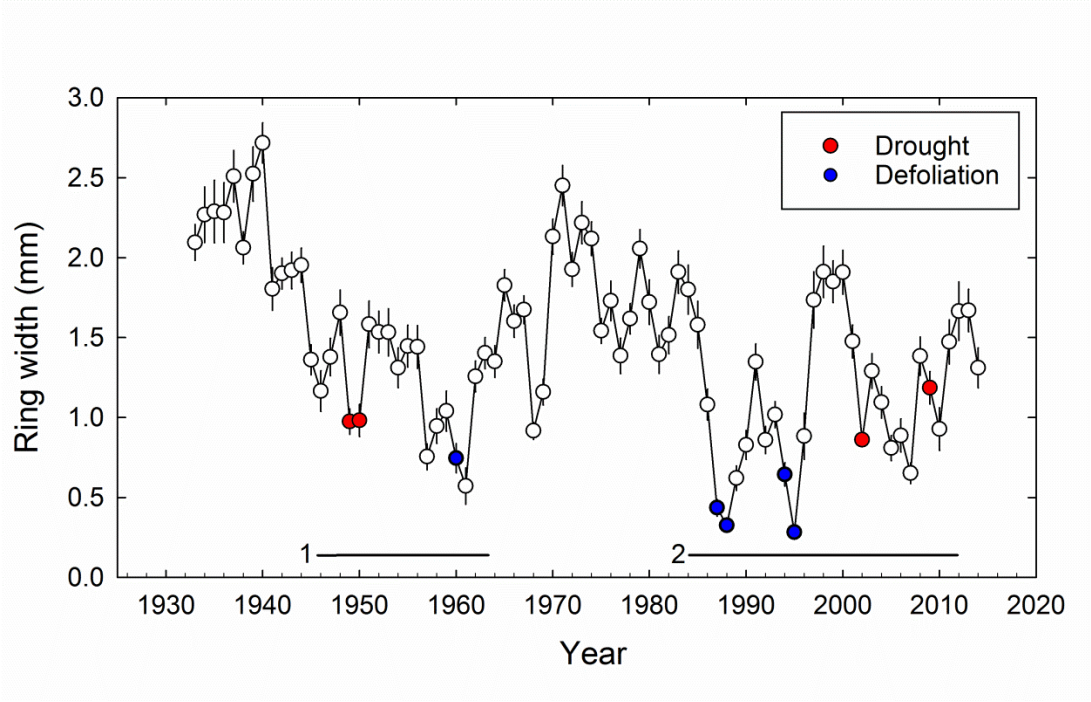

Figure 3.1
Chronology of aspen ring width. Points in red indicate years with Climate Moisture Index (CMI) values lower than -15 cm, indicating a severe drought. Points in blue indicate years with "white rings," a sign of defoliation. Horizontal black bars indicate the lengths of the series which were chosen for further wood anatomy measurements: 1946-1963 (Age Group 1) and 1984-2012 (Age Group 2), respectively. Error bars indicate standard error of the mean (n=40).

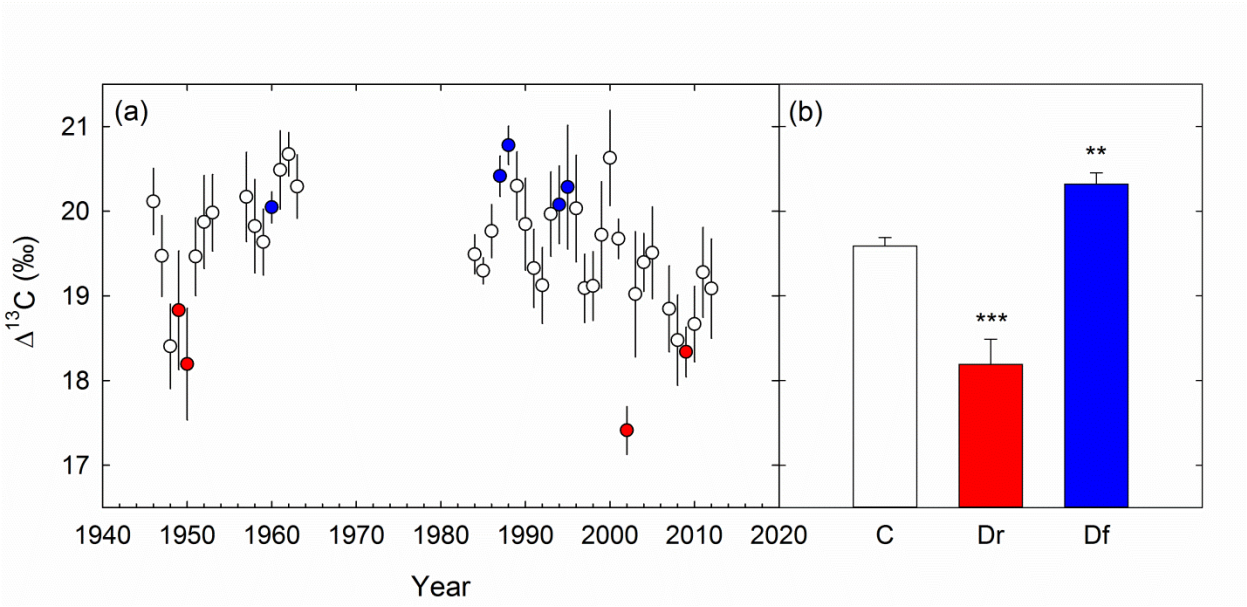

Figure 3.2

Chronology of $\Delta^{13}C$ values for both Age Groups, n=4 (a). Points in red indicate drought, and points in blue indicate defoliation years. Right (b), the mean $\Delta^{13}C$ values for each group are presented with an ANOVA test of significance comparing drought to control values and defoliation with control. Error bars indicate standard error of the mean and stars indicate significant differences at a $P<0.001$*** and $P<0.01$**; C=control, Dr=drought, Df=defoliation.

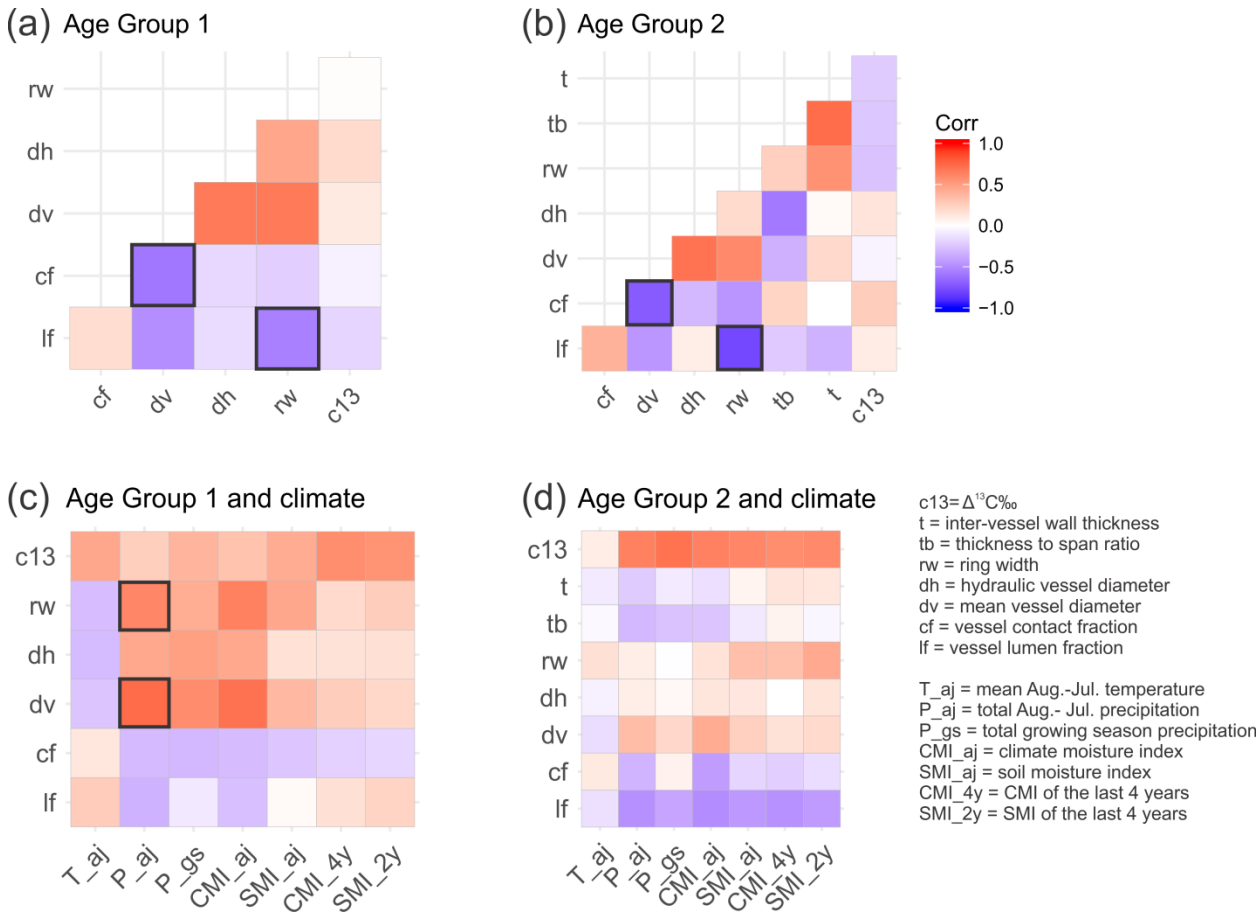

Figure 3.3

Pearson's r correlations of wood anatomical variables with other wood anatomical variables in Age Group 1 (a) and Age Group 2 (b). Pearson's r correlations of wood anatomical and climate variables for Age Group 1(c) and Age Group 2 (d), in which years of defoliation were removed from the analyses. Wood anatomy correlations with climate were generally stronger with Age Group 1: here, mean vessel diameter (*dv*) showed a strong positive relationship with annual and seasonal precipitation variables – a slightly stronger relationship than ring width (*rw*) and precipitation. For *rw*, only the rings used for anatomical measurements were included in these analyses. Resulting *P*-values for these correlations can be found in Tables S1-S4. Black outlines indicate wood anatomy relationships that are explored in more depth in Figs. 4-7. Due to time constraints and section quality, *t* and *tb* were only measured for Age Group 2.

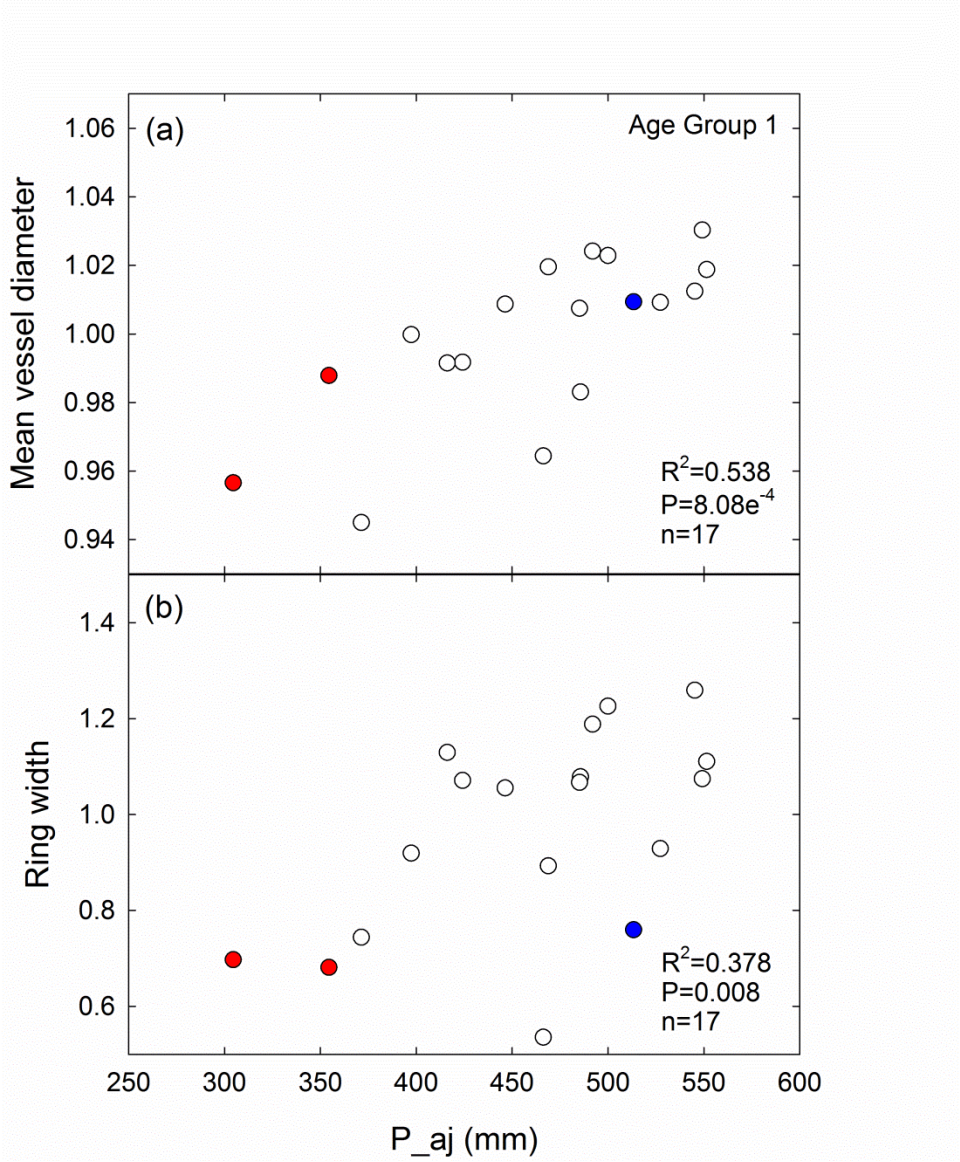

Figure 3.4

A significant correlation was found between the standardized mean vessel diameter values and August to July precipitation (P_aj) in Age Group 1 (a). A still significant, though weaker, correlation was found for the standardized ring width values and P_aj (b). Red points indicate drought and blue points indicate years of defoliation. Defoliation years were removed from the analysis.

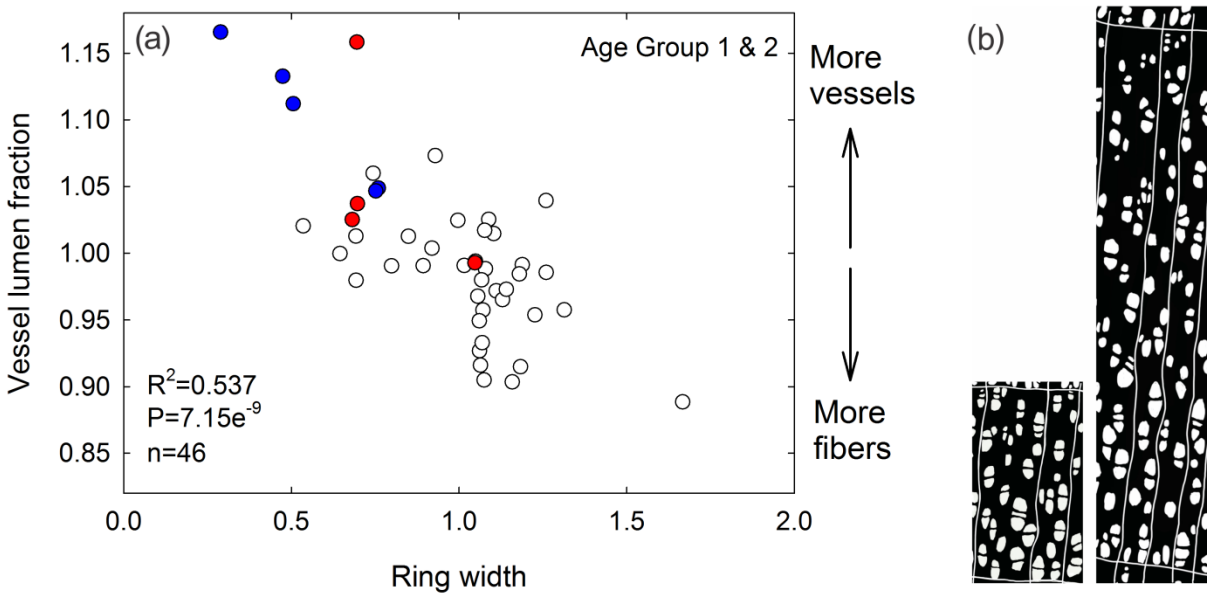

Figure 3.5

Ring width vs. vessel lumen fraction (standardized values) for both Age Groups (a). Vessel lumen fraction represents the proportion of vessel lumen area per xylem area across the entire ring. Within both groups, the defoliation years are characterized by small ring width and high vessel lumen fraction. Red points indicate years of drought and blue points indicate years of defoliation. The semi-ring porous nature of aspen tree rings is illustrated: larger rings tend to have less vessel lumen area, as the trees produce smaller vessels and a higher proportion of fiber area in the latewood (b).

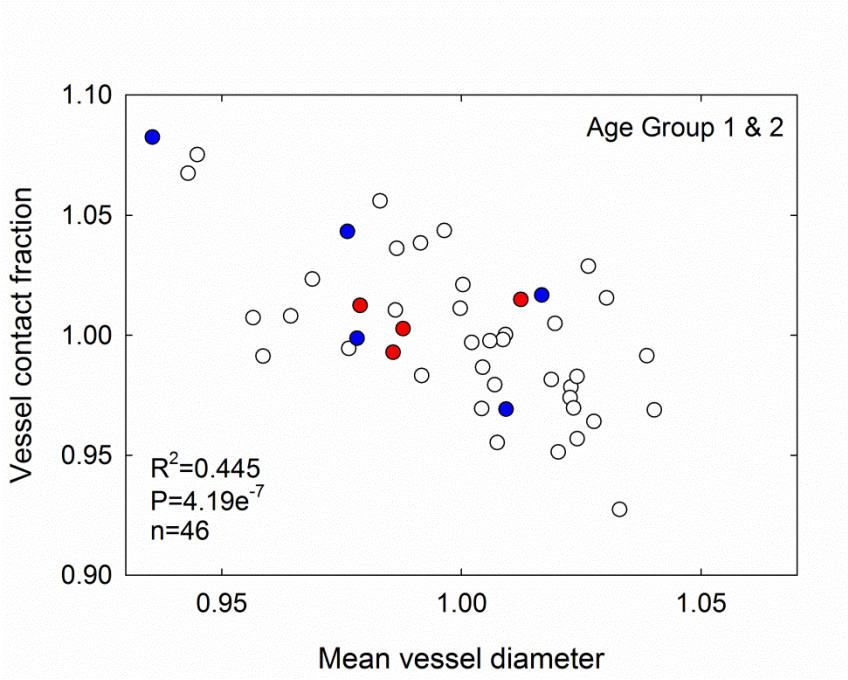

Figure 3.6

Mean vessel diameter vs. vessel contact fraction (standardized values) for both wood Age Groups. Across both groups, tree rings with smaller vessels tend to also have vessels in greater contact with each other. Red points indicate years of drought, and blue points indicate years of defoliation.

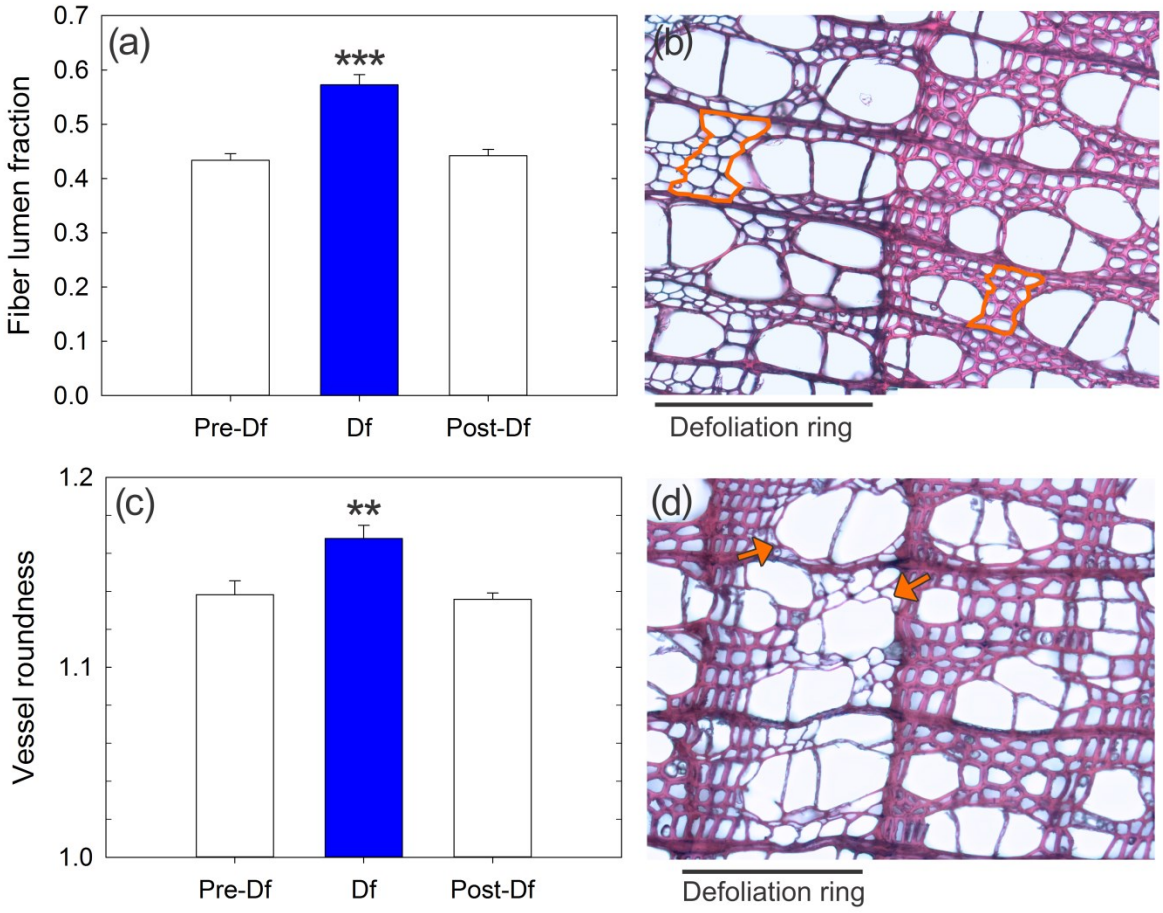

Figure 3.7

Bar graph showing the mean fiber lumen fraction for rings in the year immediately preceding, during, and post a 1 or 2 year defoliation event; bars represent the mean of all tree rings per all relevant years (Pre-Df=18, Df=30, Post-Df=18) (a). Cross section of two adjacent tree rings; circles in orange exemplify how fiber lumen fraction was measured (b). Vessel roundness in the year immediately preceding, during, and post a 1 or 2 year defoliation, measured for rings in Age Group 2 (Pre-Df=10, Df=20, Post-Df=10). A value of 1 indicates a perfect circle while values higher than 1 are less circular (c). Cross section of two adjacent tree rings with visibly less round vessels in the years of defoliation, as indicated by arrow (d). Error bars indicate standard error of the mean. Stars indicate significant differences at a $P<0.001$*** and $P<0.01$**; Df=Defoliation.

3.9 Supporting Information

Table 3.S1. P-values for Pearson's r correlations of wood anatomical variables with other wood anatomical variables in Age Group 1.

Values < 0.05 are in bold. Abbreviations are as follows: vessel lumen fraction (lf), vessel contact fraction (cf), mean vessel diameter (dv), hydraulic vessel diameter (dh), ring width (rw), $\Delta^{13}C$ (c13).

	lf	cf	dv	dh	rw	c13
lf						
cf	0.463					
dv	**0.038**	**0.010**				
dh	0.560	0.512	**0.003**			
rw	**0.018**	0.407	**0.003**	0.055		
c13	0.530	0.834	0.684	0.506	0.966	

Table 3.S2. P-values for Pearson's r correlations of wood anatomical variables with other wood anatomical variables in Age Group 2.

Values < 0.05 are in bold. Abbreviations are as follows: vessel lumen fraction (lf), vessel contact fraction (cf), mean vessel diameter (dv), hydraulic vessel diameter (dh), ring width (rw), vessel thickness to span ratio (tb), intervessel wall thickness (t), $\Delta^{13}C$ (c13).

	lf	cf	dv	dh	rw	tb	t	c13
lf								
cf	**0.034**							
dv	**0.017**	**0.000**						
dh	0.632	0.109	**0.000**					
rw	**0.000**	**0.014**	**0.001**	0.343				
tb	0.231	0.251	0.080	**0.001**	0.207			
t	0.087	0.991	0.301	0.895	**0.002**	**0.000**		
c13	0.624	0.186	0.802	0.462	0.175	0.224	0.267	

Table 3.S3. P-values for Pearson's r correlations of wood anatomical variables with climate variables for Age Group 1.

Values < 0.05 are in bold. Abbreviations are as follows: vessel lumen fraction (lf), vessel contact fraction (cf), mean vessel diameter (dv), hydraulic vessel diameter (dh), ring width (rw), $\Delta^{13}C$ (c13), August-July temperature (T_aj), August to July precipitation (P_aj), May to September "growing season" precipitation (P_gs), August to July Climate Moisture Index (CMI_aj), August to July Soil Moisture Index (SMI_aj), 4-year mean Climate Moisture Index (CMI_4y), 2-year mean Soil Moisture Index (SMI_2y).

	lf	cf	dv	dh	rw	c13
T_aj	0.293	0.627	0.333	0.256	0.276	0.103
P_aj	0.195	0.251	**0.001**	0.068	**0.009**	0.381
P_gs	0.706	0.231	**0.013**	**0.044**	0.088	0.171
CMI_aj	0.284	0.265	**0.002**	0.069	**0.006**	0.271
SMI_aj	0.910	0.350	0.144	0.548	0.064	0.126
CMI_4y	0.533	0.448	0.313	0.557	0.455	**0.030**
SMI_2y	0.381	0.506	0.432	0.538	0.307	0.041

Table 3.S4. P-values for Pearson's r correlations of wood anatomical variables with climate variables for Age Group 2.

Values < 0.05 are in bold. Abbreviations are as follows: vessel lumen fraction (lf), vessel contact fraction (cf), mean vessel diameter (dv), hydraulic vessel diameter (dh), ring width (rw), vessel thickness to span ratio (tb), intervessel wall thickness (t), $\Delta^{13}C$ (c13), August-July temperature (T_aj), August to July precipitation (P_aj), May to September "growing season" precipitation (P_gs), August to July Climate Moisture Index (CMI_aj), August to July Soil Moisture Index (SMI_aj), 4-year mean Climate Moisture Index (CMI_4y), 2-year mean Soil Moisture Index (SMI_2y).

	lf	cf	dv	dh	rw	tb	t	c13
T_aj	0.686	0.425	0.344	0.463	0.732	0.866	0.576	0.979
P_aj	**0.001**	**0.020**	**0.042**	0.429	0.314	**0.029**	**0.026**	**0.000**
P_gs	**0.003**	0.240	0.201	0.797	0.707	0.059	**0.025**	**0.000**
CMI_aj	**0.000**	**0.008**	**0.020**	0.318	0.211	**0.039**	0.070	**0.000**
SMI_aj	**0.000**	**0.038**	0.094	0.584	0.101	0.166	0.192	**0.000**
CMI_4y	**0.000**	0.075	0.209	0.892	0.084	0.456	0.443	**0.000**
SMI_2y	**0.000**	0.060	0.143	0.637	**0.044**	0.277	0.333	**0.000**

4 Defoliation constrains xylem and phloem functionality

4.1 Summary

Insect defoliation contributes to tree mortality under drought conditions. Defoliation-induced alterations to the vascular transport structure may increase tree vulnerability to drought; however, this has been rarely studied. To evaluate the response of tree vascular function following defoliation, 2-year old balsam poplar were manually defoliated and both physiological and anatomical measurements were made after allowing for re-foliation. Hydraulic conductivity measurements showed that defoliated trees had both increased vulnerability to embolism and decreased water transport efficiency, likely due to misshapen xylem vessels. Anatomical measurements revealed novel insights into defoliation-induced alterations to the phloem. Phloem sieve tube diameter was reduced in the stems of defoliated trees, suggesting reduced transport capability. And, phloem fibers were absent, or reduced in number, in stems, shoot tips, and petioles of new leaves. The reduction in phloem fiber area may reduce the stability of the vascular tissue, but also potentially allows for the continued function of previous year's sieve tubes in the stem. Results from this study suggest that defoliation leads to trees with increased risk for vascular dysfunction and drought-induced mortality through alterations in the vascular structure.

4.2 Introduction

Forest dieback and mortality due to climate warming and drought has been reported on a global scale (Allen et al. 2010). The mechanism of drought-induced mortality is often discussed through the lens of resource limitation, while noting that biotic agents such as insect pests may have a strong amplifying effect on tree stress (McDowell et al. 2008; Anderegg et al. 2015). Although

many studies have focused on the impacts of drought stress, "insect defoliation is one of a number of periodic stressors of trees that is rarely brought to bear on ongoing discussions of carbon (C) starvation or hydraulic limitation hypotheses" (Foster 2017, p. 1152).

One way insect attacks may promote tree mortality is through induced structural and functional alterations, especially in the vascular tissue. The plant vascular tissue provides the essential functions of water and sugar transport within the cells of the xylem and phloem (Evert 2006). The evaluation of changes in xylem anatomy allows for inferences to be made about associated changes in water transport function (Fonti et al. 2010). And, hydraulic measurements give direct insight into the functioning of the xylem: measures of hydraulic conductivity provide a characterization of water transport efficiency, while measures of xylem vulnerability to cavitation and embolism characterize transport safety (Gleason et al. 2016). Plasticity of these traits has been exhibited in relation to factors such as drought (Beikircher & Mayr 2009; Corcuera et al. 2011), nutrient fertilization (Plavcová et al. 2013), salinity (Janz et al. 2012), and shade conditions (Schoonmaker et al. 2010; Plavcová & Hacke 2012).

Insect damage as a cause for changes in xylem structure and function, however, has been less studied. Insect pest species differ in the timing of their predation, and their impact on forests (Pureswaran et al. 2018), leading to a variety of potential impacts on tree physiology. For example, bark beetle attack may alter water movement by inducing reductions in transpiration (Hubbard et al. 2013). Measurements of xylem function have shown that Hemlock woolly adelgid infestation alters xylem specific conductivity in trees, potentially because of changes in xylem tracheid diameter (Domec et al. 2013; Huggett et al. 2018). However, changes in the xylem structure of aspen (*Populus tremuloides* Michx.) due to insect defoliation suggest that the xylem will be more

vulnerable to cavitation (Hillabrand et al. 2018) and the impact of this defoliation on phloem has not been assessed at all.

Trembling aspen and the closely related species balsam poplar (*Populus balsamifera* L.) are known to be defoliated by the forest tent caterpillar (*Malacosoma disstria* Hbn) (Hildahl & Reeks 1960; Peterson & Peterson 1992). Defoliation by the caterpillar is a significant factor affecting inter-annual growth in aspen forests (Hogg et al. 2005) and prolonged outbreaks have been observed to cause significant mortality in the forest over-story (Man & Rice 2010). This is a potential concern in western Canada, where insect outbreaks that affect trembling aspen forests may be triggered by warmer spring temperatures (Chen et al. 2017). However, the full influence of forest tent caterpillar defoliation on tree functioning is still yet to be understood.

The forest tent caterpillars hatch just as bud-burst and first leaf emergence occurs, and their predation can lead to complete defoliation of their hosts (Fitzgerald 1995). Outbreaks of the caterpillar can occur in cyclic patterns (Cooke & Lorenzetti 2006). In terms of stem tissue, the most characteristic result of severe defoliation is the formation of abnormal tree rings which appear pale-colored in dried samples. These rings are termed "white rings" and are found in balsam poplar as well as aspen (Hogg & Schwarz 1999; Hogg et al. 2002), contain fibers with thinner walls (Sutton & Tardif 2005), and irregularly shaped xylem vessels (Hillabrand et al. 2018). Xylem fibers with thinner walls, adjacent to vessels, may be unable to allow vessels to resist implosion (Jacobsen et al. 2005), likely explaining the observed reduced roundness of vessels. These changes in the xylem anatomy imply a reduction in the safety of water transport, by way of increased vulnerability to cavitation. However hydraulic measurements have not yet been conducted to confirm this.

Additionally, there is a lack of information concerning the impact of defoliation on phloem anatomy and physiology. With such pronounced changes observed in the xylem, it is conceivable that the loss of early spring photosynthates also alters phloem structure and function. As the tissue through which sugars are transported, the phloem is vital to plant functioning (Evert 2006). Though it is difficult to study, the ties between the phloem and the xylem suggest that stress such as drought may negatively influence phloem transport (Sevanto 2014, 2018). It has been observed that water stress can reduce phloem conduit diameters in trees, lowering the potential phloem conductivity and efficiency of transport (Woodruff 2013; Dannoura et al. 2018). It remains to be seen if defoliation also produces observable changes in the phloem anatomy.

In this experiment, our objective was to study the impacts of insect defoliation on the development and function of both xylem and phloem. By experimentally defoliating 2-year old balsam poplar, we aimed to determine the effect of defoliation on tree hydraulic conductivity and vulnerability to cavitation, hypothesizing that the xylem of defoliated trees would be more vulnerable. And secondly, we aimed to investigate potential alterations in function of the phloem through anatomical measurements.

4.3 Methods

Plant material and treatment

Two year-old potted balsam poplar trees, originated from branch cuttings, were brought into a growth chamber in mid-January 2018, after overwintering outdoors. Conditions in the growth chamber were controlled for daily temperatures of 21°C and nightly temperatures of 19°C with a day length of 16 hours. Trees were fertilized twice a week with a 30:8:8 N:P:K solution. From a total of ten trees, five trees were assigned as controls. A complete defoliation of five other

trees occurred on February 22nd after all trees in the experiment showed leaf expansion. Trees were defoliated again every four days for the following two weeks to mimic an infestation of the forest-tent caterpillar. Trees were harvested for conductivity and anatomical measurements eight weeks after the initial defoliation, after allowing for new apical growth and growth of new leaves in the defoliation treatment.

Hydraulic measurements

All trees were harvested for hydraulic conductivity measurements. A sample segment consisting of a stem with two years of growth cut to 14.2 cm in length was collected from each individual tree. This gave a sample size of five for each treatment. Hydraulic conductivity was measured with a flow-balance system and recorded as bulk flow divided by the pressure gradient (Sperry et al. 1988). Following measurements of native conductivity, one hour of vacuum infiltration was used to remove embolism from the samples. Each stem sample was spun to increasingly negative pressures using the standard centrifuge method (Alder et al. 1997; Hacke et al. 2015). At each pressure, the hydraulic conductivity of each stem was measured and recorded. The values of hydraulic conductivity were converted into percent loss of conductivity (PLC) from their maximum, and then averaged for each treatment to create vulnerability curves. These values were divided by the xylem area of each stem sample to create curves of xylem specific conductivity (K_s); both xylem rings in each tree were assumed to be conductive. Leaf specific conductivity (LSC) was calculated by dividing the native and maximum values of hydraulic conductivity by all leaf area attached to and distal from the sample segments. Additionally, the leaf area of each sample was also divided by the xylem area to calculate the leaf area to sapwood area ratio (A_L:A_S).

Anatomical measurements

For anatomical measurements of the vascular tissue, one sample from each of three different locations (stem, shoot tip, petiole) were saved from each individual tree. Stems with 2 years of growth were saved from the conductivity measurements (stems), and samples of new, post-defoliation apical growth were collected 4 cm from the shoot tip (shoot tips). Petiole samples also were taken from leaves of similar developmental age from growth produced after the treatment near the shoot tip (between 4 and 6 leaves down from the apical meristem) in both control and defoliated trees (petioles). All samples used in the preparation of micro-sections were fixed in FAA (Formalin-Acetic-Alcohol) for one week and then embedded in paraffin wax. Micro-sections 8 µm in thickness were created using a rotary microtome (Leica RM 2125) and double stained with safranin and aniline blue. Due to the trees being 2 years-old, the sections were quite wide and broke at the cambium during sectioning, causing separation between the xylem and phloem tissues in samples from both the control and defoliation treatments.

In stems and shoot tips, measurements of vessel diameter (dv) were made as an average of all vessels across a ring of xylem between 3-4 xylem rays in the outermost annual ring which was formed after defoliation. This measurement was done at 3 points around a cross section and averaged to create a grand mean per tree. Vessel diameters were converted to hydraulic vessel diameters (dh) (Sperry et al. 1994) with the equation:

$$dh = \frac{\sum dv^5}{\sum dv^4} \quad (4.1)$$

Ten vessels per each cross section of stem and shoot tip tissue within ±5 microns of the mean hydraulic vessel diameter were measured for vessel roundness and were averaged per tree. Vessel roundness was calculated by ImagePro Premier with the ratio:

$$roundness = \frac{Perimeter^2}{4\pi Area} \quad (4.2)$$

where a value of 1 represents the ratio of a perfect circle (note this equation is the correct form, Hillabrand et al. (2018) erroneously flipped the numerator and denominator in their depiction of the equation). Values greater than 1 indicate deviation from the ideal shape.

The phloem tissue was stained by aniline blue and sieve tubes were distinguished from companion and parenchyma cells by size and shape. Sieve tube diameter was measured across bands of sieve tubes in the center of the annually produced phloem between 3-4 phloem rays in stems and shoot tips. This measurement was also done at 3 points around each cross section and averaged to create a grand mean per tree. Sieve tubes with diameters within ±2 microns of the mean were also measured for roundness. Additionally, in the 2 year-old stems, sieve tube roundness was also measured in the previous year's phloem. This was done to examine how altered phloem development in the current year influenced the older phloem structure. Sieve element length was measured from longitudinal sections of shoot tips only in order to be sure that phloem measured was produced in the year of defoliation.

To make observations of relative xylem and phloem growth, additional measurements were made in stems, shoot tips, and petioles. Ratios of the current year xylem area to phloem area, and the phloem fiber area to total current year phloem area were made radially across the area contained between the extent of the same parenchyma rays through both xylem and phloem. Additionally, a count was made of the number of phloem cell layers produced by the cambium in the stem and shoot tip samples. All measurements were made using Image Pro Premier (ImagePro Premier, Media Cybernetics, Rockville, MD, USA).

Statistical Analysis

Statistical analyses were performed using the software R (R core team 2016). The normality of the data for each measurement was assessed with the Shapiro-Wilk test. Bartlett's test was used to assess equality of variances between treatments. Student's t tests were performed to determine significant differences between treatments for hydraulic and anatomical measurements. The ratio of phloem fiber area to total phloem area measurements for stems and petioles contained multiple zeros for the defoliation treatment leading to unequal variances between treatments. Therefore, the presence or absence of phloem fibers was considered as categorical data for stems and petioles and the Z test of proportions was used to test for treatment differences.

4.4 Results

Xylem vulnerability curves, showing percent loss of conductivity of stems of defoliated trees and those in the control treatment were significantly different at several xylem pressures (-1.25, -1.5, and -2.0 MPa), showing increased vulnerability to cavitation in the defoliation treatment (Fig. 4.1a). Xylem specific conductivity of the defoliated trees was also lower than in control trees across the entire pressure range, showing reduced efficiency. The difference was significant at -1.25, -1.5, and -2.0 MPa (Fig. 4.1b). Though the maximum xylem specific conductivity (0 MPa) and other points along the curve were lower for the defoliated trees, these differences were not statistically significant, possibly a result of the low sample size. Additionally, native xylem specific conductivity values indicated that control trees were experiencing greater levels of embolism (Table 4.1). Leaf specific conductivity values did not differ significantly between treatments, however, again these values suggested greater amounts of native embolism in the

control treatment (Table 4.1). The leaf area to sapwood area ratio was significantly decreased in defoliated trees (Table 4.1).

The defoliation treatment produced narrow rings: these rings were reduced in area as compared to the xylem rings in the control treatment (Fig. 4.2). Characteristic of forest-tent caterpillar defoliation, these rings visually appeared to be white and less dense with thinner fiber walls (Fig 4.2, arrows) and irregularly shaped vessels (Fig. 4.2, asterisks). And, in cross sections stained with safranin and aniline blue, there was more blue staining in the narrow rings, as the safranin did not stain the xylem as strongly (Fig. 4.2, arrows). This suggests that some portions of the rings were less lignified.

Anatomical measurements of vascular tissue characteristics in the same stem samples as the hydraulic measurements showed no difference in xylem vessel diameter (Fig 4.3a), but did show reduced vessel roundness, or increased vessel shape irregularity, in the defoliation treatment (Fig. 4.3b). Interestingly, phloem sieve tube diameter was significantly decreased in the defoliation treatment (Fig. 4.3c). Measurements of sieve tube roundness in the stem indicated that current year sieve tubes were slightly more irregularly shaped in the defoliation treatment, though not significantly (Fig. 4.4a). However, sieve tubes produced in the previous year were significantly more round in the defoliation treatment (Fig. 4.4b).

Across all plant organs (stems, shoot tips, petioles), ratios of xylem area, phloem area, and phloem fiber cap area for tissue produced in the year of defoliation (2018) showed treatment differences. The phloem fiber to total phloem area ratio was consistently and significantly lower in the defoliated trees (Fig. 4.5a-c). In stems of control trees, the division between current year's phloem and the previous year's phloem was marked by wide bands of phloem fibers (fiber cap) (Fig. 4.6a, arrow). In contrast, current year phloem fibers were often completely absent in stems

of defoliated trees (Fig. 4.6b, arrow), instead showing a division with the previous year's phloem marked by a line of small cells. As well, phloem fibers were often absent in the petioles of leaves produced after defoliation (Fig. 4.7). The ratio of xylem area to phloem area was unchanged in shoot tips and petioles; however the absolute areas were, as expected, much larger in stems of the control treatment, where 4-fold more xylem was produced than in the defoliation treatment (Table 4.2).

For an additional measure of phloem production, the number of layers of phloem cells (sieve tubes) produced in the current year were counted. In stems, the average phloem cell count was slightly smaller in the defoliation treatment, but not significantly different (Table 4.2). This measurement and several anatomical characteristics were also assessed in samples collected from the shoot tip. No significant differences were found between treatments: these results are available in Table 4.S1.

4.5 Discussion

Our first objective was to study the effects of defoliation on xylem hydraulic conductivity and vulnerability to cavitation. Consistent with our hypothesis, the xylem of defoliated trees was more vulnerable to cavitation. This reduction in transport safety was likely caused by defoliation-induced changes in xylem fiber properties. Fibers with thin and potentially less lignified cell walls, as visually observed in this study and previously (Sutton & Tardif 2005; Hillabrand et al. 2018), are providing reduced structural support to vessels as evidenced by vessels which are more irregular in shape. These partially imploded vessel walls then may allow for air seeding through micro-fractures in the wall or through stretching of pit membranes (Jacobsen et al. 2005). An increased vulnerability to cavitation and embolism increases the risk for tree mortality due to

drought (Anderegg et al. 2016), indicating a potential method in which insect defoliation intensifies the stress of drought on tree function.

Water transport efficiency was also reduced in defoliated trees. Measurements of xylem specific conductivity indicated that when stem conductivity was normalized by xylem area, the defoliated trees' conductivity was lower. This finding indicates that balsam poplar do not have a compensatory response in xylem production and efficiency to defoliation as has been observed in other species (Salleo et al. 2003; Huggett et al. 2018). Because mean vessel diameter was not significantly different between treatments, it is possible that the lower conductivity values can also be attributed to misshapen xylem vessels; deviations in shape from the ideal circle can greatly reduce the efficiency of laminar flow through vessels according to the Hagen-Poiseuille model (Tyree & Zimmerman 2002).

Though xylem hydraulic measurements showed both reduced transport safety and efficiency, it is notable that the native conductivities of defoliated trees indicated lower levels of embolism. After the defoliation treatment, and subsequent re-growth of leaves, the leaf area to sapwood area ratio was significantly decreased compared to trees in the control treatment. Likely, the reduced number of leaves transpiring induced less negative water potentials. However, in contrast to the findings of Domec et al. (2013) for defoliated hemlock, there was a lack of a coinciding increase in leaf specific conductivity with the decrease in A_L:A_S. This finding is also indicative of impaired, or less efficient xylem supplying water to the leaves. Though initially the loss of leaves benefits the water status of defoliated trees, when the leaf area recovers in subsequent years, water transport functionality may still be impaired. Diffuse-porous trees utilize multiple rings, and the xylem produced during the year of defoliation will remain reduced in both safety and efficiency.

Our second objective was to investigate whether defoliation alters phloem development and putative function. Observations of the phloem anatomy of the two-year old main stem revealed further insights into the impacts of defoliation on the vascular tissue. Anatomical measurements of the phloem indicated a 20% reduction in stem sieve tube diameters (Fig. 4.3c). Smaller sieve tubes have been observed previously due to water stress, likely impacting transport efficiency, and it has been suggested that low turgor pressure at the time of cell development may drive this anatomical change (Woodruff 2013; Dannoura et al. 2018). Cell expansion is a turgor driven process that requires both water and solutes (Taiz & Zeiger 2006). However instead of experiencing a lack of water, the reduced ability of defoliated trees to photosynthesize may instead lead to a lack of adequate solutes for sieve tube expansion. Visually, the idea that sieve tube members do not fully expand may be corroborated by the finding that these sieve tubes were slightly more irregularly shaped (Fig. 4.4a) and appeared compressed and lacking in organization when compared to the previous year's phloem (See Fig. 4.6a-b).

An interesting finding was the reduction in phloem fiber area within trees of the defoliation treatment. These phloem fibers have been noted to occasionally be absent from aspen stems in small increment growth years (Davis & Evert 1968), suggesting that when resources are low, fiber development is inhibited. Fibers strengthen the bark and may function as a barrier against attacks by insects and fungi (Franceschi et al. 2005); however, the reduction or absence of phloem fiber area may also have negative effects on the phloem function. Due to the thickened cell walls of fibers, it is likely that phloem fiber caps contribute to the structural integrity of the phloem as well as the entire vasculature before secondary growth of woody tissue is completed. Defoliated trees did not grow as tall; however they did put on new apical growth after the treatment. The observation that phloem fiber caps, though reduced in area, were still more present within the shoot

tips of defoliated trees than the stems of defoliated trees (where they were often entirely absent in the current year's phloem), suggests that they were at least partially conserved in the shoot tips out of necessity to support stem elongation and the new vascular tissue. Indeed, the ability of the stem to resist bending is maximized by having the stiffest material in the periphery (Niklas 1992).

Notably, when comparing the phloem between trees of the control and defoliation treatments, the previous year's sieve tubes are significantly more round in defoliated trees (Fig 4.4b), and appear to remain uncrushed (Fig. 4.6a-b). Unlike the cells in the previous year's phloem of the control treatment, the roundness of these cells indicates pressurization. This presents the possibility that a greater proportion of sieve tubes may yet remain functional later into the growing season. And, this appearance may be an additional result of the lack of phloem fibers in the defoliated trees. The normal development of fibers may inevitably crush older sieve tubes; without the development of fibers, it is possible that older sieve tubes remain functional. Although this does not preclude the possibility that the sieve plates of old phloem are plugged and therefore non-functional (Van Bel 2003), based on cell appearance there remains a potential for transport within these cells.

Overall, this study highlights the strong impact of defoliation on the fiber structure and transport capability of both the xylem and phloem, and illustrates an interaction between carbon and hydraulic limitations. In the xylem, the most direct result of defoliation was observed in the fiber wall thickness, while alterations in vessel structure were likely an indirect consequence of a weaker matrix around the vessels. These alterations to fibers under the carbon limited conditions of defoliation indicate a potential route through which carbon starvation influences hydraulic failure when considering mechanisms of tree death. Similarly, within the phloem, the reductions in fiber area and sieve tube diameters because of defoliation suggest ways in which carbon

limitation interacts with the functionality of phloem transport. Though this experiment utilized small trees, the previous observations of defoliation-induced alterations in xylem structure in mature trees (Sutton & Tardif 2005; Hillabrand et al. 2018) suggest that alterations to the phloem can also be found in mature trees. Likely, alterations in vascular transport may be observed in mature trees as well.

4.6 Conclusions

Taken together, these observations of defoliation-induced changes in the anatomy and physiology of balsam poplar suggests that defoliated trees are at a greater risk for mortality from drought. Hydraulic conductivity measurements indicated that defoliated trees were more vulnerable to cavitation and also had lower xylem-specific conductivities, supporting our hypothesis and indicating both reduced transport safety and efficiency. The reduced leaf area to xylem area ratio did not increase maximum leaf specific conductivity in defoliated trees, again indicating xylem with reduced efficiency. Anatomical measurements yielded novel insight into potential effects of defoliation on phloem function. Observations of reduced sieve tube diameters in defoliated trees also implied reduction in transport efficiency. Reduced phloem fiber production may lead to a reduction in the stability of new vascular tissue, but could allow for the continued function of old sieve tubes. The lack of early season photosynthates appeared to have a wide impact on the functioning of the entire vascular transport system, and indicated mechanisms through which defoliation contributes to tree dysfunction and mortality under drought conditions. Further research in this area could examine how long the physiological effects of defoliation impact these trees for a greater understanding of mortality risks.

4.7 References

Allan C.D., Macalady A.K., Chenchouni H., Bachelet D., Mcdowell N., Vennetier M., ..., Cobb N. (2010) A global overview of drought and heat-induced tree mortality reveals emerging climate change risks for forests. *Forest Ecology and Management* 259: 660-684.

Alder N.N., Pockman W.T., Sperry J.S. & Nuismer S. (1997) Use of centrifugal force in the study of xylem cavitation. *Journal of Experimental Botany* 48: 665-674.

Anderegg W.R.L., Hicke J.A., Fisher R.A., Allen C.D., Aukema J., Bentz B., …, Zeppel M. (2015) Tree mortality from drought, insects, and their interactions in a changing climate. *New Phytologist* 208:674-683.

Anderegg W.R.L., Klein T., Bartlett M., Sack L., Pellegrini A.F.A., Choat B., Jansen S. (2016) Meta-analysis reveals that hydraulic traits explain cross-species patterns of drought-induced tree mortality across the globe. *PNAS* 113: 5024-5029.

Beikircher B. & Mayr S. (2009) Intraspecific differences in drought tolerance and acclimation in hydraulics of *Ligustrum vulgare* and *Viburnum lantana*. *Tree Physiology* 29: 765-775.

Chen L., Huang J., Dawson A., Zhai L., Stadt K.J., Comeau P.G., Whitehouse C. (2018) Contributions of insects and droughts to growth decline of trembling aspen mixed boreal forest of western Canada. *Global Change Biology* 24: 655-667.

Cooke B.J. & Lorenzetti F. (2006) The dynamics of forest tent caterpillar outbreaks in Quebec, Canada. *Forest Ecology and Management* 226: 110-121.

Corcuera L., Cochard H., Gil-Pelegrin E., Notivol E. (2011) Phenotypic plasticity in mesic populations of *Pinus pinaster* improves resistance to xylem embolism (P_{50}) under severe drought. *Trees* 25: 1033-1042.

Dannoura M., Epron D., Desalme D., Massonnet C., Tsuji S., Plain C., Priault P., Gérant D. (2018) The impact of prolonged drought on phloem anatomy and phloem transport in young beech trees. *Tree Physiology*. https://doi.org/10.1093/treephys/tpy070

Davis J.D. & Evert R.F. (1968) Seasonal Development of the Secondary Phloem in *Populus tremuloides*. *Botanical Gazette* 129: 1-8.

Domec J.C., Rivera L.N., King J.S., Peszlen I., Hain F., Smith B., Frampton J. (2013) Hemlock woolly adelgid (*Adelges tsugae*) infestation affects water and carbon relations of eastern hemlock (*Tsuga canadensis*) and Carolina hemlock (*Tsuga caroliniana*). *New Phytologist* 199: 452-463.

Evert R.F. (2006) Esau's Plant Anatomy: meristems, cells, and tissues of the plant body: their structure, function, and development (3rd ed.). Hoboken, NJ: Wiley-Interscience.

Fitzgerald T.D. (1995) The Tent Caterpillars. Ithaca, NY: Cornell University Press.

Fonti P., von Arx G., García-González I., Eilmann B., Sass-Klaassen U., Gärtner H., Eckstein D. (2010) Studying global change through investigation of the plastic responses of xylem anatomy in tree rings. *New Phytologist* 185:42-53.

Foster J.R. (2017) Xylem traits, leaf longevity and growth phenology predict growth and mortality response to defoliation in northern temperate forests. *Tree Physiology* 37: 1151-1165.

Franceschi V.R., Krokene P., Christiansen E., Krekling T. (2005) Anatomical and chemical defenses of conifer bark against bark beetles and other pests. *New Phytologist* 167: 353-376.

Gleason S.M., Westoby M., Jansen S., Choat B., Hacke U.G., Pratt R.B., … Zanne A.E. (2016) Weak tradeoff between xylem safety and xylem-specific hydraulic efficiency across the world's woody plant species. *New Phytologist* 209: 123-136.

Hacke U.G., Venturas M.D., MacKinnon E.D., Jacobsen A.L., Sperry J.S & Pratt R.B. (2015) The standard centrifuge method accurately measures vulnerability curves of long-vesselled olive stems. *New Phytologist* 205: 116-127.

Hildahl V. & Reeks W.A. (1960) Outbreaks of the forest tent caterpillar, *Malacosoma disstria* Hbn., and their effects on stands of trembling aspen in Manitoba and Saskatchewan. *The Canadian Entomologist* 92: 199-209.

Hillabrand R.M., Lieffers V.J., Hogg E.H., Martinez-Sancho E., Menzel A., Hacke U.G. (2018) Functional xylem anatomy of aspen exhibits greater change due to insect defoliation than to drought. *Tree Physiology*. https://doi.org/10.1093/treephys/tpy075

Hogg E.H., Brandt J.P., Kochtubajda B. (2005) Factors affecting interannual variation in growth of western Canadian aspen forests during 1951-2000. *Canadian Journal of Forest Research* 35:610-622.

Hogg E.H., Hart M., Lieffers V.J. (2002) White tree rings formed in trembling aspen saplings following experimental defoliation. *Canadian Journal of Forest Research* 32: 1929-1934.

Hogg E.H. & Schwarz A.G. (1999) Tree-ring analysis of declining aspen stands in west-central Saskatchewan. Information Report Nor-X-359. Forestry Canada, Northern Forestry Centre, Edmonton, Alberta.

Hubbard R.M., Rhoades C.C., Elder K., Negron J. (2013) Changes in transpiration and foliage growth in lodgepole pine trees following mountain pine beetle attack and mechanical girdling. *Forest Ecology and Management* 289: 312-317.

Huggett B.A., Savage J.A., Hao G., Preisser E.L., Holbrook N.M. (2018) Impact of hemlock woolly adelgid (*Adelges tsugae*) infestation on xylem structure and function and leaf physiology in eastern hemlock (*Tsuga canadensis*). *Functional Plant Biology* 45: 501-508.

Jacobsen A.L., Ewers F.W., Pratt R.B., Paddock III W.A., Davis S.D. (2005) Do xylem fibers affect vessel cavitation resistance? *Plant Physiology* 139:546-556.

Janz D., Lautner S.,Wildhagen H., BehnkeK., Schnitzler J.P., Rennenberg H.,…, Polle A. (2012) Salt stress induces the formation of a novel type of pressure wood' in two *Populus* species. *New Phytologist* 194, 129–141.

McDowell N., Pockman W.T., Allen C.D., Breshears D.D., Cobb N., Kolb T., ..., Yepez E.A. (2008) Mechanisms of plant survival and mortality during drought: why do some plants survive while others succumb to drought? *New Phytologist* 178: 719-739.

Man R. & Rice J.A. (2010) Response of aspen stands to forest tent caterpillar defoliation and subsequent overstory mortality in northeastern Ontario, Canada. *Forest Ecology and Management* 260: 1853-1860.

Niklas K.J. (1992) Plant Biomechanics. Chicago: The University of Chicago Press.

Plavcová L., Hacke U.G. (2012) Phenotypic and developmental plasticity of xylem in hybrid poplar saplings subjected to experimental drought, nitrogen fertilization, and shading. *Journal of Experimental Botany* 63: 6481-6491.

Plavcová L., Hacke U.G., Almeida-Rodriguez A.M., Li E., Douglas C.J. (2013) Gene expression patterns underlying changes in xylem structure and function in response to increased nitrogen availability in hybrid poplar. *Plant, Cell & Environment* 36: 186-199.

Peterson E.B. & Peterson N.M. (1992) Ecology, management, and use of aspen and balsam poplar in the Prairie Provinces. Special Report 1. Forestry Canada, Northern Forestry Centre, Edmonton, Alberta.

Pureswaran D., Roques A., Battisti A. (2018) Forest Insects and Climate Change. *Current Forestry Reports* 4: 35-50.

R Core Team (2016) R: A language and environment for statistical computing. R Foundation for Statistical Computing, Vienna, Austria. URL http://www.R-project.org/.

Salleo S., Nardini A., Raimondo F., Assunta Lo Gullo M., Pace F., Giacomich P. (2003) Effects of defoliation caused by the leaf miner *Cameraria ohridella* on wood production and efficiency in *Aesculus hippocastanum* growing in north-eastern Italy. *Trees* 17: 367-375.

Schoonmaker A.L., Hacke U.G., Landhausser S.M., Lieffers V.J., Tyree M.T. (2010) Hydraulic acclimation to shading in boreal conifers of varying shade tolerance. *Plant, Cell & Environment* 33: 382-393.

Sevanto S. (2014) Phloem transport and drought. *Journal of Experimental Botany* 65: 1751-1759.

Sevanto S. (2018) Drought impacts on phloem transport. *Current Opinion in Plant Biology* 43: 76-81.

Sperry J.S., Donnelly J.R. & Tyree M.T. (1988) A method for measuring hydraulic conductivity and embolism in xylem. *Plant, Cell and Environment* 11: 35-40.

Sperry J.S., Nichols K.J., Sullivan J.E.M., Eastlack S.E. (1994) Xylem embolism in ring-porous, diffuse-porous, and coniferous trees of northern Utah and interior Alaska. *Ecology* 75: 1736-1752.

Sutton A. & Tardif J. (2005) Distribution and anatomical characteristics of white rings in *Populus tremuloides*. *IAWA Journal* 26:221-238.

Taiz L. & Zeiger E. (2006) Plant Physiology (4th ed.). Sunderland, MA: Sinauer Associates, Inc.

Tyree M.T. & Zimmerman M. (2002) Xylem Structure and the Ascent of Sap. Berlin: Springer Verlag.

Van Bel A.J.E. (2003) The phloem, a miracle of ingenuity. *Plant, Cell and Environment* 26: 125-149.

Woodruff D.R. (2014) The impacts of water stress on phloem transport in Douglas-fir trees. *Tree Physiology* 34: 5-14.

4.8 Figures and Tables

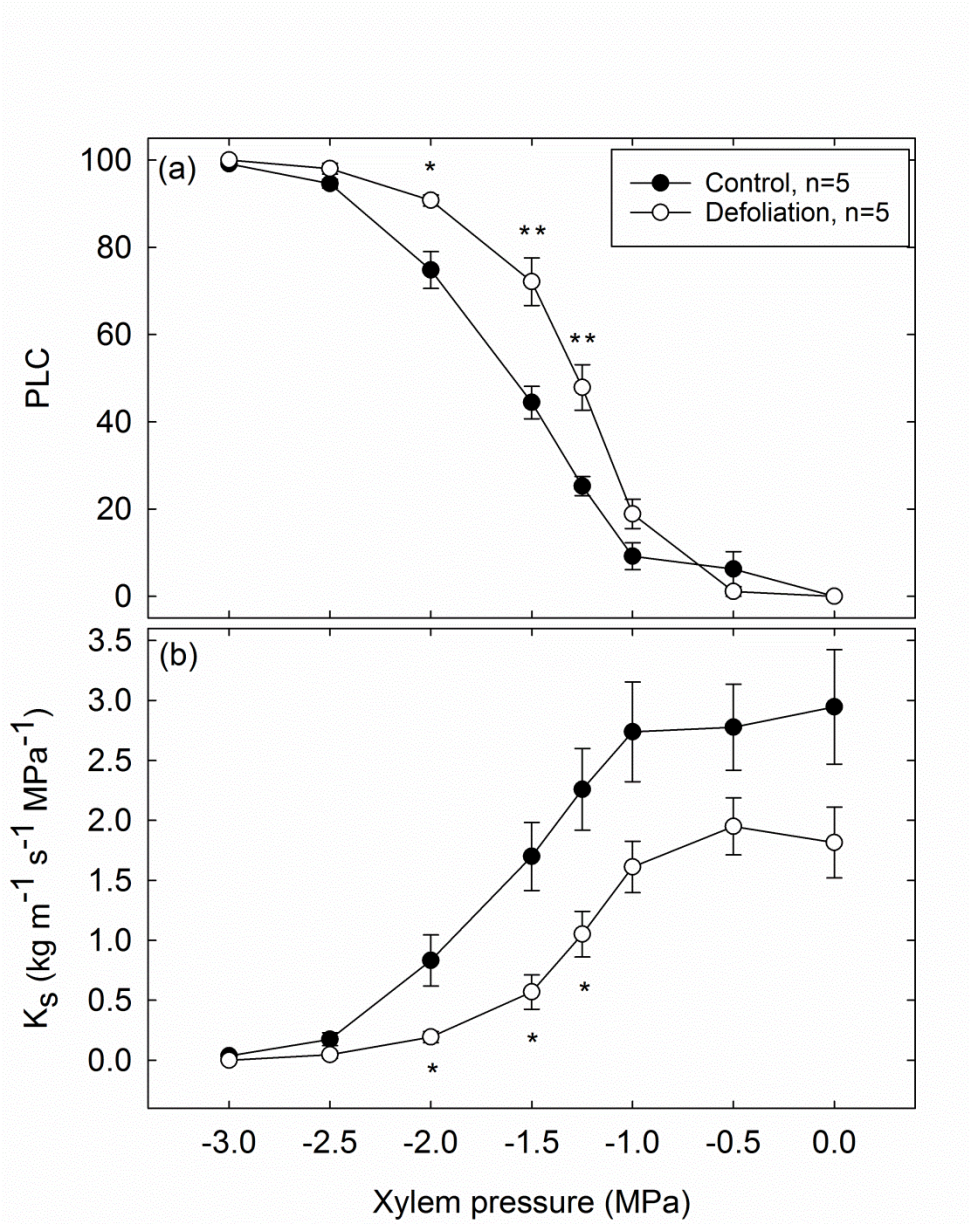

Figure 4.1
Percent loss of conductivity (PLC) and xylem specific conductivity (K_s) for the trees in the control and defoliation treatments. Error bars indicate standard error of the mean. Stars indicate significant differences between treatments (P<0.05*, P<0.01**).

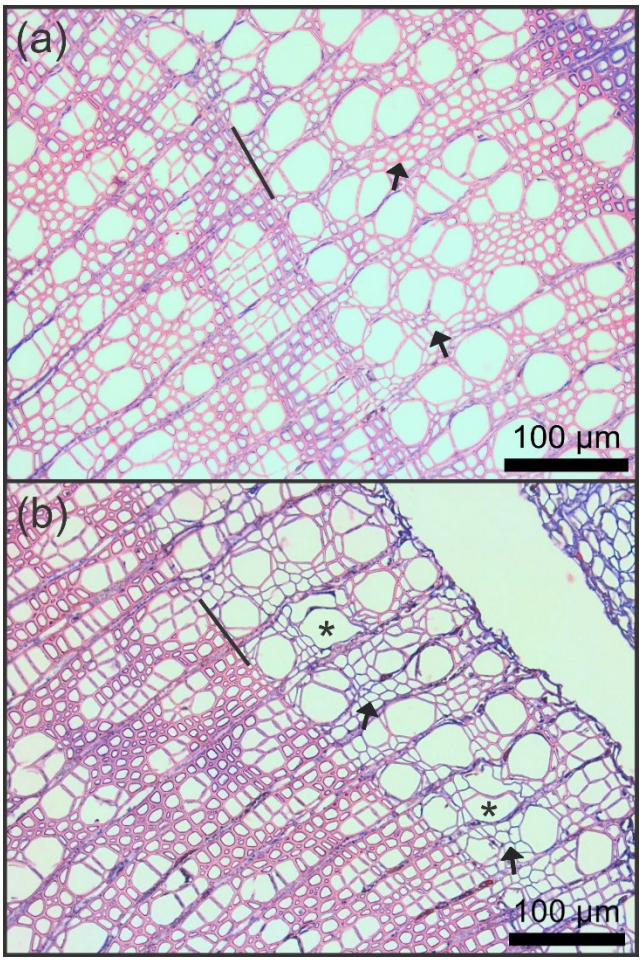

Figure 4.2
Image of a stem cross section from a control tree (a) and defoliated tree (b) showing the structural distinctions in xylem produced for the current year. A black bar denotes the ring boundary where the current year's xylem is to the right. A much narrower xylem ring was produced after defoliation (b) and this ring is seen rupturing at the vascular cambium. Arrows point to areas of fibers with visibly thicker (a) and thinner (b) walls in the current year's xylem. Sections were double-stained with safranin and aniline blue. Patches of fibers were not as strongly stained red by the safranin (b), indicating lower lignin content. Also note the wavy shape of some of the vessels that were produced after defoliation (b; asterisks).

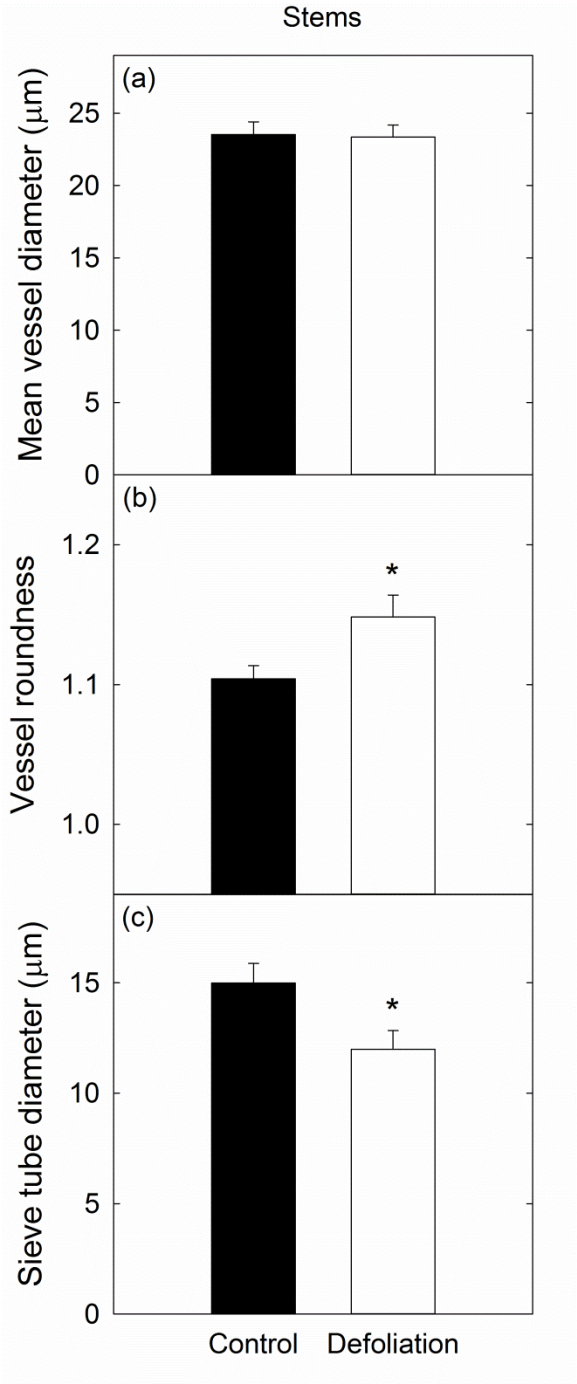

Figure 4.3
Stem anatomical measurements. Mean vessel diameter (a), vessel roundness (b), and mean sieve tube diameter (c) per treatment (n=5 trees). Vessels with roundness values greater than 1 are more irregular in shape. Error bars indicate standard error of the mean. Stars indicate significant differences between treatments (P<0.05*).

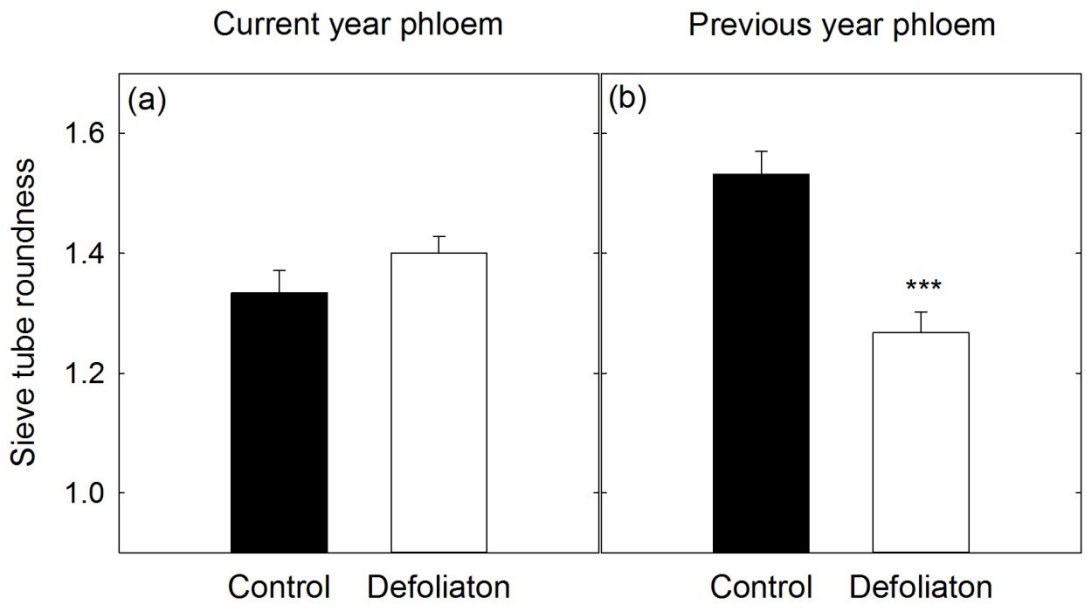

Figure 4.4
Measurements of sieve tube roundness for two years of phloem in the main stems: the current year (a) and the previous year (b). Sieve tube roundness was calculated the same as vessel roundness where values greater than 1 show more irregularity in shape. Graphed values represent the grand means of sieve tube diameters from n=5 stems per treatment. Error bars indicate standard error of the mean. Stars indicate significant differences between treatments (P<0.001***).

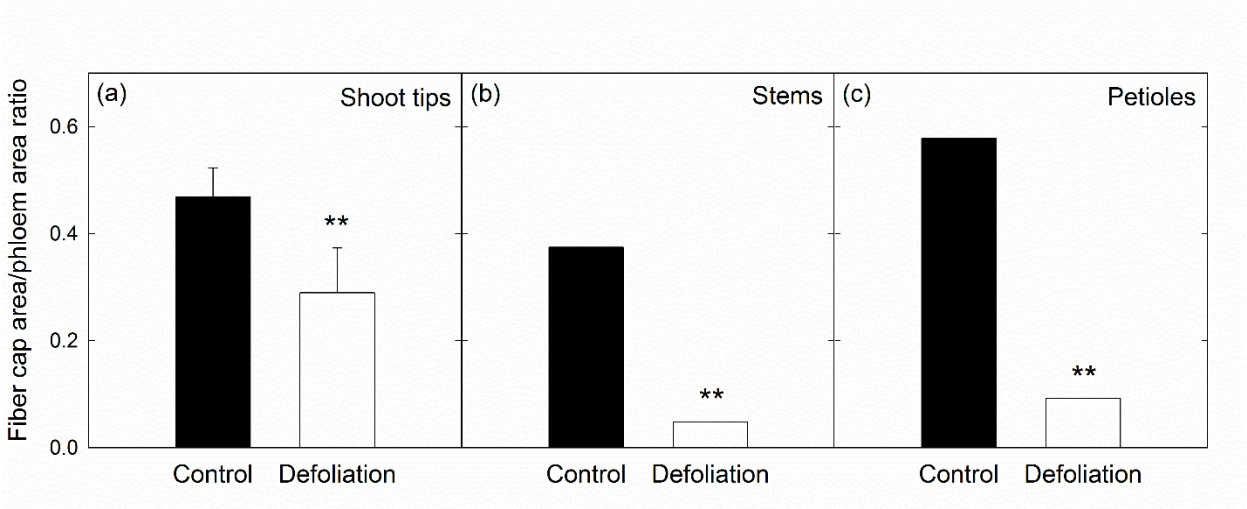

Figure 4.5

Mean values of the ratio of the phloem fiber area to total phloem area in shoot tips (a), for current year's phloem in stems (b) and in petioles of leaves produced post-treatment (c), n=5. Shoot tip data was analyzed with a t-test. Because of multiple zero values for this ratio in the defoliation treatments for stems and petioles, the presence or absence of phloem fibers was treated as categorical for stems and petioles, and analyzed with a Z test of proportions. Error bars represent standard error of the mean for data analyzed with a t-test. Stars indicate significant differences between treatments as determined by a t-test or Z test of proportions (P<0.01**).

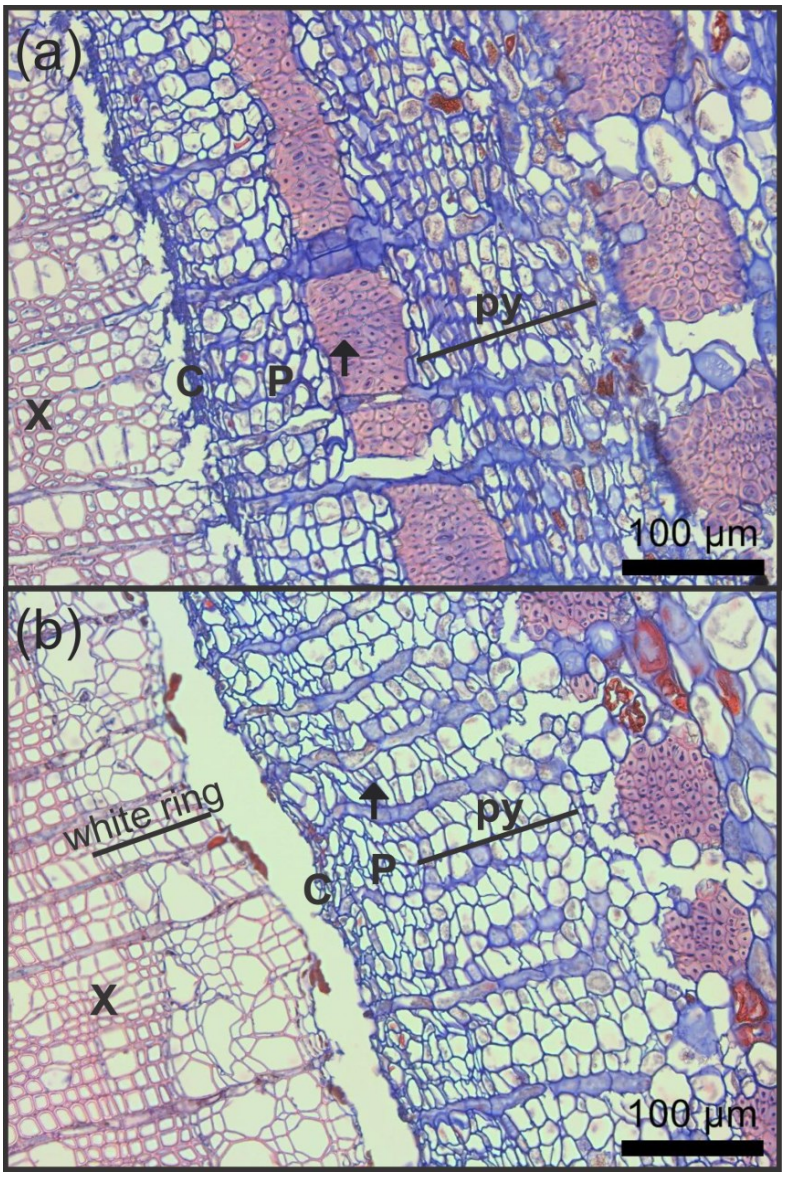

Figure 4.6
Cross sections showing phloem from the main stem with secondary growth in the control treatment (a) and in the defoliation treatment (b). Arrows point to current year phloem fibers (a) and the absence of current year phloem fibers (b) which mark the division between the previous and current year's phloem growth. Letters refer to xylem (X), the cambium (torn) (C), current year's phloem (P), and the previous year's phloem (py; underlined).

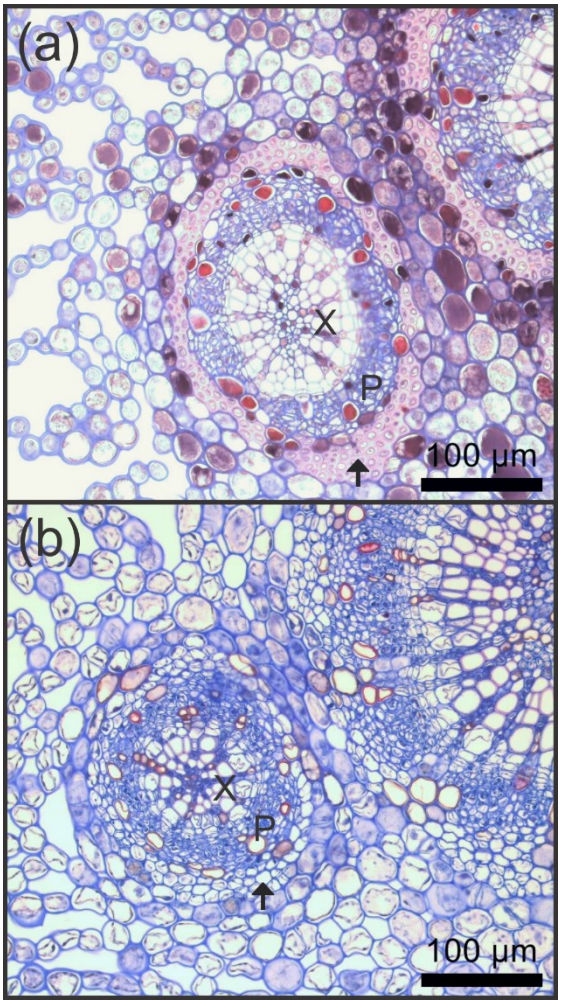

Figure 4.7
Cross sections of petioles from new leaves that developed post-treatment showing vascular bundles from a control tree (a) and a defoliated tree (b). Arrows point to phloem fibers (a) and the absence of phloem fibers (b). Letters refer to xylem (X), and phloem (P).

Table 4.1 Stem and leaf physiological traits

Comparison of treatment means (± s.e.) for the native and maximum values of xylem specific conductivity (K_s) and leaf specific conductivity (LSC), as well as the leaf area to sapwood area ratio (A_L:A_S), n=5 plants per treatment. Stars indicate significant differences between treatments (P<0.05*).

	Control	**Defoliation**
K_s (kg m^{-1} MPa^{-1} s^{-1})		
native	2.14 ±0.50	1.46 ±0.17
max	2.95 ±0.48	1.82 ±0.30
LSC (10^{-4} kg m^{-1} MPa^{-1} s^{-1})		
native	2.77 ±0.72	3.17 ±0.46
max	3.84 ±0.86	3.73 ±0.37
A_L: A_S (m^2 cm^{-2})	0.83 ±0.08	0.50 ±0.10*

Table 4.2 Additional measured anatomical characteristics

Treatment means (± s.e.) for additional measured anatomical characteristics made for the current year xylem and phloem in stems and petioles, n=5 plants per treatment. Phloem cell count refers to the number of layers of phloem cells produced by the cambium. Stars indicate significant differences between treatments (P<0.05*).

	Control	Defoliation
Stems		
Hydraulic vessel diameter (μm)	35.67 ±1.50	32.06 ±1.97
Xylem/phloem area	8.19 ±2.06	1.96 ±0.30*
Phloem cell count	8.87 ±0.55	7.47 ±0.56
Petioles		
Xylem/phloem area	1.06 ±0.11	1.06 ±0.08

4.9 Supporting Information

Table 4.S1 Anatomical characteristics of shoot tips

Treatment means (± s.e.) for measured anatomical characteristics in current year xylem and phloem in new shoot tip growth. n=5 plants per treatment. Phloem cell count refers to the number of layers of phloem cells produced by the cambium.

	Control	Defoliation
Shoot tips		
Vessel diameter (μm)	13.78 ±1.75	17.26 ±0.91
Hydraulic vessel diameter (μm)	19.62 ±1.94	23.74 ±1.02
Vessel roundness	1.13 ±0.01	1.12 ±0.01
Sieve tube diameter (μm)	10.66 ±0.92	9.81 ±0.53
Sieve tube length (μm)	96.53 ±5.46	93.59 ±3.77
Xylem/phloem area	2.31 ±0.56	2.14 ±0.27
Phloem cell count	8.93 ±0.73	8.53 ±0.67

5 Conclusions

5. 1 Drought-induced changes to the vascular tissue

Both Chapters 2 and 3 examined the influence of drought on the xylem of *Populus* species. Together the results of these research chapters suggest a mechanism of increased vulnerability to drought and the influence of age in tree's response to drought conditions.

Beginning with the xylem ultrastructure, the examination of xylem pit membranes revealed likely irreversible increases in both xylem pit membrane pore size and the number of visibly porous membranes due to drought. This observation supported pit membrane damage as a mechanism for cavitation fatigue, a phenomenon observed not only in *Populus* but in other species as well (Hacke et al. 2001). This increased vulnerability to cavitation following a drought can persist multiple years in stands, especially in diffuse-porous species which utilize multiple rings of xylem (Anderegg et al. 2013). Though a phenomenon observed across species, knowledge of the variations in species response may be useful to achieve even greater understanding of the impact of cavitation fatigue. Damage to pit membranes implies that recovery of a pre-fatigue vulnerability to cavitation may be achieved by growth of new xylem. However, the length of time to achieve recovery may vary between species depending on the amount of functional sapwood used by the trees. Additionally, a recent study has suggested that seasonality may play a role in resistance of pit membranes to damage, and the resulting degree of fatigue exhibited (Zhang et al. 2018). These findings suggest a mechanism through which drought induces physical damage to the xylem, and provides a starting point for future studies of tree vulnerability to drought.

At a much broader scale, xylem structural alterations examined through tree ring chronologies can reveal tree hydraulic adjustments to stress over many years (Fonti et al. 2010; Bryukhanova & Fonti 2013). In Chapter 3, this idea was utilized to understand the response of

xylem to both drought and defoliation stress. The main finding regarding drought-stress was that the xylem vessel diameter was more strongly influenced by precipitation when the trees were young than when they were mature. Mature stands may be less susceptible to the effects of drought because of larger root systems. Stronger correlations between ^{13}C and climate also suggested better regulation of transpiration in mature trees through greater stomatal sensitivity to drought. It is notable that measurements of xylem anatomical traits did not reveal significant alterations within years considered severe drought, and suggests a resilience of the water transport structure and function to drought in mature trees, at least until drought-stress becomes severe enough to be associated with xylem pit membrane damage (Chapter 2).

5.2 Defoliation-induced changes to the vascular tissue

The influence of insect defoliation on both xylem and phloem was observed in Chapters 3 and 4. Collectively, these observations present new information and inform us about the ways in which defoliation-induced structural alterations lead to vascular dysfunction.

The most apparent way in which trees are stressed through defoliation is through carbon limitation; reductions in stored carbon due to defoliation have been documented in various *Populus* species (Kosola et al. 2001; Landhäusser & Lieffers 2012). Notably, the results from this thesis research revealed ways through which this carbon resource limitation directly influences vascular transport function. When compared with drought-stress, insect defoliation induced more pronounced changes to the xylem in tree rings (Chapter 3). The observations of reduced wall thickness in xylem fibers and misshapen xylem vessels in tree rings implied that defoliation may lead to xylem that is more vulnerable to cavitation in the event of a drought. Hydraulic conductivity measurements supported this hypothesis (Chapter 4). Potentially, mortality from defoliation that

has been documented in aspen is facilitated by these changes to the xylem structure. In fact, observations of dieback, especially crown dieback, in poplar due to defoliation (Kosola et al. 2001; Moulinier et al. 2014) support this idea. Dieback due to increased vulnerability to cavitation may manifest first at branch tips as they will experience the lowest water potentials.

The examination of phloem anatomy in Chapter 4 revealed entirely novel information about phloem structure and function in response to defoliation. Analysis of phloem sieve tube diameter showed that phloem sieve tubes were reduced in the main stem of defoliated trees, suggesting that phloem flow would be less efficient. This is similar to findings for water-stressed trees (Woodruff 2013; Dannoura et al. 2018), though the mechanism for reduced turgor in cells may be driven by solute limitations rather than water limitations. Reductions in phloem transport efficiency may therefore be similarly expected in response to both drought and defoliation. However, the impact of the absence of phloem fiber cells in the main stem is less clear. In areas absent of fibers, the previous years' sieve tubes appeared to have more turgor. It seems possible that phloem sieve tubes not crushed by fibers may still be functional and could provide transport pathways. However, the lack of fibers may also reduce structural support to the newly produced vascular tissue, potentially negatively impacting transport safety. Though defoliation induced strong alterations to phloem structure, there remains more to be learned about phloem function in response to this stress.

5.3 The prioritization of transport capability over mechanical strength

As suggested by research supporting hydraulic traits as best predictors of mortality (Skelton et al. 2015; Anderegg et al. 2016; Adams et al. 2017), transport function is critical to tree survival under stress. At a certain stress severity, i.e. low water potentials, transport failure is

unavoidable due to embolism and loss of hydraulic conductivity (Tyree & Sperry 1988). And similarly, irreversible damage to xylem pit membranes may be unavoidable (Chapter 2). However, the research described in this thesis also emphasizes trees' prioritization of critical transport functions when producing new vascular tissue under stress. Additionally, this appears to come at the cost of reducing resources to cells providing mechanical strength. Anatomical measurements (Chapter 3, Chapter 4) showed that both xylem and phloem fibers exhibited the most pronounced alterations in structure due to defoliation. Although fibers weakened through reduced cell wall thickness led to proximate vessel shape changes in the xylem, the development of vessels was not affected directly. In the absence of drought stress, these misshapen vessels may contribute normally to water transport.

The lack of resource allocation to phloem fiber production was also prominent. However the lack of fiber cells did not reflect a lack of sieve tubes. Although defoliated trees showed reduced phloem sieve tube diameters, the production of these cells appeared to be unaffected. This was evidenced by the number of sieve tubes produced being similar between defoliated and non-defoliated trees. This seems to be the case even for drought stress; in water-stressed trees the number of sieve tubes produced also did not differ from the number produced by control trees, though they were smaller in diameter (Dannoura et al. 2018). Together, these observations show that when resources are limited, alterations to the vascular structure are more pronounced in the cells contributing to mechanical strength.

5.4 Future research areas

Future research into vascular tissue structure and function should take into further account the potential lagged effects of defoliation. Though xylem structure appeared to recover in the year

following defoliation (Chapter 3), there may be potential lasting effects of the altered xylem's contribution to water transport. For example, cavitation fatigue has been measured in trees several years following a drought (Anderegg et al. 2013), but it is unclear how long defoliated trees may show increased vulnerability to embolism. Potentially, defoliation may also affect pit membranes characteristics. Besides porosity, pit membrane thickness is also tied to a tree's vulnerability to cavitation (Li et al. 2016), and could be altered. Future studies may also investigate if the wood produced during a defoliation year remains functional in the years following. Even without functional xylem from a defoliation year, decreases in xylem area-specific conductivity may remain until enough new sapwood has been produced. These observations would help us to understand for how many years after a defoliation trees may be more vulnerable to water stress.

Additionally, one aspect of tree response that this thesis project did not examine is the impact of a combined drought and defoliation event. It is possible that severe drought and defoliation would occur in the same year, especially as major outbreaks of forest tent caterpillar may last multiple years (Cooke & Roland 2000; 2007). Though it is clear that defoliated aspen and poplar may be more susceptible to drought, whether or not experiencing both stresses at the same time amplifies physiological and anatomical alterations is still uncertain. On a broader scale, understanding the impact of combined drought and defoliation stress on forests may be more complicated. Multiple factors may play into the amount of damage sustained by trees due to coinciding water stress and insect infestation: the insect feeding behavior, the affected tree part, and the severity of water stress (Jactel et al. 2012). This variability inherent in insect interactions with drought reinforces the need to study this scenario across many species.

5.5 Summary

The study of alterations to the structure and function of the vascular tissue provides evidence for mechanisms of tree dieback. This information collected from *Populus*, unknown prior to this research, include observations of xylem pit membrane damage as a mechanism for cavitation fatigue, changing xylem vessel diameter sensitivity to drought in aspen over time, increased vulnerability to cavitation in defoliated trees via decreased xylem vessel roundness, and reduced sieve tube diameters and fiber area in the phloem in response to defoliation. Together these observations illustrate processes through which drought and defoliation influence tree vulnerability to dieback and mortality.

5.6 References

Adams H.D., Zeppel M.J.B., Anderegg W.R.L., Hartmann H., Landhäusser S.M., Tissue D.T., …, McDowell N.G. (2017) A multi-species synthesis of physiological mechanisms in drought-induced tree mortality. *Nature Ecology & Evolution* 1: 1285-1291.

Anderegg W.R.L., Plavcová L., Anderegg L.D.L., Hacke U.G., Berry J.A. & Field C.B. (2013) Drought's legacy: Multiyear hydraulic deterioration underlies widespread aspen forest die-off and portends increased future risk. Global *Change Biology* 19:1188-1196.

Anderegg W.R.L., Klein T., Bartlett M., Sack L., Pellegrini A.F.A., Choat B. & Jansen S. (2016) Meta-analysis reveals that hydraulic traits explain cross-species patterns of drought-induced tree mortality across the globe. *PNAS* 113: 5024-5029.

Bryukhanova M. & Fonti P. (2013) Xylem plasticity allows rapid hydraulic adjustment to annual climatic variability. *Trees* 27: 485-496.

Cooke B.J. & Roland J. (2007) Trembling aspen responses to drought and defoliation by forest tent caterpillar and reconstruction of recent outbreaks in Ontario. *Canadian Journal of Forest Research* 37:1586-1598.

Cooke B.J. & Roland J. (2000) Spatial analysis of large-scale patterns of forest tent caterpillar outbreaks. Écoscience 7:410-422.

Dannoura M., Epron D., Desalme D., Massonnet C., Tsuji S., Plain C., Priault P., Gérant D. (2018) The impact of prolonged drought on phloem anatomy and phloem transport in young beech trees. *Tree Physiology,* https://doi.org/10.1093/treephys/tpy070

Fonti P., von Arx G., García-González I., Eilmann B., Sass-Klaassen U., Gärtner H., Eckstein D. (2010) Studying global change through investigation of the plastic responses of xylem anatomy in tree rings. *New Phytologist* 185:42-53.

Hacke U.G., Stiller V., Sperry J.S., Pittermann J. & McCulloh K.A. (2001) Cavitation Fatigue. Embolism and refilling cycles can weaken the cavitation resistance of xylem. *Plant Physiology* 125: 779-786.

Jactel H., Petit J., Desprez-Loustau M., Delzon S., Piou D., Battisti A. & Koricheva J. (2012) Drought effects on damage by forest insects and pathogens: a meta-analysis. *Global Change Biology* 18: 267-276.

Kosola K.R., Dickmann D.I., Paul E.A. & Parry D. (2001) Repeated insect defoliation effects on growth, nitrogen acquisition, carbohydrates, and root demography of poplars. *Oecologia* 129: 65-74.

Landhäusser SM, Lieffers VJ (2012) Defoliation increases risk of carbon starvation in root systems of mature aspen. Trees 26:653-661.

Li S., Lens F., Espino S., Karimi Z., Klepsch M., Schenk H.J., …, Jansen S. (2016) Intervessel pit membrane thickness as a key determinant of embolism resistance in angiosperm xylem. *IAWA Journal* 37: 152-171.

Moulinier J., Lorenzetti F. & Bergeron Y. (2014) Growth and mortality of trembling aspen (*Populus tremuloides*) in response to artificial defoliation. *Acta Oecologica* 55: 104-112.

Skelton R.P., West A.G. & Dawson T.E. (2015) Predicting plant vulnerability to drought in biodiverse regions using functional traits. *PNAS* 112: 5744-5749.

Tyree M.T. & Sperry J.S. (1988) Do woody plants operate near the point of catastrophic dysfunction caused by dynamic water-stress – answers from a model. *Plant Physiology* 88: 574-580.

Woodruff D.R. (2014) The impacts of water stress on phloem transport in Douglas-fir trees. *Tree Physiology* 34: 5-14.

Zhang W., Feng F. & Tyree M.T. (2018) Seasonality of cavitation and frost fatigue in *Acer mono* Maxim. *Plant, Cell and Environment* 41: 1278-1286.

Cumulative Bibliography

Adams H.D., Zeppel M.J.B., Anderegg W.R.L., Hartmann H., Landhäusser S.M., Tissue D.T., …, McDowell N.G. (2017) A multi-species synthesis of physiological mechanisms in drought-induced tree mortality. *Nature Ecology & Evolution* 1: 1285-1291.

Agresti A. (1990) Categorical Data Analyses. New York: John Wiley & Sons.

Alder N.N., Pockman W.T., Sperry J.S. & Nuismer S. (1997) Use of centrifugal force in the study of xylem cavitation. *Journal of Experimental Botany* 48: 665-674.

Allan C.D., Macalady A.K., Chenchouni H., Bachelet D., Mcdowell N., Vennetier M., ..., Cobb N. (2010) A global overview of drought and heat-induced tree mortality reveals emerging climate change risks for forests. *Forest Ecology and Management* 259: 660-684.

Anderegg W.R.L., Plavcová L., Anderegg L.D.L., Hacke U.G., Berry J.A. & Field C.B. (2013) Drought's legacy: Multiyear hydraulic deterioration underlies widespread aspen forest die-off and portends increased future risk. *Global Change Biology* 19:1188-1196.

Anderegg W.R.L. (2014) Spatial and temporal variation in plant hydraulic traits and their relevance for climate change impacts on vegetation. *New Phytologist* 205: 1008-1014.

Anderegg W.R.L., Flint A., Huang C., Flint L., Berry J.A., Davis F.W., Sperry J.S. & Field C.B. (2015a) Tree mortality predicted from drought-induced vascular damage. *Nature Geoscience* 8: 367-371.

Anderegg W.R.L., Hicke J.A., Fisher R.A., Allen C.D., Aukema J., Bentz B., …, Zeppel M. (2015b) Tree mortality from drought, insects, and their interactions in a changing climate. *New Phytologist* 208:674-683.

Anderegg W.R.L., Klein T., Bartlett M., Sack L., Pellegrini A.F.A., Choat B. & Jansen S. (2016) Meta-analysis reveals that hydraulic traits explain cross-species patterns of drought-induced tree mortality across the globe. *PNAS* 113: 5024-5029.

Arend M. & Fromm J. (2007) Seasonal change in the drought response of wood cell development in poplar. *Tree Physiology* 27: 985-992.

Beikircher B. & Mayr S. (2009) Intraspecific differences in drought tolerance and acclimation in hydraulics of *Ligustrum vulgare* and *Viburnum lantana*. *Tree Physiology* 29: 765-775.

Braatne J.H., Rood S.B. & Heilman P.E. (1996) Life history, ecology, and conservation of riparian cottonwoods in North America. In Biology of *Populus* (eds R.F Stettler, H.D. Bradshaw Jr., P.E. Heilman, & T.M. Hinckley), pp. 57-85. Ottawa: NRC Research Press.

Bryukhanova M. & Fonti P. (2013) Xylem plasticity allows rapid hydraulic adjustment to annual climatic variability. *Trees* 27: 485-496.

Bunn A.G. (2008) A dendrochronology program library in R (dplR). *Dendrochronologia* 26:115-124.

Carlquist S. (1984) Vessel grouping in dicotyledon wood. *Aliso* 10:505-525.

Chen L., Huang J., Dawson A., Zhai L., Stadt K.J., Comeau P.G. & Whitehouse C. (2018) Contributions of insects and droughts to growth decline of trembling aspen mixed boreal forest of western Canada. *Global Change Biology* 24: 655-667.

Chen H.Y.H. & Luo Y. (2015) Net aboveground biomass declines of four major forest types with forest ageing and climate change in western Canada's boreal forests. *Global Change Biology* 21: 3675-3684.

Choat B., Ball M., Luly J. & Holtum J. (2003) Pit membrane porosity and water stress-induced cavitation in four co-existing dry rainforest tree species. *Plant Physiology* 131: 41-48.

Choat B., Cobb A.R. & Jansen S. (2008) Structure and function of bordered pits: new discoveries and impacts on whole-plant hydraulic function. *New Phytologist* 177: 608-626.

Choat B., Jansen S., Zwieniecki M.A., Smets E. & Holbrook N.M. (2004) Changes in pit membrane porosity due to deflection and stretching: the role of vestured pits. *Journal of Experimental Botany* 55: 1569-1575.

Cooke B.J. & Lorenzetti F. (2006) The dynamics of forest tent caterpillar outbreaks in Quebec, Canada. *Forest Ecology and Management* 226: 110-121.

Cooke B.J. & Roland J. (2007) Trembling aspen responses to drought and defoliation by forest tent caterpillar and reconstruction of recent outbreaks in Ontario. *Canadian Journal of Forest Research* 37:1586-1598.

Cooke B.J. & Roland J. (2000) Spatial analysis of large-scale patterns of forest tent caterpillar outbreaks. *Écoscience* 7:410-422.

Corcuera L., Camarero J.J. & Gil-Pelegrin E. (2004) Effects of a severe drought on *Quercus ilex* radial growth and xylem anatomy. *Trees* 16: 83-92.

Corcuera L., Cochard H., Gil-Pelegrin E., Notivol E. (2011) Phenotypic plasticity in mesic populations of *Pinus pinaster* improves resistance to xylem embolism (P_{50}) under severe drought. *Trees* 25: 1033-1042.

Dannoura M., Epron D., Desalme D., Massonnet C., Tsuji S., Plain C., Priault P., Gérant D. (2018) The impact of prolonged drought on phloem anatomy and phloem transport in young beech trees. *Tree Physiology,* https://doi.org/10.1093/treephys/tpy070

Davis J.D. & Evert R.F. (1968) Seasonal Development of the Secondary Phloem in *Populus tremuloides*. *Botanical Gazette* 129: 1-8.

DeBell D.S., Singleton R., Harrington C.A. & Gartner B.L. (2002) Wood density and fiber length in young *Populus* stems: Relation to clone, age, growth rate, and pruning. *Wood and Fiber Science* 34:529-539.

Diamandis S. & Koukos P. (1992) Effect of bacteria on the mechanical and chemical properties of wood in poplars damaged by frost cracks. *Forest Pathology* 22:362-370.

Domec J.C., Rivera L.N., King J.S., Peszlen I., Hain F., Smith B., Frampton J. (2013) Hemlock woolly adelgid (*Adelges tsugae*) infestation affects water and carbon relations of eastern hemlock (*Tsuga canadensis*) and Carolina hemlock (*Tsuga caroliniana*). *New Phytologist* 199: 452-463.

Eilmann B., Zweifel R., Buchmann N., Fonti P. & Rigling A. (2009) Drought-induced adaptation of xylem in Scots pine and pubescent oak. *Tree Physiology* 29: 1011-1020.

Evert R.F. (2006) Esau's Plant Anatomy: meristems, cells, and tissues of the plant body: their structure, function, and development (3rd ed.). Hoboken, NJ: Wiley-Interscience.

Fitzgerald T.D. (1995) The Tent Caterpillars. Ithaca, NY: Cornell University Press.

Fonti P., von Arx G., García-González I., Eilmann B., Sass-Klaassen U., Gärtner H. & Eckstein D. (2010) Studying global change through investigation of the plastic responses of xylem anatomy in tree rings. *New Phytologist* 185:42-53.

Foster J.R. (2017) Xylem traits, leaf longevity and growth phenology predict growth and mortality response to defoliation in northern temperate forests. *Tree Physiology* 37: 1151-1165.

Franceschi V.R., Krokene P., Christiansen E., Krekling T. (2005) Anatomical and chemical defenses of conifer bark against bark beetles and other pests. *New Phytologist* 167: 353-376.

Fritts H.C. (1976) Tree rings and climate. London: Academic Press Inc.

Galvez D.A., Landhäusser S.M. & Tyree M.T. (2011) Root carbon reserve dynamics in aspen seedlings: Does simulated drought induce reserve limitation? *Tree Physiology* 31:250-257.

Gärtner H. & Schweingruber F. (2013) Microscopic preparation techniques for plant stem analysis. Remagen: Verlag Dr. Kessel.

Gleason S.M., Westoby M., Jansen S., Choat B., Hacke U.G., Pratt R.B., … Zanne A.E. (2016) Weak tradeoff between xylem safety and xylem-specific hydraulic efficiency across the world's woody plant species. *New Phytologist* 209: 123-136.

Hacke U.G., Sperry J.S. & Pittermann J. (2004) Analysis of circular bordered pit function II. Gymnosperm tracheids with torus-margo pit membranes. *American Journal of Botany* 91: 386-400.

Hacke U.G., Sperry J.S., Pockman W.T., Davis S.D. & McCulloh K.A. (2001) Trends in wood density and structure are linked to prevention of xylem implosion by negative pressure. *Oecologia* 126:457-461.

Hacke U.G., Spicer R., Schreiber S.G. & Plavcová L. (2017) An ecophysiological and developmental perspective on variation in vessel diameter. *Plant, Cell and Environment* 40:831-845.

Hacke U.G., Stiller V., Sperry J.S., Pittermann J. & McCulloh K.A. (2001) Cavitation Fatigue. Embolism and refilling cycles can weaken the cavitation resistance of xylem. *Plant Physiology* 125: 779-786.

Hacke U.G., Venturas M.D., MacKinnon E.D., Jacobsen A.L., Sperry J.S & Pratt R.B. (2015) The standard centrifuge method accurately measures vulnerability curves of long-vesselled olive stems. *New Phytologist* 205: 116-127.

Hart M., Hogg E.H. & Lieffers V.J. (2000) Enhanced water relations of residual foliage following defoliation in *Populus tremuloides*. *Canadian Journal of Botany* 78:583-590.

Hildahl V. & Reeks W.A. (1960) Outbreaks of the forest tent caterpillar, *Malacosoma disstria* Hbn., and their effects on stands of trembling aspen in Manitoba and Saskatchewan. *The Canadian Entomologist* 92: 199-209.

Hillabrand R.M., Hacke U.G. & Lieffers V.J. (2016) Drought-induced xylem pit membrane damage in aspen and balsam poplar. *Plant, Cell and Environment* 39:2210-2220.

Hillabrand R.M., Lieffers V.J., Hogg E.H., Martinez-Sancho E., Menzel A., Hacke U.G. (2018) Functional xylem anatomy of aspen exhibits greater change due to insect defoliation than to drought. *Tree Physiology*. https://doi.org/10.1093/treephys/tpy075

Hogg E.H. (1994) Climate and the southern limit of the western Canadian boreal forest. *Canadian Journal of Forest Research* 24:1835-1845.

Hogg E.H., Barr A.G. & Black T.A. (2013) A simple soil moisture index for representing multi-year drought impacts on aspen productivity in the western Canadian interior. *Agricultural and Forest Meteorology* 178-179:173-182.

Hogg E.H., Brandt J.P. & Kochtubajda B. (2005) Factors affecting interannual variation in growth of western Canadian aspen forests during 1951-2000. *Canadian Journal of Forest Research* 35:610-622.

Hogg E.H., Brandt J.P. & Michaelian M. (2008) Impacts of a regional drought on the productivity, dieback, and biomass of western Canadian aspen forests. *Canadian Journal of Forest Research* 38: 1373-1384.

Hogg E.H., Hart M. & Lieffers V.J. (2002) White tree rings formed in trembling aspen saplings following experimental defoliation. *Canadian Journal of Forest Research* 32:1929-1934.

Hogg E.H. & Schwarz A.G. (1999) Tree-ring analysis of declining aspen stands in west-central Saskatchewan. Information Report Nor-X-359. Forestry Canada, Northern Forestry Centre, Edmonton, Alberta.

Holmes R.L. (1983) Computer-assisted quality control in tree-ring dating and measurement. *Tree-Ring Bulletin* 43:70-78.

Hubbard R.M., Rhoades C.C., Elder K., Negron J. (2013) Changes in transpiration and foliage growth in lodgepole pine trees following mountain pine beetle attack and mechanical girdling. *Forest Ecology and Management* 289: 312-317.

Huggett B.A., Savage J.A., Hao G., Preisser E.L., Holbrook N.M. (2018) Impact of hemlock woolly adelgid (*Adelges tsugae*) infestation on xylem structure and function and leaf physiology in eastern hemlock (*Tsuga canadensis*). *Functional Plant Biology* 45: 501-508.

Jacobsen A.L., Ewers F.W., Pratt R.B., Paddock III W.A. & Davis S.D. (2005) Do xylem fibers affect vessel cavitation resistance? *Plant Physiology* 139:546-556.

Jactel H., Petit J., Desprez-Loustau M., Delzon S., Piou D., Battisti A. & Koricheva J. (2012) Drought effects on damage by forest insects and pathogens: a meta-analysis. *Global Change Biology* 18: 267-276.

Jansen S., Choat B. & Pletsers A. (2009) Morphological variation of intervessel pit membranes and implications to xylem function in angiosperms. *American Journal of Botany* 96: 409-419.

Jansen S., Pletsers A. & Sano Y. (2008) The effect of preparation techniques on SEM-imaging of pit membranes. *IAWA Journal* 29: 161-178.

Janz D., Lautner S.,Wildhagen H., BehnkeK., Schnitzler J.P., Rennenberg H.,…, Polle A. (2012) Salt stress induces the formation of a novel type of pressure wood' in two *Populus* species. *New Phytologist* 194, 129–141.

Jarbeau J.A., Ewers F.W. & Davis S.D. (1995) The mechanism of water-stress-induced embolism in two species of chaparral shrubs. *Plant, Cell and Environment* 18: 189-196.

Jones B., Tardif J. & Westwood R. (2004) Weekly xylem production in trembling aspen (*Populus tremuloides*) in response to artificial defoliation. *Canadian Journal of Botany* 82:590-597.

Kitin P., Voelker S.L., Meinzer F.C., Beeckman H., Strauss S.H. & Lachenbruch B. (2010) Tyloses and phenolic deposits in xylem vessels impede water transport in low-lignin transgenic poplars: A study by cryo-fluorescence microscopy. *Plant Physiology* 154:887-898.

Knoblauch M. & Peters W.S (2010) Münch, morphology, microfluidics – our structural problem with the phloem. *Plant, Cell and Environment* 33: 1439- 1452.

Knoblauch M., Knoblauch J., Mullendore D.L., Savage J.A., Babst B.A., Beecher S.D., …, Holbrook N.M. (2016) Testing the Münch hypothesis of long distance phloem transport in plants. *eLife* 5.

Kosola K.R., Dickmann D.I., Paul E.A. & Parry D. (2001) Repeated insect defoliation effects on growth, nitrogen acquisition, carbohydrates, and root demography of poplars. *Oecologia* 129: 65-74.

Koubaa A., Hernandez R.E., Beaudoin M. & Poliquin J. (1998) Interclonal, intraclonal, and within-tree variation in fiber length of poplar hybrid clones. *Wood and Fiber Science* 30:40-47.

Lachenbruch B., Moore J. & Evans R. (2011) Radial variation in wood structure and function in woody plants, and hypotheses for its occurrence. In: Meinzer F.C., Lachenbruch B. & Dawson T.E. (eds) Size- and Age-Related Changes in Tree Structure and Function. Springer, Dordrecht, pp. 121-164.

Landhäusser S.M. & Lieffers V.J. (2012) Defoliation increases risk of carbon starvation in root systems of mature aspen. *Trees* 26:653-661.

Leal S., Pereira H., Grabner M. & Wimmer R. (2004) Tree-ring structure and climatic effects in young *Eucalyptus globulus* Labill. grown at two Portuguese sites: preliminary results. *Dendrochronologia* 21:139-146.

Lee J., Holbrook N.M. & Zwieniecki M. A. (2012) Ion induced changes in the structure of bordered pit membranes. *Frontiers in Plant Science* 3: 55.

Lens F., Sperry J.S., Christman M.A., Choat B., Rabaey D. & Jansen S. (2011) Testing hypotheses that link wood anatomy to cavitation resistance and hydraulic conductivity in the genus *Acer*. *New Phytologist* 190: 709-723.

Lens F., Tixier A., Cochard H., Sperry J.S., Jansen S. & Herbette S. (2013) Embolism resistance as a key mechanism to understand adaptive plant strategies. *Current Opinion in Plant Biology* 16: 287-292.

Li S., Lens F., Espino S., Karimi Z., Klepsch M., Schenk H.J., …, Jansen S. (2016) Intervessel pit membrane thickness as a key determinant of embolism resistance in angiosperm xylem. *IAWA Journal* 37: 152-171.

Loepfe L., Martinez-Vilalta J., Piñol J., Mencuccini M. (2007) The relevance of xylem network structure for plant hydraulic efficiency and safety. *Journal of Theoretical* Biology 247:788-803.

Martínez-Sancho E., Dorado-Liñán I., Heinrich I., Helle G. & Menzel A. (2017) Xylem adjustment of sessile oak at its southern distribution limits. *Tree Physiology* 37:903-914.

McCarroll D. & Loader N.J. (2004) Stable isotopes in tree rings. *Quaternary Science Reviews* 23: 771-801.

Mbogga M.S., Hamann A. & Wang T. (2009) Historical and projected climate data for natural resource management in western Canada. *Agricultural and Forest Meteorology* 149: 881-890.

McDowell N., Pockman W.T., Allen C.D., Breshears D.D., Cobb N., Kolb T., ..., Yepez E.A. (2008) Mechanisms of plant survival and mortality during drought: why do some plants survive while others succumb to drought? *New Phytologist* 178: 719-739.

Man R. & Rice J.A. (2010) Response of aspen stands to forest tent caterpillar defoliation and subsequent overstory mortality in northeastern Ontario, Canada. *Forest Ecology and Management* 260: 1853-1860.

Michaelian M., Hogg E.H., Hall R.J. & Arsenault E. (2011) Massive mortality of aspen following severe drought along the southern edge of the Canadian boreal forest. *Global Change Biology* 17: 2084-2094.

Moulinier J., Lorenzetti F. & Bergeron Y. (2014) Growth and mortality of trembling aspen (*Populus tremuloides*) in response to artificial defoliation. *Acta Oecologica* 55: 104-112.

Mullendore D.L., Froelich D.R., Beecher S., Ross-Elliott T.J., Knoblauch J. & Knoblauch M. (2015) Investigation of Structure-Function relationship of Long-Distance transport in plants: new imaging tools to answer old questions. *Microscopy and Microanalysis* 21:1491-1492.

Natural Resources Canada (2017) Statistical Data, Forests: https://cfs.nrcan.gc.ca/statsprofile.

Niklas K.J. (1992) Plant Biomechanics. Chicago: The University of Chicago Press.

Noyer E., Lachenbruch B., Dlouhá J., Collet C., Ruelle J., Ningre F. & Fournier M. (2017) Xylem traits in European beech (*Fagus sylvatica* L.) display a large plasticity in response to canopy release. *Annals of Forest Science* 74:1-11.

Pan Y., Birdsey R.A., Fang J., Houghton R., Kauppi P.E., Kurz W.A., …, Hayes D. (2011) A large and persistent carbon sink in the world's forests. *Science* 333: 988-993.

Peng C., Ma Z., Lei X., Zhu Q., Chen H., Wang W., …, Zhou X. (2011) A drought-induced pervasive increase in tree mortality across Canada's boreal forests. *Nature Climate Change* 1: 467-471.

Pesacreta T.C., Groom L.H. & Rials T.G. (2005) Atomic force microscopy of the intervessel pit membrane in the stem of *Sapium sebiferum* (Euphorbiaceae). *IAWA Journal* 26: 397-426.

Peterson E.B. & Peterson N.M. (1992) Ecology, management, and use of aspen and balsam poplar in the Prairie Provinces. Special Report 1. Forestry Canada, Northern Forestry Centre, Edmonton, Alberta.

Phillips N.G., Ryan M.G., Bond B.J., McDowell N.G., Hinckley T.M. & Čermák J. (2003) Reliance on stored water increases with tree size in three species in the pacific northwest. *Tree Physiology* 23:237-245.

Pinno B.D., Lieffers V.J. & Stadt K.J. (2001) Measuring and modelling the crown and light transmission characteristics of juvenile aspen. *Canadian Journal of Forest Research* 31:1930-1939.

Plavcová L. & Hacke U.G. (2012) Phenotypic and developmental plasticity of xylem in hybrid poplar saplings subjected to experimental drought, nitrogen fertilization, and shading. *Journal of Experimental Botany* 63: 6481-6491.

Plavcová L., Hacke U.G. & Sperry J.S. (2011) Linking irradiance-induced changes in pit membrane ultrastructure with xylem vulnerability to cavitation. *Plant, Cell and Environment* 34: 501-513.

Plavcová L., Hacke U.G., Almeida-Rodriguez A.M., Li E. & Douglas C.J. (2013) Gene expression patterns underlying changes in xylem structure and function in response to increased nitrogen availability in hybrid poplar. *Plant, Cell and Environment* 36: 186-199.

Plavcová L., Jansen S., Klepsch M. & Hacke U.G. (2013) Nobody's perfect: can irregularities in pit structure influence vulnerability to cavitation? *Frontiers in Plant Science* 4: 453.

Pureswaran D., Roques A., Battisti A. (2018) Forest Insects and Climate Change. *Current Forestry Reports* 4: 35-50.

R Core Team (2016) R: A language and environment for statistical computing. R Foundation for Statistical Computing, Vienna, Austria. URL http://www.R-project.org/.

Régnière J., St.-Amant R. & Béchard A. (2016) BioSIM 10.0 User's Manual, Information Report LAU-X-137E. Natural Resources Canada, Canadian Forest Service, Ottawa, ON, Canada.

Rodgers P.C. (2017) Guide to Quaking Aspen Ecology and Management. BLM-UT-G1017-001-8000. Western Aspen Alliance, Utah State University, Logan, Utah.

Sala A., Piper F. & Hoch G. (2010) Physiological mechanisms of drought-induced tree mortality are far from being resolved. *New Phytologist* 186: 274-281.

Salleo S., Nardini A., Raimondo F., Assunta Lo Gullo M., Pace F., Giacomich P. (2003) Effects of defoliation caused by the leaf miner *Cameraria ohridella* on wood production and efficiency in *Aesculus hippocastanum* growing in north-eastern Italy. *Trees* 17: 367-375.

Sano Y. (2005) Inter- and intraspecific structural variations among intervascular pit membranes, as revealed by field-emission scanning electron microscopy. *American Journal of Botany* 92: 1077-1084.

Sano Y. & Jansen S. (2006) Perforated pit membranes in imperforate tracheary elements of some angiosperms. *Annals of Botany* 97: 1045-1053.

Savage J.A., Clearwater M.J., Haines D.F., Klein T., Mencuccini M., Sevanto S., Turgeon R. & Zhang C. (2016) Allocation, stress tolerance and carbon transport in plants: how does phloem physiology affect plant ecology. *Plant, Cell and Environment* 39: 709-725.

Schenk H.J., Steppe K. & Jansen S. (2015) Nanobubbles: a new paradigm for air-seeding in xylem. *Trends in Plant Science* 20: 199-205.

Schneider L. & Gärtner H. (2013) The advantage of using a starch based non-Newtonian fluid to prepare micro sections. *Dendrochronologia* 31:175-178.

Scholz F.G., Phillips N., Bucci S., Meinzer F.C. & Goldstein G. (2011) Hydraulic capacitance: Biophysics and functional significance of internal water sources in relation to tree size. In: Meinzer F.C., Lachenbruch B. & Dawson T.E. (eds) Size- and Age-Related Changes in Tree Structure and Function. Springer, Dordrecht, pp. 341-361.

Scholz A., Rabaey D., Stein A., Cochard H., Smets E. & Jansen S. (2013) The evolution and function of vessel and pit characters with respect to cavitation resistance across 10 *Prunus* species. *Tree Physiology* 33: 684-694.

Schoonmaker A.L., Hacke U.G., Landhausser S.M., Lieffers V.J., Tyree M.T. (2010) Hydraulic acclimation to shading in boreal conifers of varying shade tolerance. *Plant, Cell and Environment* 33: 382-393.

Schreiber S.G., Hacke U.G., Hamann A. & Baltzer J. (2015) Variation of xylem vessel diameters across a climate gradient: Insight from a reciprocal transplant experiment with a widespread boreal tree. *Functional Ecology* 29:1392-1401.

Schreiber S.G., Hacke U.G., Hamann A. & Thomas B.R. (2011) Genetic variation of hydraulic and wood anatomical traits in hybrid poplar and trembling aspen. *New Phytologist* 190:150-160.

Settler R.F., Bradshaw Jr. H.D., Heilman P.E. & Hinckley T.M. (1996) Biology of *Populus* and its Implications for Management and Conservation. Ottawa: NRC Research Press.

Sevanto S., McDowell N.G., Dickman L.T., Pangle R. & Pockman W.T. (2014) How do trees die? A test of the hydraulic failure and carbon starvation hypotheses. *Plant, Cell and Environment*, 37, 153-161.

Sevanto S. (2014) Phloem transport and drought. *Journal of Experimental Botany* 65: 1751-1759.

Sevanto S. (2018) Drought impacts on phloem transport. *Current Opinion in Plant Biology* 43: 76-81.

Shane M.W., McCully M.E. & Canny M.J. (2000) Architecture of branch-root junctions in maize: structure of the connecting xylem and the porosity of the pit membranes. *Annals of Botany* 85: 613-624.

Skelton R.P., West A.G. & Dawson T.E. (2015) Predicting plant vulnerability to drought in biodiverse regions using functional traits. *PNAS* 112: 5744-5749.

Sperry J.S. & Love D.M. (2015) What plant hydraulics can tell us about responses to climate-change droughts. *New Phytologist* 207: 14-17.

Sperry J.S., Donnelly J.R. & Tyree M.T. (1988) A method for measuring hydraulic conductivity and embolism in xylem. *Plant, Cell and Environment* 11: 35-40.

Sperry J.S. & Hacke U.G. (2004) Analysis of circular bordered pit function I. Angiosperm vessels with homogenous pit membranes. *American Journal of Botany* 91: 369-385.

Sperry J.S., Nichols K.J., Sullivan J.E.M. & Eastlack S.E. (1994) Xylem embolism in ring-porous, diffuse-porous, and coniferous trees of northern Utah and interior Alaska. *Ecology* 75: 1736-1752.

Sperry J.S., Perry A.H. & Sullivan J.E.M. (1991) Pit membrane degradation and air-embolism formation in ageing xylem vessels of *Populus tremuloides* Michx. *Journal of Experimental Botany* 42: 1399-1406.

Sperry J.S. & Tyree M.T. (1988) Mechanism of water stress-induced xylem embolism. *Plant Physiology* 88: 581-587.

Speer J.H. (2010) Fundamentals of tree ring research. Tucson: The University of Arizona Press.

Stiller V. & Sperry J.S. (2002) Cavitation fatigue and its reversal in sunflower (*Helianthus annuus* L.) *Journal of Experimental Botany* 53: 1155-1161.

Suarez M.L. & Kitzberger T. (2008) Recruitment patterns following a severe drought: long-term compositional shifts in Patagonian forests. *Canadian Journal of Forest Research*, 38, 3002-3010.

Sutton A. & Tardif J. (2005) Distribution and anatomical characteristics of white rings in *Populus tremuloides*. *IAWA Journal* 26:221-238.

Taiz L. & Zeiger E. (2006) Plant Physiology (4th ed.). Sunderland, MA: Sinauer Associates, Inc.

Tixier A., Herbette S., Jansen S., Capron M., Tordjeman P., Cochard H. & Badel E. (2014) Modelling the mechanical behavior of pit membranes in bordered pits with respect to cavitation resistance in angiosperms. *Annals of Botany* 114: 325-334.

Tyree M.T. & Sperry J.S. (1988) Do woody plants operate near the point of catastrophic dysfunction caused by dynamic water-stress – answers from a model. *Plant Physiology* 88: 574-580.

Tyree M.T. & Zimmerman M. (2002) Xylem Structure and the Ascent of Sap. Berlin: Springer Verlag.

Van Bel A.J.E. (2003) The phloem, a miracle of ingenuity. *Plant, Cell and Environment* 26: 125-149.

Venturas M.D., MacKinnon E.D., Dario H.L., Jacobsen A.L., Pratt R.B. & Davis S.D. (2016) Chaparral shrub hydraulic traits, size, and life history types relate to species mortality during California's historic drought of 2014. *PLOS ONE* 11:e0159145.

Voelker S.L., Lachenbruch B., Meinzer F.C., Kitin P. & Strauss S.H. (2011) Transgenic poplars with reduced lignin show impaired xylem conductivity, growth efficiency and survival. *Plant, Cell and Environment* 34:655-668.

Warton D.I., Wright I.J., Falster D.S. & Westoby M. (2006) Bivariate line-fitting methods for allometry. *Biological Reviews* 81:259-291.

Weed A.S., Ayres M.P. & Hicke J. (2013) Consequences of climate change for biotic disturbances in North American forests. *Ecological Monographs* 83: 441-470.

Wheeler J.K., Sperry J.S., Hacke U.G. & Hoang N. (2005) Inter-vessel pitting and cavitation in woody Rosaceae and other vesselled plants: a basis for a safety versus efficiency trade-off in xylem transport. *Plant, Cell and Environment* 28: 800-812.

Woodruff D.R. (2014) The impacts of water stress on phloem transport in Douglas-fir trees. *Tree Physiology* 34: 5-14.

Worrall J.J., Egeland L., Eager T., Mask R.A., Johnson E.W., Kemp P.A. & Shepperd W.D. (2008) Rapid mortality of *Populus tremuloides* in southwestern Colorado, USA. *Forest Ecology and Management* 255:686-696.

Worrall J.J., Marchetti S.B., Egeland L., Mask R.A., Eager T. & Howell B. (2010). Effects and etiology of sudden aspen decline in southwestern Colorado, USA. *Forest Ecology and Management* 260: 638-648.

Worrall J.J., Rehfeldt G.E., Hamann A., Hogg E.H., Marchetti S.B., Michaelian M. & Gray L.K. (2013) Recent declines of *Populus tremuloides* in North America linked to climate. *Forest Ecology and Management* 299: 35-51.

Zhang W., Feng F. & Tyree M.T. (2018) Seasonality of cavitation and frost fatigue in *Acer mono* Maxim. *Plant, Cell and Environment* 41: 1278-1286.

Zimmerman M. (1983) Xylem Structure and the Ascent of Sap. Berlin: Springer Verlag.